Role of PET and PET/CT in inflammation and infection

Essay
Submitted for the fulfillment of M.Sc. degree in nuclear medicine

By
Shaimaa Ahmed Abdelmonem Elrasad
M.B.B.CH

Under supervision of
Prof. Dr.Saleh Abdo Mohammed Goda
Professor of radioisotopes-nuclear medicine
Faculty of medicine – Cairo University

Assist. Prof. Dr.Shahenda Sabry Salem
Assistant Professor of nuclear medicine
Faculty of medicine – Cairo University

Faculty of medicine
Cairo University
2012

Acknowledgement

First of all I must be grateful for Allah for his limitless help and guidance.

My sincere appreciation is due to my professor Dr.Shahenda Salem, professor of nuclear medicine, Faculty of Medicine, Cairo University, for providing me with her valuable advice and experience.

My special thanks to professor Dr. Saleh Abdo, professor of radioisotopes, nuclear medicine, Faculty of Medicine, Cairo University, for his kind supervision.

I would like also to express my deep gratitude to Dr. Mahasen Amin, lecturer of nuclear medicine, Faculty of Medicine, Cairo University, for her continuous generous care and outstanding support.

To my mother and my father, my profound love and appreciation for all what they have done for me to be what I am

To my husband for his treasured help and efforts to provide me the suitable circumstances I've needed. And to my brother for his continuous encouragement and support.

Also, I would like to thank all my senior staff and colleagues in nuclear department, for their support and encouragement.

Shaimaa Ebrasad

Table of contents

List of figures

List of tables:

List of abbreviations:

-2D: 2 dimensional
-3D: 3 dimensional
-ABVD: Adriamycine-bleomycine-vinblastine-dacarbazine
-**ADPKD:** Autosomal Dominant Polycystic Kidney Disease
-AGA: Anti-granulocyte antibody
-**AIDS:** Acquired immuno deficiency syndrome
-AIP: Autoimmune pancreatitis
-ARA: American Rheumatism Association
-ARA: Arachedonic acid
-**ARDS:** Adult respiratory distress syndrome
-AS: Ankylosing spondylitis
-BGO: Bismuth germinates
-BIP: Bleomycin-induced pneumonitis
-CCP: Cyclic citrullinated peptide
-CGP: Circulating granulocyte pools
-CMV: Cytomegalovirus
-COP: Cryptogenic organizing pneumonia
-CRP: C-reactive protein
-Cs: Cesium
-CT: Computed Tomography
-**CTDs:** Connective tissue diseases
-DJD: Degenerative joint disease
-**DMARDs**: Disease modifying anti rheumatic drugs
-**DMSA**: Dimercaptosuccinic acid
-DTPI: Dual time point imaging
-EPLs: Extra pancreatic lesions
-EPTB: Extra-pulmonary tuberculosis
-ESR: Erythrocyte sedimentation rate
-FBP: Filtered back projection
-**FDG**: Fluoro-2-deoxy-D-glucose
-FOV: Field of view

-**FUO**: Fever of undetermined origin
-Ga: Gallium
-GCA: Giant cell arteritis
-Ge: Germanium
-GIT: Gastrointestinal tract
-GLUT: Glucose transporter
-HDL: Correlated with high density lipoprotein
-HIV: Human immunodeficiency virus
-HL: Hodgkin lymphoma
-HMPAO: Hexamethylpropylene-amine-oxime
-IBD: Inflammatory Bowel Disease
-IgG: Immunoglobulin G
-IIPs: Idiopathic interstitial pneumonias
-IL-2: Interleukin-2
-In: Indium
-IPF: Idiopathic pulmonary fibrosis
-**IVP:** Intravenous pyelography
-**JIA**: Juvenile idiopathic arthritis
-JRA: Juvenile rheumatoid arthritis
-KeV: Kilo-electron volt
-**LOC:** Line of coincidence
-LLD: Lower level discriminator
-LSO: Lutetium oxyorthosilicate
-LVV: Large vessel vasculitis
-LYSO: Lutetium yettrium oxyorthosilicate
-MAI: Mycobacterium avium infection
-MDP: Methylene diphosphonate
-MGP: Marginating granulocyte pools
-MIP: Maximum intensity projection
-MLBP: Mechanical low back pain
-ML-EM: Maximum-likelihood expectation maximization
-**MMP:** Matrix metalloproteinase
-MPM: Malignant pleural mesothelioma
-MRI: Magnetic resonance image

-mRNA: Messenger radionuclide acid
-MTP: Metatarsophalangeal
-MTP: Methylpredensolone
-MTX: Methotrexate
-MVP: Metabolic volumetric product
-NES: Noise equivalent count
-**NHL:** Non- Hodgkin lymphoma
-NSAIDS: Non-steroidal anti-inflammatory drugs
-NSIP: Nonspecific interstitial pneumonia
-OA: Osteoarthritis
-**OS-EM:** Ordered-subsets expectation-maximization
-PC: Pancreatic carcinoma
-PCP: Pneumocystis carinii pneumonia
-PET: Positron emission tomography
-PMR: Polymyalgia rheumatica
-PMT: Photomultiplier tube
-PWV: Pulse wave velocity
-RA: Rheumatoid arthritis
-RF: Rheumatoid factor
-RI-SUV: Retention index-standard uptake value
-SD: Standard deviation
-SF: Scatter fraction
-SI: Spinal infection
-SLE: Systemic lupus erythematosus
-SPECT: Single photon emission tomography
-SST: Selective serotonin
-SSTR: Selective serotonin receptor
-**SUV:** Standard uptake value
-TA: Takayasu arteritis
-TBR: Target to background ratio
-Tc: Technetium
-TNF: Tumor necrotic factor
-TVS: Total vascular score
-ULD: Upper level discriminator

-US: Ultrasonography
-VAP-1: Vascular adhesion protein 1
-**WBCs:** White blood cells

Introduction

Inflammation is part of the non-specific immune response that occurs in reaction to any type of body injury and that the cardinal signs of inflammation can be explained by increased blood flow, elevated cellular metabolism, vasodilatation, release of soluble mediators, extravasation of fluids and cellular influx. In some disorders the inflammatory process, which under normal conditions is self-limiting, becomes continuous and chronic inflammatory disease develops (1).

Inflammation has very specific characteristics, whether acute or chronic, and the innate immune system plays a pivotal role, as it mediates the first response. Infiltration of innate immune system cells, specifically neutrophils and macrophages, characterizes the acute inflammation, while infiltration of T lymphocytes and plasma cells are features of chronic inflammation. Monocytes/macrophages play a central role in both, contributing to the final consequence of chronic inflammation which is represented by the loss of tissue function due to fibrosis develops subsequently (1).

Positron emission tomography is a tomographic scintigraphic technique in which a computer-generated image of local radioactive tracer distribution in tissues is produced through the detection of annihilation photons that are emitted when radionuclides introduced into the body decay and release positrons.

Combined positron emission tomography/computed tomography devices provide both the metabolic information from 18-fluoro-2-deoxy-D-glucose PET and the anatomic information from CT in a single examination. As shown in some clinical scenarios, the information obtained by PET/CT appears to be more accurate in evaluating patients with known or suspected malignancies than does the information obtained from either PET or CT alone or the results obtained from PET and CT separately but interpreted side by side (2).

Timely identification and localization of infectious and inflammatory process are of critical importance in the treatment of patients presenting

with suspicion of infection and inflammation. Whilst other radiological techniques (CT, MRI, US) are used for the localization of infectious foci, they rely merely on anatomical changes. Therefore, there has to be a reasonable elapse of time before the infection is diagnosed. In contrast, scintigraphic detection of infection and inflammation is a non-invasive method of whole-body scanning based on functional tissue changes. Several radiopharmaceuticals are currently employed for the scintigraphic imaging of infection and inflammation (3).

Nuclear medicine plays an important role in the evaluation of infection and inflammation. Fluorine 18 fluorodeoxyglucose (FDG) is a readily available radiotracer that offers rapid, exquisitely sensitive high-resolution tomography. In patients with acquired immunodeficiency syndrome, FDG PET accurately helps localize foci of infection and is particularly useful for differentiating central nervous system lymphoma from toxoplasmosis (3).

FDG PET can also help localize the source of fever of undetermined origin (FUO), thereby guiding additional testing. In the musculoskeletal system, FDG PET accurately helps diagnose spinal osteomyelitis, and in inflammatory conditions such as sarcoidosis and vasculitis, it appears to be useful for defining the extent of disease and monitoring response to treatment. FDG PET may be of limited usefulness in postoperative patients and in patients with a failed joint prosthesis or a tumor. Nevertheless, this relatively new imaging technique promises to be helpful in the diagnosis of infection and inflammation. FDG PET will likely assume increasing importance in assessing FUO, spinal osteomyelitis, vasculitis, and sarcoidosis and may even become the radionuclide imaging procedure of choice in the evaluation of some or all of these pathologic conditions (3).

Aim of work:

1- To review clinical applications & uses of FDG-PET/CT in diagnosis and localization of infectious and inflammatory sites.

2- To view the recent advances in accurate diagnosis of infection and inflammation by FDG-PET/CT in comparison to other diagnostic modalities

Pathology of Inflammation

Introduction:

Inflammation was described as early as 3000 BC in an Egyptian papyrus and is still a common problem despite continuous advancements in prevention and treatment methods. The delineation of the site and extent of inflammation is crucial to the clinical management of infection and for monitoring the response to therapy. This issue is relevant to nuclear medicine since physiologic along with morphologic imaging has an important role in achieving this goal (4).

Inflammation is a complex tissue reaction to injury. Injury may be caused by living microbes, i.e., bacteria, viruses, or fungi, leading to infection, or by injurious chemical, physical, immunological, or radiation agents:

Physical agents:
–Trauma.
–Heat.

Chemical agents:
–Chemotherapy.
–Industrial accidents.

Immunological agents:
-Antigen-antibody reactions.

Radiation:
-Radiotherapy.
-Nontherapeutic radiation exposure.

Inflammation is fundamentally a protective reaction against the cause of cell injury as well as the consequence of such injury. However, inflammation is harmful and may even be life threatening. Inflammation is generally considered a nonspecific response, because it happens in the same way regardless of the stimulus and the number of exposures to the stimulus (4).

Classification of Inflammation:

Inflammation may be classified as acute or chronic.

Acute inflammation:

Is the immediate or early response to injury and is of relatively short duration. It lasts for minutes, hours, or at most a few days.

Chronic inflammation:

On the other hand, is of longer duration and may last from weeks to years. The distinction between acute and chronic inflammation, however, depends not only on the duration of the process but also on other pathological and clinical features.

Pathophysiological Changes of Inflammation

Local Pathophysiological Changes of Inflammation

Acute Inflammation:

Acute inflammation continues only until the threat to the host has been eliminated, which usually takes 8–10 days, although this is variable. Inflammation is generally considered to be chronic when it persists for longer than 2 weeks. Many regional and systemic changes accompany acute inflammation, are mediated by certain chemicals produced endogenously called chemical mediators and are behind the spread of the acute inflammatory response following injury to a small area of tissue into uninjured sites (5).

These chemical mediators include mediators released from cells such as histamine and prostaglandins and others in plasma which are released by the systems contained in the plasma; these are the four enzymatic cascade systems, the complement system, the kinins, the coagulation factors and the fibrinolytic system, which produce several inflammatory mediators (5).

Table 1 summarizes the main chemical mediators of inflammation. Acute inflammation is characterized by the following major regional components.

Chemical mediators of inflammation:

Mediator	Characteristics and role in inflammation
A. Cell factors	
Histamine	Stored in mast cells, basophil and eosinophil leukocytes, and platelets. Release from sites of storage is stimulated by complement components C3a and C5a, and by lysosomal proteins released from neutrophils. Responsible for vasodilatation and the immediate phase of increased vascular permeability
Lysosomal compound	Released from neutrophils and includes cationic proteins, which may increase vascular permeability, and neutral proteases, which may activate complement
Prostaglandins	Long-chain fatty acids derived from arachidonic acid and synthesized by many cell types. Some prostaglandins potentiate the increase in vascular permeability caused by other compounds
Leukotrienes	Synthesized from arachidonic acid, especially in neutrophils, and have vasoactive properties
5-Hydroxytryptamine (serotonin)	A potent vasoconstrictor present in high concentrations in mast cells and platelets
Lymphokines	Released by lymphocytes and may have vasoactive or chemotactic effects
B. Plasma factors	
Products of complement activation:	
C5a	Chemotactic for neutrophils; increases vascular permeability; releases histamine from mast cells.
C3a	Similar to but less active than C5a.
C567	Chemotactic for neutrophils.
C56789	Cytolytic activity.
C4b, 2a, 3b	Facilitates phagocytosis of bacteria by macrophages (opsonization of bacteria)
Kinin system	Bradykinin included in the system is the most important vascular permeability factor, also a mediator for pain which is a major feature of acute inflammation
Coagulation factors	Responsible for the conversion of soluble fibrinogen into fibrin, a major component of the acute inflammatory exudate
Fibrinolytic system	Plasmin included in the fibrinolytic system is responsible for the lysis of fibrin into fibrin degradation products, which have a local effect on vascular permeability

Table1. Chemical mediators of inflammation (5).

Local Vascular Changes

1. Vasodilation following transient vasoconstriction is one of the most important changes that accompany acute inflammation and it persists until the end of the process. It involves first the arterioles and then results in the opening of new capillary beds in the area.

2. Increased vascular permeability due to:

– Contraction of endothelial cells with widening of intercellular gaps

– Direct endothelial injury, resulting in endothelial cell necrosis and detachment

– Leukocyte-mediated endothelial injury: Leukocytes adhere to the endothelium, which becomes activated, thereby releasing toxic oxygen species and proteolytic enzymes and causing endothelial injury.

– Angiogenesis: With inflammation, endothelial cells may proliferate and form new capillaries and venular beds (angiogenesis). These capillary sprouts remain leaky until endothelial cells differentiate.

3. Stasis (slowing of circulation):

Increased permeability with extravasation of fluid into the extravascular spaces results in concentration of red blood cells in the small vessels and increased viscosity of blood, with slowing of circulation in the local vessels. Figures 1 illustrate the main vascular changes.

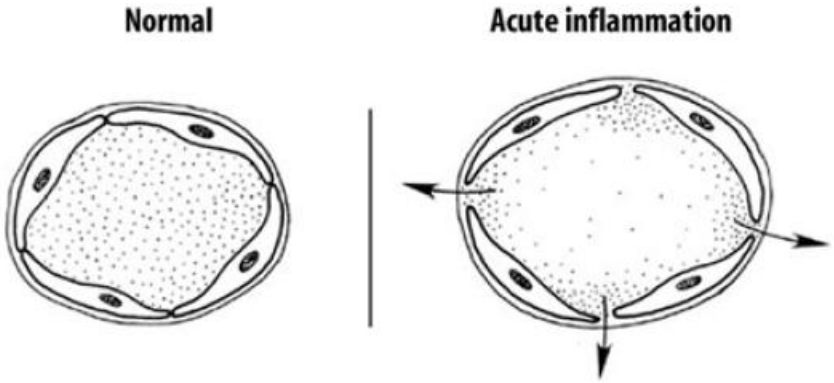

Fig.1. Vasodilation of vessels and opening of the intercellular gaps in inflammation (6).

Local Cellular Events

Granulocyte Physiology:

Mature granulocytes are highly specialized, short-lived, non-dividing cells with a multi-lobulated nucleus, numerous cytoplasmic granules and a diameter of 12–15μm.Thematuration time of granulocytes in hematopoietic bone marrow is about 15 days. The mean residence time in the circulation is about 10h. And survival time in tissues (if they migrate into them) up to about 4 days. The factors controlling granulocyte maturation and their release from, bone marrow are poorly understood (6).

The leukocytosis caused by epinephrine (adrenaline) is largely a result of the release of granulocytes from the marginating granulocyte pool; hydrocortisone and endotoxin, however, probably cause leukocytosis by multiple mechanisms including accelerated release of young granulocytes from bone marrow (6).

In response to an acute infection, as an example of an inflammatory process, the following sequence of events occurs:

1. Margination:

After stasis develops, leukocytes will be peripherally oriented along the vascular endothelium, a process called leukocytic margination (Figure 2).

2. Diapedesis: (emigration)

Leukocytes emigrate from the microcirculation and accumulate at the site of injury.

3. Chemotaxis:

Once outside the blood vessel, the cells migrate at varying rates of speed in interstitial tissue towards a chemotactic stimulus in the inflammatory focus. Through chemoreceptors at multiple locations on their plasma membranes, the cells are able to detect where the highest concentrations of chemotactic factors are and to migrate in their direction (6).

Granulocytes, including the eosinophils, basophils, and some lymphocytes, respond to such stimuli and aggregate at the site of inflammation. The primary chemotactic factors include bacterial products, complement components C5a and C3a, kallikrein and plasminogen activators, products of fibrin degradation, prostaglandins, and fibrin peptides (6).

Histamine is not a chemotactic factor but facilitates the process. Some bacterial toxins, particularly from gram-negative bacteria and streptococcal streptolysins, inhibit neutrophil chemotaxis (6).

4. Phagocytosis:

The polymorph nuclear leukocytes and macrophages ingest debris and foreign particles. Various factors, collectively called opsonins, bind to foreign material including damaged autologous cells (opsonization), thereby identifying them for phagocytosis by granulocytes. The principal opsonins are serum immunoglobulin and activated components of the complement system. The latter include components of the classical pathway, activated by specific antibody binding to the foreign cell surface, and components of the alternative pathway which can be activated in the absence of specific antibody. Both pathways go through C3, which is therefore of crucial importance (5).

Granulocytes express Fc receptors which bind the Fc region of antibody, while the Fab region, the end conferring the antibody's specificity, binds to the foreign cell (the antigen). They also express C3b receptors and, with the Fc receptor. After ingestion a phagocytic vacuole, termed the phagosome, containing the particle is formed (5).

The next stage involves the digestion of the foreign particle by the liberation into the phagosome of a variety of enzymes. Some of these enzymes are also released extra-cellularly and these may contribute to the tissue injury sustained during the inflammatory process (5).

Granulocytes are metabolically stimulated during phagocytosis. The first step in the process is granulocyte priming, during which the cell changes its shape, Priming is important in the context of imaging

because recent evidence suggests that it is the process most closely linked to the uptake of fluorodeoxyglucose (5).

Because primed cells are less deformable, they display a prolonged transit through the pulmonary vasculature and this is the basis for the sustained high lung uptake seen in labeled leukocyte studies in patients with severe systemic inflammation.

The main metabolic consequence of priming is a greatly amplified secretion of hydrogen peroxide and other highly reactive oxygen species (such as the hydroxyl radical and superoxide) in response to appropriate “secretagogues”. This, the “respiratory burst”, results in an increase in oxygen uptake by the granulocyte.

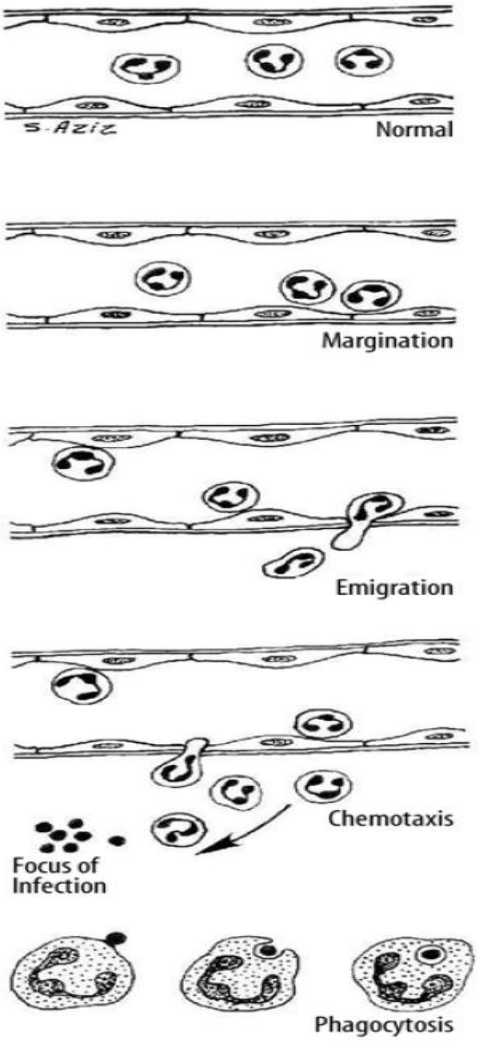

Fig.2. Sequence of cellular changes that accompany inflammation. (6)

Lifespan in the Circulation:

Granulocytes have a mean residence time in blood of about 10 h (corresponding to a half-life of 7 h). Their clearance from blood is essentially exponential, i.e. their removal is random rather than age-dependent. This seems inconsistent with programmed cell death and it may be that granulocyte apoptosis is relevant only to the resolution of inflammation. Since labeled granulocytes are cleared from the blood within 24 h of injection, uptake of activity into an inflammatory focus is essentially complete by this time. It is possible that there is a proportion of granulocytes that is longer lived than 10 h, as suggested by the presence of a slower exponential in radiolabeled granulocyte clearance studies (6).

Granulocyte Kinetics

Granulocyte kinetics can be subdivided into granulocyte distribution, lifespan in blood, and disposal sites.

Distribution:

Granulocytes in blood are in dynamic equilibrium between two pools, the marginating (MGP) and circulating (CGP) granulocyte pools.

This is based on that within about 20 min of intravenous administration, 50% of labeled granulocytes have left the circulation, and that this can be increased up to 80%, by administration of epinephrine (adrenaline) or by strenuous exercise. Granulocyte migration in the form of endothelial rolling is the prelude to migration, is induced by the activation of E-selectin, and is pathological. Most of the MGP is accounted for by granulocyte pooling within organs (7).

Local Sequel of Acute Inflammation

Acute inflammation has several possible local squeal. These include resolution, suppuration (formation of pus), organization and progression to chronic inflammation.

Resolution means complete restoration of tissues to normal. Organization of tissues is their replacement by granulation tissue with formation of large amounts of fibrin, new capillaries growing into fibrin, macrophages migrating into the zone and proliferation of fibroblasts resulting in fibrosis and the consequent organization of exudate.

Chronic Inflammation:

Acute inflammation may progress to a chronic form characterized by reduction of the number of polymorph nuclear leukocytes but proliferation of fibroblasts with collagen production.

Commonly, chronic inflammation may be primary with no preceding acute inflammatory reaction. Chronic inflammation, whether following acute inflammation or not, is characterized by a proliferative (fibroblastic) rather than an exudative response with predominantly mononuclear cell infiltration (macrophages, lymphocytes, and plasma cells). Vascular permeability is also abnormal, but to a lesser extent than in acute inflammation with formation of new capillaries.

Abscess Formation:

Abscess is defined as a collection of pus in tissues, organs, or confined spaces, usually caused by bacterial infection.

The abscess formation starts by a phase of cellulitis, characterized by hyperemia, leukocytosis, and edema, without cellular necrosis or suppuration.

It may be followed by necrosis, liquefaction and formation of pyogenic membrane surrounding the pus, which results in abscess formation that can be present with both acute and chronic inflammation.

Systemic Pathophysiological Changes of Inflammation:

Three major systemic changes are associated with inflammation:

Leukocytosis, fever, and an increase in plasma proteins.

-Leukocytosis is an increased production of leukocytes due to stimulation by several products of inflammation such as complement component C3a and colony-stimulating factors.

-A febrile response is due to the pyrogens.

-The increase in plasma proteins is due to stimulation of the liver by some products of inflammation, leading to increased synthesis of certain proteins referred to as acute-phase reactants which include C-reactive protein, fibrinogen- and haptoglobin and are anti-inflammatory (8).

Inflammation Imaging

Timely identification and localization of infectious and inflammatory processes is a critical step toward appropriate treatment of patients with known or suspected of such disorders. Diagnosis and localization of infection by clinical and laboratory methods is often difficult. The results frequently are nonspecific and imaging is usually needed (9).

Radiologic techniques including computed tomography, magnetic resonance imaging, X-ray, and ultrasonography have been frequently utilized for this purpose. However, these techniques rely solely on structural changes, and therefore discrimination of active infectious and inflammatory processes from alterations following surgery or other intervention remain difficult with these modalities (9).

Also, infectious and inflammatory disorders cannot be detected in the early stages of their development because of the lack of substantial structural derangements, which render anatomic techniques insensitive for early diagnosis. Furthermore, these techniques, based on current standards, provide information on only a limited part of the body. However, because of advance made in recent years, it becomes feasible to scan the entire body within a short period of time (9).

Imaging of infection can be also achieved by either nuclear medicine or other strictly morphological methods. Several nuclear medicine modalities are used to diagnose and localize inflammation and infections. These include ^{111}In-labeled white blood cells, ^{67}Ga citrate, IgG polyclonal antibodies labeled with ^{111}In or ^{99m}Tc, monoclonal antibodies such as anti-granulocyte antibodies, ^{99m}Tc HMPAO-labeled white blood cells, ^{99m}Tc Nano-colloid, ^{99m}Tc DMSA, ^{99m}Tc glucoheptonate, ^{99m}TcMDPmultiphase bone scan, ^{111}In-labeled chemotactic peptide analogs (10).

Conventional nuclear medicine modalities, such as ^{67}Ga imaging and labeled leukocyte studies, have been useful in diagnosing some infectious disease and have contributed significantly to the management of such patients during the past three decades. Non-specific radiolabeled

compounds such as ^{67}Ga-citrate and radiolabeled polyclonal human immunoglobulin accumulate in inflammatory foci due to enhanced vascular permeability. Specific accumulation of radiolabeled compounds in inflammatory lesions results from binding to activated endothelium (e.g., radiolabeled anti-E selectin), the enhanced influx of leukocytes (e.g., radiolabeled autologous leukocytes, anti-granulocyte antibodies or cytokines), the enhanced glucose uptake by activated leukocytes (^{18}F-fluorodeoxyglucose) or direct binding to microorganisms (e.g., radiolabeled ciprofloxacin or antimicrobial peptides). However, these techniques suffer from many shortcomings (10).

Recent developments in the field have substantially improved the ability of the radiotracer imaging techniques to detect infectious disease. These new methods are based on utilizing radiolabeled chemostatic peptides radiolabel liposomes , Avidin-mediated agents radiolabeled antibodies, radiolabeled antibiotics, and positron-emitting compounds, such as [^{18}F] fluorodeoxyglucose (FDG) (11).

Imaging of Soft Tissue Inflammation

No Localizing Signs Present:

When no localizing clinical signs are present, which is common in cancer and immunosuppressed patients, nuclear medicine procedures are often the imaging modalities chosen. The ability to screen the entire body is particularly important for many such cases. The optimal choice of radiotracer again depends on the duration of infection (Fig. 3) (12).

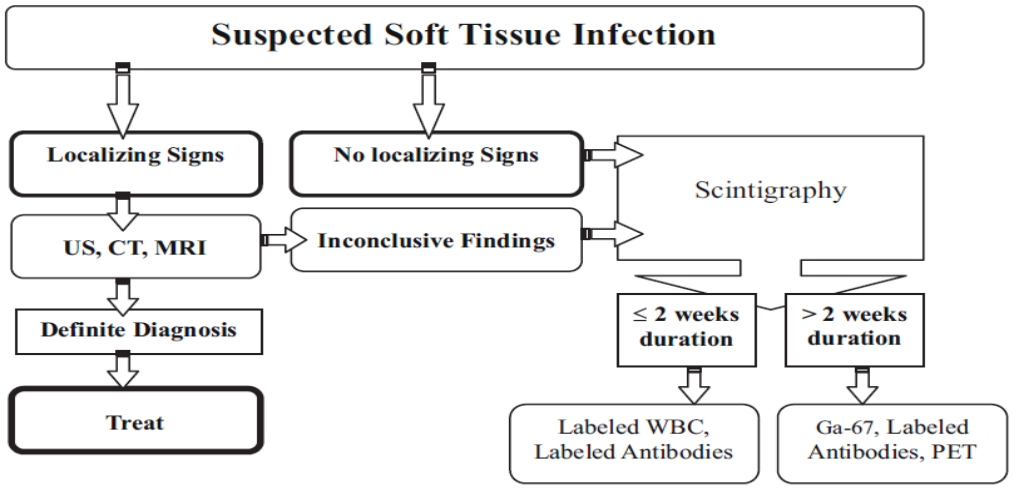

Fig.3. Suggested diagnostic algorithm for soft tissue infections. Note that in case of suspected renal infection, 99mTc DMSA scan is preferred; in infections of relatively long duration, labeled WBC may be used, but if negative, ^{67}Ga or other labeled antibodies should follow before excluding chronic active infection due to possible false-negative results with labeled WBC (12).

Indium-111-labeled white blood cells are the most specific for acute infections, but false-positive results have been reported with some tumors, swallowed infected sputum, GI bleeding, and sterile inflammation. False-negative results have been reported in infections present for more than 2 weeks. More rarely, such false-negative results occur for infections present for only 1 week. Gallium-67 is less specific than labeled WBCs, as it is taken up by many tumors, and by sterile inflammation. Labeled antibodies and peptides have the potential for a specific diagnosis of infection when the localizing signs are present (table 2) (12).

Correlation with morphological modalities after successful radionuclide localization of infection can be of great help. For example, this correlation provides anatomical information prior to surgical interventions. X-rays, CT, MRI, and US usually yield fast results but unfortunately may not distinguish infected from non-infected tissue. Figure3. Illustrates suggested algorithms for the diagnosis of soft tissue infections (12).

Pathological change at the site of infection	Scintigraphic pattern
Hyperemia	Locally increased accumulation of several radiotracers, increased flow and blood pool activity on bone scan; hyperemic pattern on delayed bone images may be present with soft tissue infection
Increased vascular permeability	Increased migration of WBCs, increased accumulation of ^{67}Ga, increased uptake of radiolabeled antibodies
Increased migration of WBCs and chemotaxis	Increased accumulation of labeled WBCs
Increased secretion of iron-containing globulin by injured and stimulated WBCs	Increased accumulation of ^{67}Ga
Localized areas of renal parenchymal damage in pyelonephritis	Areas of reduced or absent DMSA uptake
Dilatation of PC system in pyelonephritis	Prominent pelvocalyceal system on DMSA images
Formation of woven bone	Increased uptake of ^{99m}Tc-MDP with prolonged accumulation of radio-tracer
Increased expression of glucose transporters on cell surface	Increased uptake of ^{18}F-FDG

Table 2. Correlation of pathophysiological features and scintigraphic findings of infection (12).

With Localizing Signs:

This will be discussed in details in the following chapters.

Instrumentation and Principles of Imaging: PET/CT

Positron emission tomography is a noninvasive modality that produces tomographic images of the distribution of a radionuclide-labeled tracer injected in the body. PET imaging is based on radionuclides that decay by positron emission (Figure 4-A) For example, fluorine-^{18} (^{18}F) decays to oxygen-^{18} (^{18}O), emitting a positron (β^+) and a neutrino (V_e) :

$$^{18}F \rightarrow {}^{18}O + \beta^+ + V_e \qquad [1]$$

The positron and an electron then undergo a process known as positron annihilation and are converted into a pair of gamma-ray photons. Because total energy is conserved, each gamma ray has energy of 511 keV, which is equivalent to the mass of the positron and of the electron according to the well-known relationship $E = mc^2$. Because total momentum is conserved, the two gamma rays travel in opposite directions with a relative angle very close to 180 degrees (13).

Thus, if a coincident pair of 511 keV gamma rays is detected, the line of coincidence connecting the two detected coordinates passes near the point in space where the annihilation event occurred and also where the positron decay occurred. When many such event pairs are detected, the activity distribution of the positron-emitting radionuclide within the volume of interest may be reconstructed. This process is the basis of PET imaging (13).

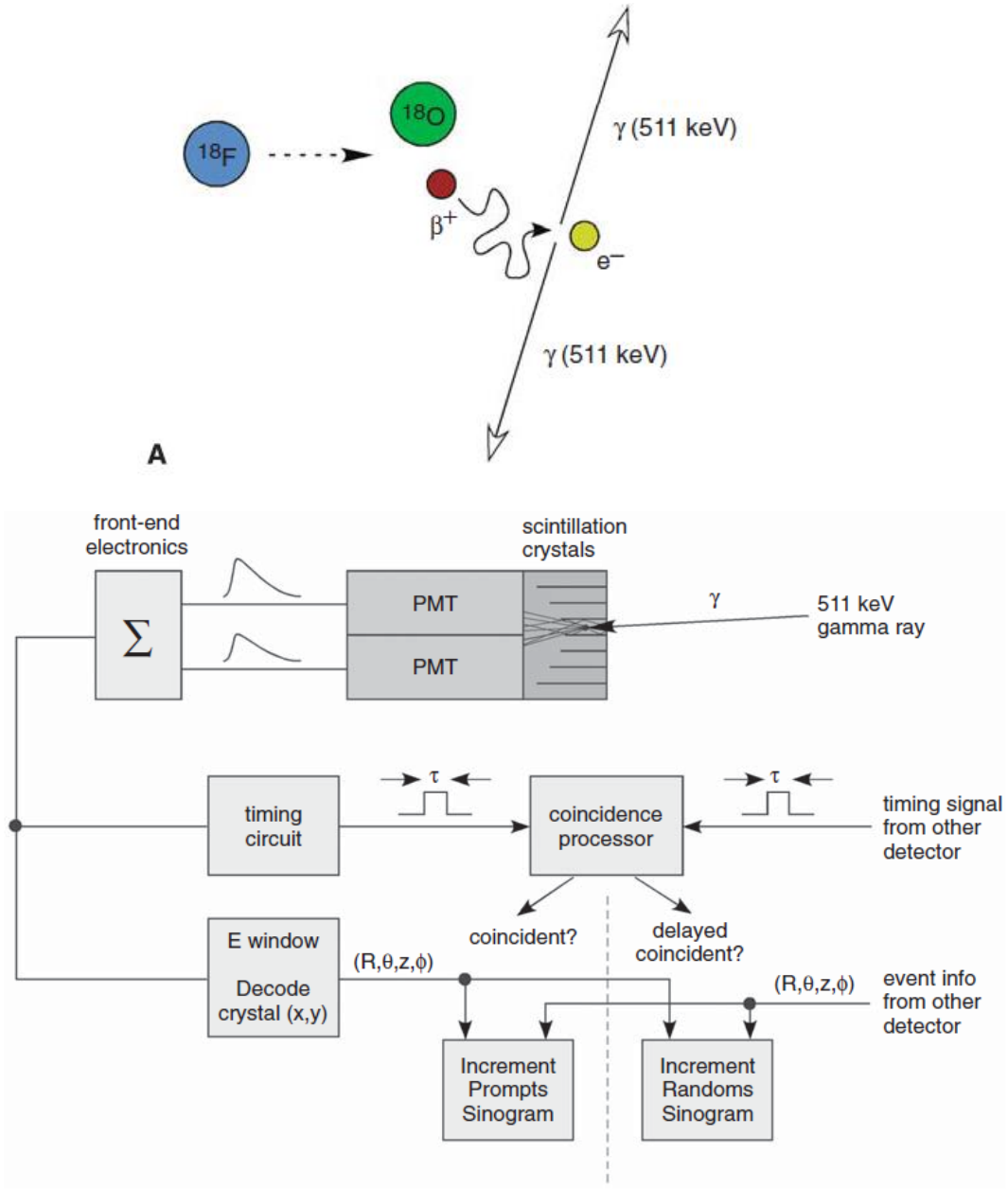

FIG. 4. Overview of PET event detection. (A) Annihilation radiation (pair of 511 keV gamma rays) results from the interaction of an electron and positron emitted by a PET radionuclide (^{18}F in this example, which decays to 18O). The positron rapidly slows down due to numerous collisions with electrons along its path, traveling only a short distance prior to annihilation. (B) Schematic of a PET scintillation detector and associated event processing (in conjunction with a coincident event recorded in an opposing detector) (13).

PET Detectors:

Detectors used in PET scanners are designed for optimal detection of 511 keV coincident gamma rays under clinical imaging conditions. A schematic of a typical PET scintillation detector is shown in Figure 4-B; it consists of several elements. First, the incident gamma ray is absorbed in a scintillation crystal and produces energetic electrons، which in turn produce a cascade of visible photons. This flash of visible light exits the crystal and is shaped by a light guide before reaching an array (often a 2×2block) of photomultiplier tubes (PMTs) (13).

The PMTs convert the flash of light into electronic pulse signals that are processed by front-end amplifiers and other electronics. The integrated signal from the group of PMTs is measured and is proportional to the total energy deposited in the crystal. The scintillation event is rejected if the detected energy is outside the allowed range for 511 keV gamma rays, set by the lower level discriminator (LLD) and upper-level discriminator (ULD) values (approximately 400 keV and 650 keV, respectively). By restricting the acceptable energy range، the number of scattered events (those interacting within the body before being detected) is minimized because the scattered gamma rays have energies lower than 511keV. In addition, a position-weighted signal is processed in order to determine the crystal of interaction, which specifies the detected location of the event (14).

The spatial resolution of the detector is limited largely by the physical size of the individual scintillation crystals. After being processed by the front-end electronics, the electronic signals associated with the scintillation events are then processed by coincidence electronics (13).

The coincidence electronics sample all detectors and accurately determine the time of each detected event, within time resolution τ. The timing pulses from all electronics banks then are compared. If two time pulses overlap, the two associated events are considered to be simultaneous and are designated as a coincidence pair. The definition of simultaneity is limited by the coincidence timing window 2τ, which is in the range of 4 to 16 ns on clinical PET scanners (13).

The coincidence timing window is set to be as small as possible so that nearly all true coincidence events are detected and as many “random”

coincidence events as possible are rejected. Random coincidences arise when two 511 keV gamma rays originating from different positron decay events are detected by chance within the coincidence timing window. For a pair of detectors having “singles” count rates of S1 and S2 for individual 511keV gamma rays, the random coincidence rate R for the pair of detectors depends linearly on the coincidence timing window and is given by:

$$R = 2\tau S_1 S_2 \qquad [2]$$

The random coincidence rate is proportional to the square of the source activity whereas the true coincidence rate is linear with respect to the source activity.Thus, the relative contribution of random coincidences rises for increasing injected dose. Both random and scatter events lead to erroneous back projection (Figure 5) and should be minimized through appropriate detector design and configuration.

An important consideration in PET detector design is the scintillation crystal material، whose characteristics directly affect PET imaging performance. The crystal’s mass density, elemental composition, and thickness together determine its ability to fully absorb 511 keV gamma rays. Since a pair of gamma rays must be detected to produce a coincident event, the PET coincidence sensitivity depends on the square of the detector sensitivity, and thus the crystal’s “stopping power” (attenuation coefficient at 511 keV) is a significant property. The scintillation light output of the crystal affects the accuracy in determining the gamma-ray energy and crystal of interaction and thereby affects the scatter rejection and intrinsic spatial resolution. In addition, the scintillation decay time of the crystal specifies the duration of the light pulse, which impacts both the dead time and timing resolution per event. A crystal with a shorter scintillation decay time is able to sustain higher count rates without saturating the detector and allows for improved rejection of random events through a more precise coincidence window. Thus, scintillation crystals with high attenuation coefficient at 511 keV, high light output, and short decay time are most appropriate for PET detectors. Modern commercial PET scanners utilize crystals of bismuth germinate (BGO), lutetium oxyorthosilicate (LSO), or gadolinium oxyorthosilicate(GSO) and more rescently lutetium yettrium oxyorthosilicate (LYSO) (15).

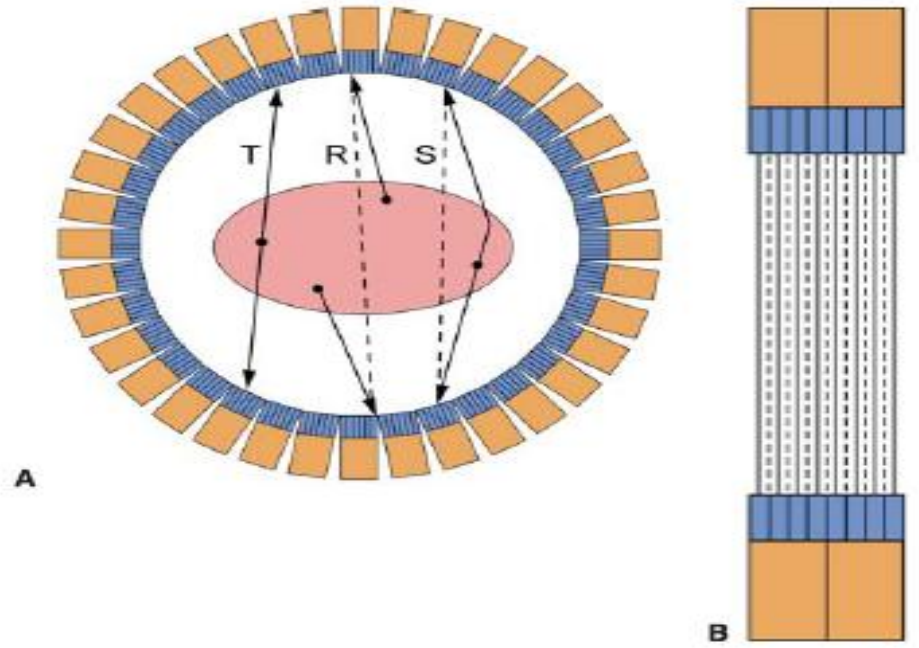

FIGURE 5. Detector configuration in PET scanners. (A) Front view showing a circular arrangement of block detectors around a patient cross section. Examples of true (T), random (R), and scatter (S) coincidence events are shown. For true events, the line of coincidence connecting the two points of detection passes near the point where the positron decay occurred. The random and scatter events result in erroneous lines of coincidence (dashed lines) and contribute to background counts. (B) Side view cross section (expanded view) illustrating the individual *N* rings and the (2*N*–1) slices defined by the ring geometry. Solid lines denote central slices; dashed lines denote in-between slices (15).

PET Scanner Design:

Modern PET scanners consist of a large number of crystals (4000 to 24,000) in a cylindrical arrangement of discrete rings (Figure 5), with typical ring diameter of 85 cm and axial field of view of 16 cm.

The N crystal rings define a total of 2N–1 slices (at the ring centers and at the midpoints between the rings). The detector geometries of PET scanners vary: Some designs use compact block detector modules and others use fewer but larger flat-panel detector components. Most PET scanners are of full ring design; however, some models employ partial rings of detectors with a rapidly rotating gantry in order to reduce cost, at the expense of reduced count sensitivity.The physical size of each crystal

is typically 4 to 8 mm in cross section and 20 to 30 mm in thickness. The crystal arrays are backed by PMTs and front-end electronics, which connect to the remaining coincidence electronics within the temperature-stabilized gantry (15).

Because imaging is based on electronic collimation, the spatial resolution of the PET scanner is limited mainly by the intrinsic spatial resolution of the detectors. Since an event location is resolved to a specific crystal, the spatial resolution is approximately that of the cross-sectional size of the crystal (4 to 8 mm). While this is true near the center of the trans-axial field of view, the spatial resolution does worsen slightly with increasing radius due to the unknown depth of interaction of the events within the thick crystals, typically increasing by 1 mm at a radius of 10 cm and by more at larger radii (15).

Many PET scanners employ axial septa to restrict the axial angle of incidence to a smaller range (Figure 6). The septa are tungsten or lead annuli located along the ring boundaries of the crystal array. The septa absorb most axially oblique gamma rays and provide some degree of collimation in the axial direction only. However, the septa are not true collimators in that electronic collimation still specifies the axial and trans-axial angles of the coincident event pairs. In several scanner models, the septa can be in the extended position (for two-dimensional (2D)-imaging mode) or in the retracted position (for 3D-imaging mode).7 other scanner models operate exclusively either with fixed septa in 2D mode or without septa in 3D mode, with the latter situation being common for newer PET/CT scanners (15).

There are advantages and disadvantages associated with PET imaging in 2D with septa as opposed to imaging in 3D without septa. Imaging with septa means that simpler 2D image reconstruction algorithms may be used since most axially oblique events are not recorded. This is done at the expense of greatly reduced count sensitivity، however. In 3D mode, a typical fourfold increase in count sensitivity is attained by recording the axially oblique events, allowing for shorter imaging times with reduced injected dose. An unwanted side effect of imaging in 3D mode is that many random and scatter coincident events arising from outside the axial field of view, which would have been absorbed by the septa, instead are detected and recorded (Figure 4, 6) Thus, use of axial septa may be

warranted in imaging situations where the high background event rate would impact image quality or quantitative accuracy (15).

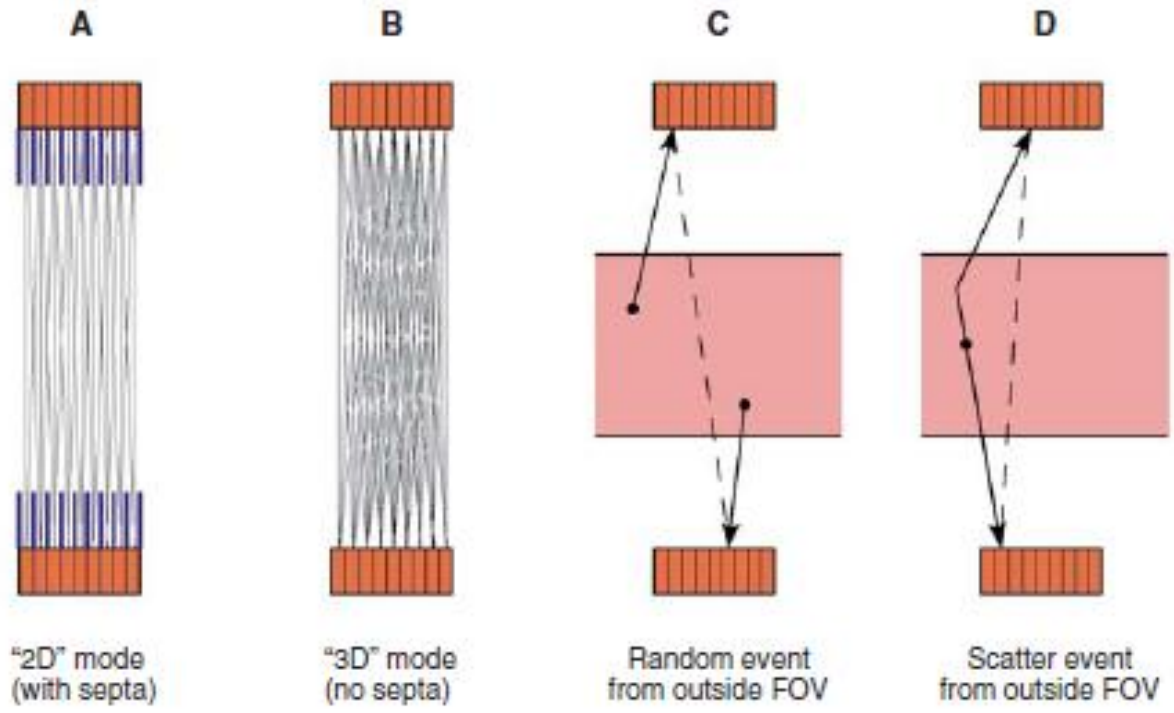

FIGURE 6. Imaging with and without axial septa. In 2D mode (A), the septa prevent most ol events from being detected, and only coincidence events within the same ring or between a rings are recorded. In 3D mode (B), the septa are removed and a much larger number of lin coincidence are detected, greatly increasing the sensitivity of the scanner. However, the rer septa in 3D mode allows random events (C) and scatter events (D) arising from activity outs axial field of view (FOV) also to be recorded, thereby increasing background counts (15).

Image quality is often characterized by noise equivalent counts (NECs) acquired. NEC is defined as:

$$NEC = \frac{T^2}{(T+S+kR)} \qquad [3]$$

Where *T*, *S*, and *R* represent true counts, scatter counts, and random counts, respectively. The factor *k* depends on the method of random correction applied and is equal to 2 for the most common case (using the delayed coincidence method and with the object being imaged occupying most of the scanner field of view).

As can be seen in this equation for NEC, true counts add beneficially to image quality, whereas random and scatter counts detract from image

quality. An important characteristic of PET scanner design is the count-rate capacity of the detectors. At low activity levels, the true coincidence rate is proportional to the activity. However, each event requires a processing time that depends on the crystal's scintillation decay time and the design of the front-end electronics. At higher event rates, an increasing fraction of events overlap in time to produce erroneous effects known as pulse pileup.

Detector saturation from pulse pileup contributes to dead-time loss, thereby reducing the total counts recorded. As a result, the count rate depends nonlinearly on activity as the degree of pulse pileup increases, eventually reaching a point above which the count rate begins to decrease. Optimal imaging generally is attained when the injected dose is such that the scanner operates on the upward slope and near the peak of the NEC curve.

NEC and imaging time are affected by many factors such as injected dose, body habitus, and activity outside the region of interest, whether septa are used, and detector dead-time characteristics. Therefore, optimal scan protocols can vary substantially among patients, studies, and scanners. Performance tests using standard phantoms are performed to assess differences in scanner characteristics (15).

Data Corrections:

In addition to excellent image quality, a goal of PET imaging is to achieve a high degree of quantitative accuracy. This goal is particularly important in cardiac imaging since relative or absolute perfusion or viability, or both, are being assessed in all regions of the myocardium. PET imaging achieves quantitative accuracy through applying corrections for many factors: detector normalization, dead-time loss, random events, body attenuation, and scatter events. Figure 7 shows a schematic of PET data processing and illustrates the steps where these corrections are implemented (15).

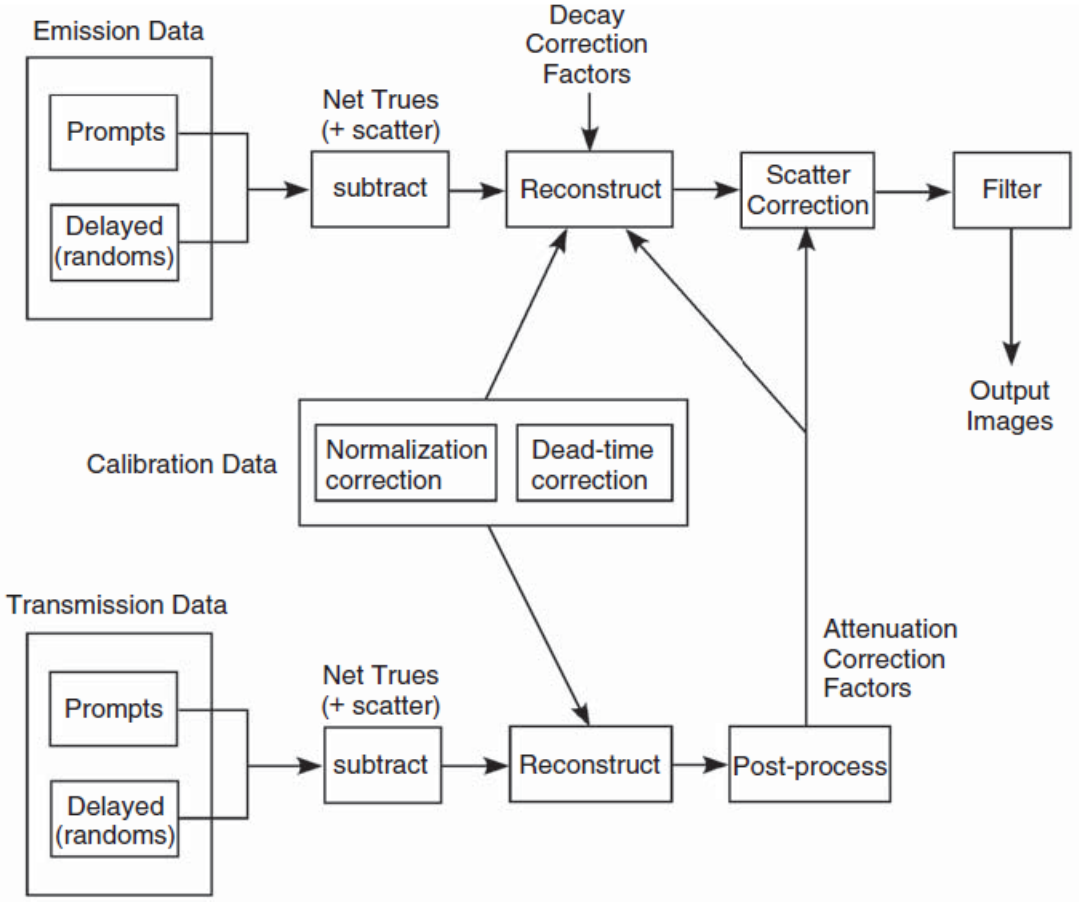

FIGURE 7. Flowchart of PET data processing and image reconstruction (15).

Detector Corrections

Detector normalization and dead-time loss corrections are based on scanner-specific calibrations done prior to imaging. Normalization data reflect the relative sensitivity of each scintillation crystal element in the scanner, which can differ substantially among crystal elements. A normalization calibration scan using a uniform source of known activity is performed at regular intervals and after tuning or servicing the detectors (15).

On a daily basis, a quality assurance scan is performed and checked against the previous system normalization data to ensure that significant drift in the detector electronics has not occurred. Detector dead-time loss is the fraction of counts lost to pulse pileup and is reflected in the count-rate characteristics of the scanner. The dead-time loss of a detector block commonly is estimated as a function of the measured singles event rate, based on prior calibration tests of the detector count rate curve. To

achieve quantitative accuracy, the raw data must be rescaled by the appropriate normalization and dead-time loss correction factors. Applying the normalization factors ensures uniform detector sensitivity and allows the reconstructed images to be expressed in terms of activity concentration or in terms of standardized uptake values (SUV), if data are normalized to injected dose and body weight or lean body mass. Applying the dead-time loss factors ensures a linear relationship between the actual count rate and the absolute activity in the field of view. These corrections serve to accurately reflect the true flux of gamma rays impinging on the crystal elements and are necessary for quantitative image reconstruction (16).

Random Correction:

PET scanners record all “prompt” coincident events that occur simultaneously within the timing resolution of the detector electronics. The prompt events (*P*) consist of true

(*T*), random (*R*), and scatter (*S*) coincident events:

P= T + R + S [4]

Since the recorded prompt events contain background events (random and scatter), they do not represent the true activity distribution. Corrections for the background events must be applied to ensure the quantitative accuracy of reconstructed images (16).

Correction for random events often is achieved by direct measurement using the delayed coincidence technique, which is based on the principle that events occurring at time intervals much longer than the detector response time are uncorrelated. A separate coincidence processor is configured to detect pairs of events occurring at a relatively large time difference compared to the event processing time.

Unlike event pairs recorded by the prompt coincidence processor, those recorded by the delayed coincidence processor are due solely to random coincidences. For each line of coincidence (LOC), the number of delayed events (D) is subtracted from the number of prompt events, thus canceling the random events (on average):

$$(P - D)_{avg} = (T + S)_{avg} \qquad [5]$$

It is important to note that this does not exactly cancel out the random events on a specific LOC because of count fluctuations (Poisson noise). During image reconstruction, there is an averaging effect over many LOCs, and the delayed subtraction method for random correction becomes quantitatively accurate in the resultant image. However, the direct subtraction of delayed coincidence counts increases the relative noise level in the images because the count fluctuations in the prompt and delayed data are additive. The noise introduced by this method can be mitigated by filtering the delayed coincidence data prior to subtraction (16).

Attenuation Correction:

A positron decay event is detected only if both 511 keV gamma rays reach the detectors and are fully absorbed by the scintillation crystals. If either of the gamma rays is scattered or absorbed by the body, then a true coincidence event is not recorded. Such count losses from body attenuation depend on the body habitus and can be surprisingly large. For example, if the total path length of the LOC through the body is 20 cm and assuming uniform attenuation equal to that of water, only 15% of 511 keV gamma-ray pairs along this LOC escape the body without absorption or scatter. If the total path length is 40 cm (as in many heavier patients), the fraction of non-attenuated gamma-ray pairs is only 2%. Because of body attenuation, regions near the edge of the body would appear much more intense in images, since the average degree of attenuation over all LOCs there is less than in the central regions of the body (16).

Fortunately, the body attenuation can be measured and corrected in a straightforward fashion. An interesting property of PET imaging is that the fraction of attenuated events along a specific LOC is constant, no matter where along this line the positron decay occurred (even from within a source placed outside the body). An external gamma-ray source produces a transmission shadow profile of the body, and by measuring the position-dependent transmission data, the attenuation factors along each LOC are measured. By rotating the transmission source around the body, tomographic attenuation data are acquired. By weighting the PET

emission data according to the attenuation data during image reconstruction, the resultant images then are corrected for attenuation (16).

Transmission sources are present in virtually all dedicated PET scanners. Many models use germanium-^{68} (^{68}Ge) rod sources that emit 511 keV gamma-ray pairs from positron decay of gallium-^{68} (^{68}Ga, the daughter radionuclide of ^{68}Ge). The transmission data are distinguished from the emission data by knowledge of the rod source location. Other PET scanners use cesium-^{137} (^{137}Cs) point sources instead, which emit (non-coincident) 662 keV gamma rays (17).

During the transmission scan, the detectors operate in singles mode instead of coincidence mode, and the higher-energy ^{137}Cs transmission gamma rays are distinguished from the 511 keV annihilation gamma rays by energy windowing. New hybrid PET/CT scanners often do not have radionuclide transmission sources and instead use the x-ray CT scanner to generate transmission data. Count statistics in transmission scans must be considered, since noise in the transmission data propagates through image reconstruction and may affect the resultant image quality. Sufficient transmission counts must be acquired to produce an attenuation map of sufficient quality, and the transmission acquisition time should account for patient body habitus and for transmission source activity as the sources decay. Depending on scanner design, the transmission acquisition time may range from 1 to 15 minutes. To further reduce noise, segmentation image processing is often performed (16).

The segmentation algorithm first distinguishes regions in the attenuation map as body tissue, lung tissue, air, or the patient table. The algorithm then assigns adjusted values to these regions based on the corresponding known or typical attenuation coefficients and produces a new and less noisy attenuation map (16).

Scatter Correction:

After the delayed coincidences are subtracted, the resultant data contain both true and scatter events. Thus scatter correction is needed for quantitative imaging, and several methods and algorithms for scatter correction have been proposed and implemented. A common implementation is to model the contribution of scattered counts based on

the theory underlying Compton scatter of gamma rays. Using the transmission attenuation map and an initial estimate of the reconstructed emission images, the corresponding scatter distribution is computed (17).

Certain approximations are made in the scatter model algorithm to accelerate computation for practical clinical use. The distribution of background counts outside the body is useful for normalizing the computed distribution with respect to the actual emission data. After subtracting the scatter contribution, the data are reconstructed once again to yield the scatter-corrected images (17).

The accuracy of scatter correction of course depends on the specific algorithm used and its ability to accurately model the actual scatter processes in the body. Usually better results are obtained with increasing sophistication of the scatter model in the algorithm. The absolute accuracy also depends on the scatter fraction (SF), that is, the relative contribution of scatter in the reconstructed image:

$$\mathrm{SF} = \frac{S}{T+S} \qquad [6]$$

A high scatter fraction has the effect of amplifying errors from scatter correction, because a larger fraction of the data must be subtracted. The scatter fraction of a particular data set depends on several factors, including the energy window (LLD and ULD values, which are set according to the energy resolution of the detectors at 511 keV), the region of the body scanned, and body habitus. In many cases, a major factor is whether axial septa are used and also the degree of side shielding of the detectors, since the septa and shielding are very effective in blocking axially oblique scatter events. For example, a standard 20 cm cylindrical phantom may exhibit a scatter fraction of 20% in 2D mode and 45% in 3D mode, and the scatter fraction in patients may be considerably higher.

Furthermore, scatter in 3D mode is significantly more complex and more difficult to model because of cross-plane events and events arising from outside the axial field of view. In situations in which a high degree of quantitative accuracy is required, imaging may be better performed in 2D mode, for which scatter correction generally is more accurate.

Data Processing and Image Reconstruction:

Sinogram Representations:

As the PET coincidence events are acquired, they are binned into data arrays according to their detected coordinates in space. First, consider the simpler 2D case of a single slice and imaging with axial septa, in which a slice is defined by events occurring within the same crystal ring or adjacent crystal rings. Each line of coincidence connecting two crystal elements within the slice is described in terms of coordinates (R, θ), which are the distance from the center and the trans axial angle. The histogram of all events binned in (R, θ) space is called a *sonogram*. Since the raw data from each slice produces a sinogram, a multi-ring PET scanner with axial septa produces a stack of 2D sinograms indexed by the slice axial coordinate z. Each sinogram is reconstructed separately, resulting in a stack of 2D tomographic images that may be displayed as a volume image. (Although the end result is a 3D volume, this mode of acquisition and reconstruction is commonly referred to as "2D imaging," since each slice is independently acquired and reconstructed.) For a multi-ring PET scanner operating without axial septa, coincident events arising from detected gamma rays on nonadjacent crystal rings also are recorded. In addition to the sinogram and slice coordinates (R, θ, z), the axial angle ϕ (or alternatively the ring difference) is another coordinate that must be specified, thus adding a fourth dimension to the complete description of the sinogram data (18).

As discussed earlier, the benefit of including multi-ring events is that the sensitivity of the PET scanner is greatly increased; however, the requirements for data storage and the complexity of image reconstruction also are increased (18).

Techniques for "fully 3D reconstruction" have been well researched, but many algorithms are too computationally intensive for routine clinical imaging. Instead, repining methods often are used to transform the complete four dimensional sinogram representations into an approximate stack of 2D sinograms. The commonly used Fourier repining algorithm has been shown to preserve the fully 3D nature of the data over a wide range of axial angles. After repining is performed, each slice may be reconstructed independently, allowing for the use of 2D image

reconstruction algorithms that are computationally much faster and more practical than fully 3D reconstruction algorithms (18).

Reconstruction:

The typical steps involved with image reconstruction and processing are summarized in (Figure 7.) Sinogram data for the emission and transmission scans are acquired separately. Random correction is applied by subtracting delayed coincidence data from the prompt coincidence data. Calibration data from a prior normalization scan and dead-time loss factors are applied, as well as a decay correction factor based on the radionuclide half-life of the injected tracer. The transmission data are reconstructed first to produce attenuation correction factors, which are then applied during subsequent reconstruction of the emission data. Scatter correction is applied using both the emission and transmission images to compute and subtract the estimated scatter component. Afterward, a smoothing filter is applied to reduce high-frequency noise and produce optimal image quality. Image reconstruction often is done using the conventional filtered back projection (FBP) algorithm, in which an apodizing filter is applied in the frequency domain to the sinogram data, followed by back projection into image space (19).

Since the FBP algorithm involves a single back projection step, it is exact and requires little computational time. However, in situations with low count density or with wide variations in activity concentration, FBP is prone to artifacts and may not produce the best-quality images. Iterative reconstruction algorithms differ from FBP in that multiple projection and Back projection steps are performed with the goal of converging toward an optimal image estimate. A common iterative algorithm is the maximum-likelihood expectation maximization (ML-EM) method, in which an image estimate first is projected and compared to the actual sinogram data, and appropriate scaling factors are computed and back projected to produce a new and more accurate image estimate. The process is repeated for a number of iterations until a final image estimate is obtained (20).

However, image noise is amplified with increasing number of iterations, and thus stopping criteria, regularization methods, or post filtering, or some combination of the three, is implemented to prevent excessive

noise in the final image. ML-EM assumes a Poisson statistical model and performs relatively well for low-count sinogram data. Since there are multiple projection and back projection steps, the algorithm is more local in nature compared to FBP and is less prone to streaking and spillover artifacts (19).

To accelerate the convergence of iterative reconstruction and to reduce computation time, the ordered-subsets expectation-maximization (OS-EM) algorithm (a modified version of ML-EM) uses ordered subsets of sinograms, such that only a fraction of the data must be processed before updating the image estimate per iteration. In recent years, OS-EM iterative reconstruction has become computationally practical in clinical settings and has become the most common reconstruction algorithm used in PET oncology studies (21).

For dynamic PET imaging using kinetic modeling to estimate absolute perfusion values, FBP is usually considered to be the better choice because of its exact nature, even though image quality often is poorer than with OS-EM. In summary, careful selection of algorithm and associated parameters should be made based on the scanner characteristics and the imaging protocol used.

PET/CT Radiopharmaceuticals in Inflammation and Infection

PET imaging differs from conventional SPECT imaging in that short - lived positron-emitting radionuclides are used as radiolabels. This has several important implications:

-First, because of the physics of positron decay, coincidence circuitry can be used, which facilitate acquisition of high resolution images with accurate attenuation correction.

-Additionally, most of the elements used as positron emitting labels are attached via covalent bonds and are commonly founding several biochemical and drug structures. This leads to much greater versatility in the development of noval PET radiopharmaceuticals (22).

For PET imaging of inflammation several radiotracers can be used such as 68Gallium (^{68}Ga) which is produced by ^{68}Ga/^{68}Ge generator and 68Gallium-labelled vascular adhesion protein-1 (VAP-1) which is an adhesion molecule that plays a key role in recruiting leucocytes into sites of inflammation but disadvantaged by its short metabolic half-life and rapid clearance. It is hypothesized that prolonging the metabolic half-life of ^{68}Ga-DOTAVAP-P1 could further improve its imaging characteristics (23).

Somatostatin tracers can be used in case of intestinal inflammation Gonkowski and Całka (24) have demonstrated a modulation of SST immuno-reactivity in the nervous structures of the porcine descending colon under experimental pathological conditions. In situations of intestinal inflammation, one can find changes in the concentration of SST as well as of SSTR (25).

But most commonly used radiotracer is FDG.

FDG synthesis:

^{18}F-FDG can be produced as a multi dose batch suitable for use throughout the workday or for distribution to imaging sites remote from

the production location. Tetraacetylmannose triflate is reacted with the fluoride ion and the acetyl protection groups are removed by basic hydrolysis. By starting with mannose, the desired optical isomer, D-glucose, is produced (23).

Mechanism of FDG uptake:

Inflammatory cells have increased glucose utilization due to over expression of membrane glucose transporters and up regulation of hexokinase activity. FDG, like glucose, is taken up by inflammatory cells via glucose transporters (GLUT) and undergoes phosphorylation (by hexokinase) within the cell to form FDG-6-phosphate; however, unlike glucose, it does not undergo further metabolism, thereby becomes trapped in metabolically active cells, accumulating in most tissues at a rate proportional to glycolysis Most tissues and tumors, apart from the liver, have relatively low level of glucose-6-phosphatase activity and therefore little ^{18}F-FDG-6-phosphate escapes the cell (26).

Technical Aspects of PET/CT Examination

Patient preparation:

A key to a successful ^{18}F-FDG PET/CT oncologic examination is adequate patient preparation. Several instructions should be followed strictly to achieve acceptable blood glucose level, minimize physiologic FDG uptake and reduce artifacts. The main goal is to achieve a good quality images and minimize false positive results (27).

Achieving acceptable blood glucose levels

Blood glucose level should be ≤ 150mg/dL. High glucose levels will compete with FDG uptake, degrading image quality, thus patients are required to fast for 4-6 hours to minimize insulin secretion in order to reduce background uptake of FDG by muscle and adipose tissue. So ^{18}F-FDG. PET/CT examination should not be performed if Blood glucose is >200mg/dL. Diabetic patients require special attention and are usually rescheduled if the blood glucose level is greater than 8-11mmol/l as giving insulin immediately before the examination is to be avoided as this encourages uptake of FDG into background tissues rather than tumor (3).

Physiologic uptake:

For skeletal muscle uptake: In the intervening period between injection and imaging, patients are requested to be still in order to minimize muscular activity, which may otherwise be a source of artifact uptake (28).

For myocardial muscle uptake: Minimizing myocardial activity is of particular importance while evaluating mediastinal or pericardial nodules. It can be done by fasting for at least 4-6 hours prior to the exam and maintaining a low carbohydrate/high protein and fat diet a day before the exam. Caffeine, nicotine and alcohol should also be avoided for 24 hours before the exam; however the caffeine effect on

myocardial uptake is variable. It may decrease myocardial activity by stimulating myocardial fatty acid metabolism (29).

For brown fat uptake: It can be reduced by decreasing the sympathetic drive and keeping the patient warm. Decreasing the sympathetic activity can be achieved by using anti adrenergic drugs such as diazepam. Drugs which stimulate the sympathetic activity (e.g. nicotine and ephedrine) should also be avoided (26).

Patient Positioning

For PET/CT it is preferable to scan the patient with the arms above the head if tolerated to avoid beam hardening artifacts which will degrade images of the upper abdomen. The exception is separate head and neck scans where the arms should be down (29).

Controlling Respiration

CT scans are acquired within a short period of time during continuous table movement, typically covering of a large axial scan range in a single breath-hold. PET scans are performed step-wise with sequential bed positions, each of them typically covering an axial FOV of approximately 15 cm. The examination time per bed position may vary from 1 to 5 min, depending on the amount of tracer applied and on the image quality desired. Thus, examination time may range between 10 and 30 min to cover a field of view from the head to the upper thighs. This necessitates the PET scan to be performed in shallow breathing (27).

Recently, respiratory gating is introduced in modern PET/CT scanners to allow a free breathing examination (Four - dimensional PET/CT) and hence, avoiding misregistration artifacts (30).

Image acquisition

A PET/CT imaging protocol usually calls for acquisition of a CT scout scan first, followed by a CT scan and a PET scan. The CT scout scan serves as an anatomic reference for the PET/CT scan. The technologist uses the scout scan to define the starting and

ending locations of the actual CT and PET acquisitions. Upon completion of the CT scan, the bed is automatically moved to position the patient in the field of view of the PET scanner. The patient is positioned so that the PET scan matches the same anatomic extent imaged during the CT acquisition. PET emission data are then acquired for 3–5 minutes per bed position covering the area of interest. The PET raw data are then reconstructed using the CT images for attenuation correction. CT scans are usually reconstructed in a 512 x 512 image matrix, whereas PET images are reconstructed in a matrix of 128 x 128. Upon reconstruction, both the PET images and the CT images are displayed side by side and overlaid (fused) in axial, lateral and sagittal frames together with maximum intensity projection (MIP). This process can be done either on the same acquisition computer or on different workstation, depending on the manufacturer (31) .

Clinical Introduction for Role of PET in Inflammation

^{18}F-Fluoro-D-deoxyglucose (FDG) positron emission tomography (PET) has developed into an accepted tool in clinical imaging. The ability to image glucose metabolism has proved to be the key to the current success of PET in different fields of medicine (32).

FDG is currently the most commonly used PET tracer. Increased glucose metabolism is often present in inflammation (33).

FDG PET is reported to be a sensitive and not specific technique in oncological imaging (32). In the early years of clinical FDG PET imaging in oncology, cases of false-positive uptake in a wide variety of infections were described. What at first seemed as a disadvantage which has been exploited in a positive manner over the last years, resulting in a number of promising reports on the potential of FDG PET imaging in different types of infection and inflammation (34).

In an experimental rat model of turpentine-induced inflammation, Yamada et al. have shown that FDG uptake is high in inflammatory tissue and that uptake is higher in chronic than in acute inflammation (36).

In another rat model of Escherichia coli infection, it has been demonstrated that FDG uptake is higher than that of other radiotracers such as 67-gallium, radiolabelled thymidine, methionine and human serum albumin. Moreover, high target-to-background ratios are reached within the first hour after FDG injection, allowing for early imaging. It was shown auto radio-graphically that FDG uptake is highest in the area of inflammatory cell infiltration surrounding the necrotic region, especially in those regions with the highest number of macrophages and polymorphonuclear leukocytes (37).

In addition, studies are demonstrating the value of FDG-PET for the evaluation of non-oncologic conditions. Based on the literature, conditions such as osteomyelitis, fever of unknown origin (FUO),

acquired immunodeficiency syndrome (AIDS), vasculitis, and inflammatory bowel disease can be successfully imaged with FDG-PET. With the approval of additional PET radiotracers in the future, there will be more widespread applications of PET for inflammatory and infectious disorders (37).

Unlike anatomic imaging modalities such as computed tomography (CT), magnetic resonance imaging (MRI), and ultrasound, PET is a molecular imaging modality that detects metabolic abnormalities present in the disease before structural abnormalities become evident. Advantages of FDG-PET as compared with the conventional nuclear medicine radiopharmaceuticals for the imaging of inflammation and infection include the ability to provide a result as early as 11/2 to 2 hours after tracer injection, the relatively low radiation dose, and the excellent spatial resolution and lesion-to-background contrast. These advantages contribute to the superior accuracy of FDG-PET for the diagnosis or exclusion of infections (37).

Indications for the use of FDG in infectious or inflammatory diseases, namely:

1. Localization of abnormal foci to guide the etiological diagnosis in the presence of fever of unknown origin (FUO)
2. Diagnosis of infection in: suspected chronic infection of bone and/or adjacent structures (osteomyelitis, spondylitis, discitis or osteitis including presence of metallic implants), diabetes with suspicion of Charcot's neuroarthropathy, osteomyelitis and/or soft tissue infection, painful hip prosthesis, vascular prosthesis, and fever in AIDS
3. Detection of the extent of inflammation in: sarcoidosis, inflammatory bowel disease, and vasculitis involving the great vessels.
4. Therapeutic follow-up of unresectable alveolar echinococcosis, in which it may be used in the search for active localization of the parasite during medical treatment and after treatment discontinuation. (32).

Diagnosis of FDG-PET in FUO

Fever of unknown origin (FUO) and unexplained signs of inflammation are challenging medical problems which are predominantly caused by infections, malignancies, autoimmune diseases and other noninfectious inflammatory diseases (38).

FUO is defined as a temperature higher than 38.3°C on several occasions and lasting longer than 3 weeks, with a diagnosis that remains uncertain after at least 1 week of investigation in a hospital (39).

Etiology of FUO :

Infections were the most frequent causes of FUO, followed by malignancies, and then noninfectious inflammatory diseases.
However, in is a more common cause of FUO than in adults, accounting for 30% to 50% of the cases, followed by connective tissue diseases (CTDs) and then neoplasm (7% to 13%). Most cases of FUO in children as well as in adults represent unusual manifestations of common diseases, rather than a common manifestation of a rare disease. The most common systemic infections in the United States that are implicated in children with FUO are salmonellosis, tuberculosis, rickettsial infections, spirochetal infections, cat-scratch disease, infectious mononucleosis, cytomegalovirus (CMV) infection, and viral hepatitis (40).

Autoimmune diseases occur with equal frequency in adults and children (10% to 20% of cases), but certain diseases such as systemic lupus erythematosus (SLE), Wegener's granulomatosis, and polyarteritis nodosa are more common in adults, whereas juvenile rheumatoid arthritis (JRA, now called juvenile idiopathic arthritis, JIA) is particularly common in children . Juvenile rheumatoid arthritis accounts for >90% of connective tissue diseases that cause FUO, followed by SLE and other types of vasculitis (40) .

Lymphoma and leukemia are the two most common malignancies presenting as FUO in children. The frequency of neoplasms decreased.

In two series, which was attributed to improved diagnostic imaging techniques (41).

Diagnosis of FUO :

Despite the fact that most children with FUO have a self-limited disease, it is still a very serious clinical problem, with mortality reaching 6% to 9% in two series studies of children with FUO. The diagnostic approach in children with FUO starts with a thorough history and physical examination, supplemented by laboratory and radiographic tests. Repeated histories and physical examination are important to better elucidate the etiology of FUO (40).

The age of the patient, history of exposure to wild or domestic animals, history of unusual dietary habits or travel, medication history, and ethnic background are very helpful in evaluating FUO. After the screening laboratory and radiographic tests, additional tests should be guided by the history and physical examination (40).

Radiographic Evaluation of patient with FUO :

After obtaining a regular chest radiograph, further radiographic examination of specific areas such as the nasal sinuses, mastoids, and gastrointestinal (GI) tract should be performed following special indications. Inflammatory bowel disease should be excluded in children with abdominal complaints, persistent fever, and elevated erythrocyte sedimentation rate (ESR), anorexia, and weight loss (42).

Echocardiograms are useful to evaluate the heart when suspecting infective endocarditis. Ultrasonography (US) is often used to investigate fluid collections, abscesses , and thrombophlebitis (42).

Computed tomography (CT) or magnetic resonance imaging (MRI) is helpful in the detection of neoplasms and abscesses in the abdomen and in the investigation of lesions in the head, neck, and chest , as well as for osteomyelitis .Magnetic resonance imaging is rarely used in the initial evaluation of FUO except in certain cases such as spinal epidural abscesses (43).

Laparotomy has been nearly replaced by noninvasive imaging techniques, especially in the search for occult abscesses or hematomas in patients with FUO. However, laparotomy is very helpful when noninvasive imaging measures are non-diagnostic and CT- or ultrasound-guided aspiration or biopsy fails to make the diagnosis (44).

Radionuclide Scans :

Gallium-67– and indium-111–labeled leukocytes have a higher overall yield than CT or US in diagnosing FUO because the images cover the whole body. In patients with FUO, gallium 67 is useful for the detection of malignancies and of granulomatous and inflammatory disorders, whereas indium-111–labeled leukocytes are more useful for detecting localized infectious and inflammatory processes (45).

Different technetium-99m (^{99m}Tc)-labeled compounds are being studied for potential clinical use in patients with FUO, such as ^{99m}Tc-hexamethylpropylene-amine-oxime (HMPAO)-labeled leukocytes, ^{99m}Tc-ciprofloxacin, and ^{99m}Tc-labeled monoclonal antibodies (46).

FDG-PET Scan :

Rationale for the Use of FDG-PET in FUO :

Many metabolically active infectious and inflammatory disorders can be readily visualized by FDG-PET scanning (Table. 3) (47).

Infections	Inflammatory/granulomatous	Neoplasms
Subphrenic abscess	Takayasu's arteritis	Hodgkin's disease
Pneumonia	Rheumatoid arthritis	Non-Hodgkin's lymphoma
Osteomyelitis	Wegener's granulomatosis	Colon carcinoma
Vascular graft infection	Sarcoidosis	Renal cell carcinoma
Tuberculosis	Thyroiditis	Sarcoma
Sinusitis	Enterocolitis	Pheochromocytoma
Mastoiditis	Myositis	
	Gastritis	
	Giant cell arteritis	

Table 3. Common causes of FUO reportedly detected by FDG-PET (47)

FDG-PET has a high accuracy in detecting chronic osteomyelitis, especially in the central skeleton, which was found to be superior to antigranulocyte antibody scintigraphy and to indium-111–labeled leukocytes. Although CT and MRI provide excellent anatomic details, they have limited capacity to differentiate postsurgical changes from infection, and, in contrast to FDG-PET, they are hindered by metal implants. Fluorodeoxyglucose-PET can differentiate between normal bone healing following a fracture or surgical intervention and osteomyelitis or malignancy. In patients with prostheses, FDG-PET can assess the presence of a superimposed infection, especially in hip prostheses and, to a lesser extent, in knee prostheses (48).

FDG-PET can be used to diagnose infections related to diabetes, especially in the evaluation of the diabetic foot (49).

FDG-PET was able to differentiate lymphoma from nonmalignant lesions in the central nervous system in HIV-positive patients (50).

Although FDG-PET cannot clearly distinguish between granulomatous diseases such as sarcoidosis and lymphoma, it can localize the active lesions, which can be biopsied for a timely and minimally invasive diagnosis (51).

The early diagnosis of vasculitis, especially large-vessel vasculitis, prevents progression to the occlusive phase of the disease. In this regard, FDG-PET has demonstrated high specificity and high sensitivity to detect and assess the activity of large-vessel vasculitis. It can noninvasively detect and quantitatively assess the disease activity in inflammatory bowel disease (52).

Fluorodeoxyglucose uptake in the synovium measured using the standard uptake values (SUVs) facilitates the quantitative assessment of synovial activity, which has been particularly helpful in assessing the disease activity in patients with rheumatoid arthritis (53).

The increase in SUV and the number of PET-positive joints correlated with swelling and tenderness of the joints, ultrasonography, synovial

thickness, and inflammatory serum markers (ESR and C-reactive protein). This facilitates the measurement of disease activity in the joints of patients with rheumatologic diseases (54).

Other infectious or inflammatory processes that can be visualized with FDG-PET are thrombophlebitis, infected implantable devices, and pleural diseases (55).

FDG-PET and Biopsy :

As opposed to the other noninvasive diagnostic approaches in FUO, biopsy is a directed invasive intervention, which is often required to make a diagnosis. The most common biopsies performed in an FUO scenario are bone marrow, liver, lymph node, temporal artery, pleura, and pericardium. However, biopsy has spatial limitations, and a negative biopsy result may well be a false-negative finding due to sampling errors. The combination of anatomic imaging and FDG-PET either through a software fusion or a combined PET-CT scanner leads to better localization of functional abnormalities. The registration of anatomic and functional images can be used to guide biopsies to the metabolically active area, which can increase the yield of this approach and decrease the need for unnecessary procedures (56).

Advantages of FDG-PET Over Anatomic Imaging:

Timely identification and localization of the source of FUO is critical for the management of patients. Therefore, FDG-PET scanning is very helpful in this regard because it can detect early changes at the molecular level before they become apparent on anatomic imaging FDG -PET images the whole body in one study. Post-therapy tissue changes such as scarring, edema, and necrosis may alter the identification of recurrent tumor with anatomic imaging. Regardless of anatomic changes after chemotherapy and radiation therapy, FDG-PET can detect residual disease and has a high negative predictive value for viable disease in a residual anatomic abnormality, reaching 97% in some cases. Therefore, equivocal radiographic findings can be accurately characterized with FDG-PET (57).

There is also increasing concern about the risk of radiation, radio contrast-induced nephropathy, and allergic reactions to patients imaged with CT. Furthermore, FDG-PET is able to detect early inflammatory and infectious lesions when anatomic imaging modalities reveal no abnormalities (58).

Advantages of FDG-PET over Other Nuclear Medicine Techniques:

Currently, gallium-67 scanning is the most commonly used radiotracer for the evaluation of FUO. However, FDG-PET has many advantages over conventional nuclear medicine techniques. It offers a better tracer kinetic, a favorable 110-minute half-life, better spatial resolution (5 to 8mm resolution for PET vs. 10 to 15mm for single photon emission computed tomography, SPECT), better lesion-to-background ratio , low dose to the patient, and the possibility for quantification decreasing the variability between readers (59).

Whole-body FDG-PET scanning is completed approximately 2 hours from the injection, which results in earlier reporting than with other radiotracers (60).

An important safety factor is that, in contrast to labeled leukocytes, in FDG-PET there is no handling of blood products. FDG-PET is more sensitive in chronic, low-grade infections, has high accuracy in the central skeleton, and a high inter-observer agreement (61).

Another major advantage of FDG-PET over gallium in the evaluation of FUO patients is the ability to visualize and assess the degree of activity in a variety of inflammatory vessel diseases (60).

It has been reported that FDG-PET can clearly visualize sarcoid lesions in the lungs and brain when concurrent gallium scans are negative (62).

Studies Regarding FDG-PET and FUO :

FDG-PET was more helpful in the diagnostic process of patients with a suspected focal infection or localized inflammation than in FUO. Only one study found that indium-111–labeled granulocyte scintigraphy had a superior diagnostic performance compared to FDG-PET in the evaluation of FUO, but in the 19 patients studied, only one patient was diagnosed with malignancy (Hodgkin's disease) (63).

In a retrospective study a review of 30 FDG-PET scans of 30 patients (aged 13 to 73 years) who were evaluated for FUO during the period between 1999 and 2004. Clinical follow-up, which included subsequent conventional imaging studies and/or pathology results, was compared to the FDG-PET scan results. FDG-PET contributed to the diagnosis of 71% of the cases. The causes of fever detected by FDG-PET included pneumonia, non-Hodgkin's lymphoma (Fig. 8), Hodgkin's disease (Fig.9), Crohn's disease (Fig10.), surgical wound infection, infected liver cysts, leukemia, and metastatic renal cell carcinoma. FDG-PET was falsely negative in three cases of colitis, peritonitis, and rejected renal transplant. Two FDG-PET scans were falsely positive in two patients with suspected abnormal activity in the abdomen; one of them had an eventual diagnosis of endocarditis (64).

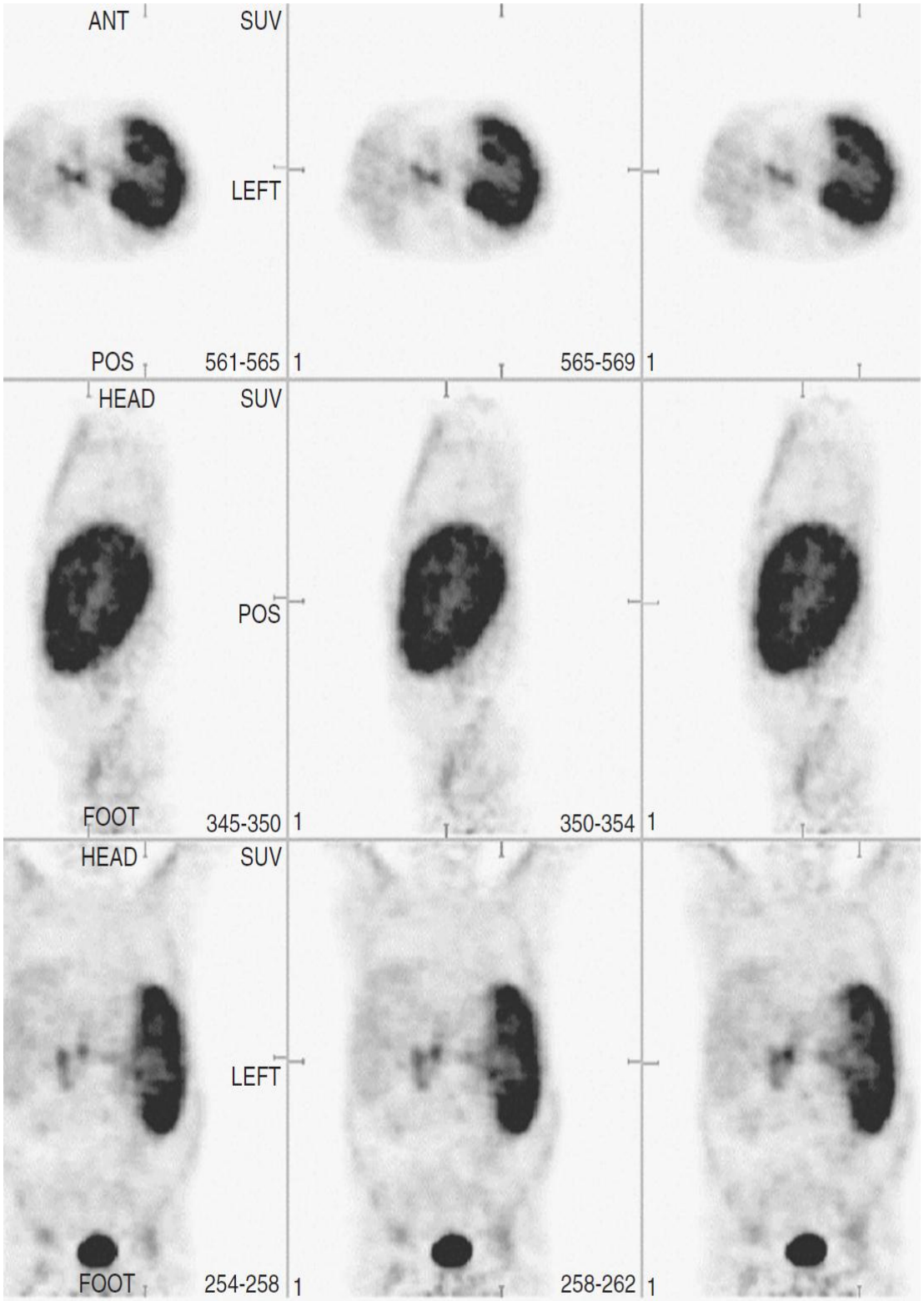

Figure 8. Intense FDG uptake is seen in the spleen, which is markedly enlarged, and two foci of abnormal uptake are visible in the upper abdomen, representing lymphadenopathy. The patient was diagnosed with non-Hodgkin's lymphoma. (64)

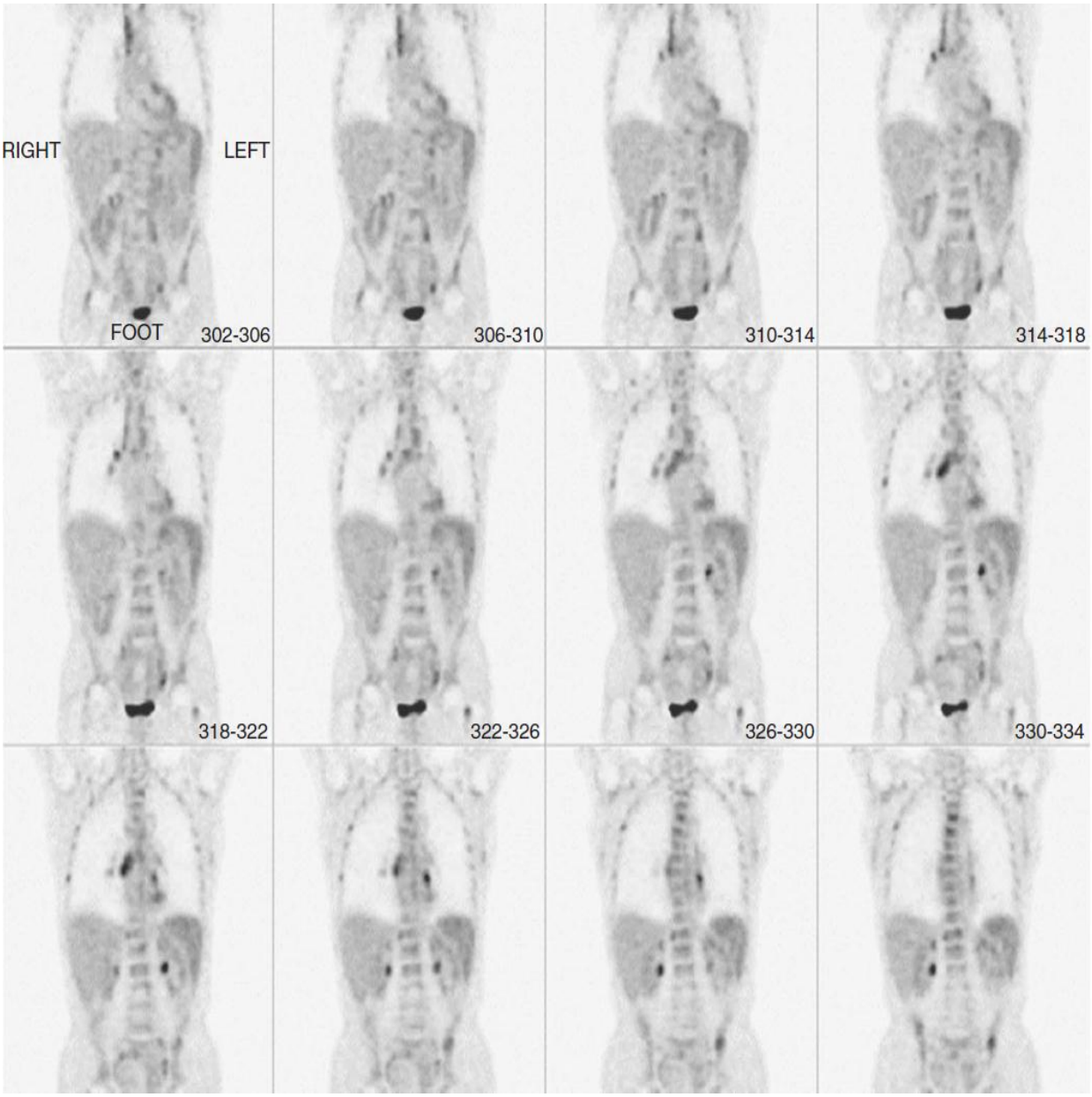

Figure 9. Abnormal FDG uptake is seen in the bone marrow, as well as in supraclavicular and mediastinal lymph nodes of a patient with FUO. The patient was diagnosed with Hodgkin's disease. (64)

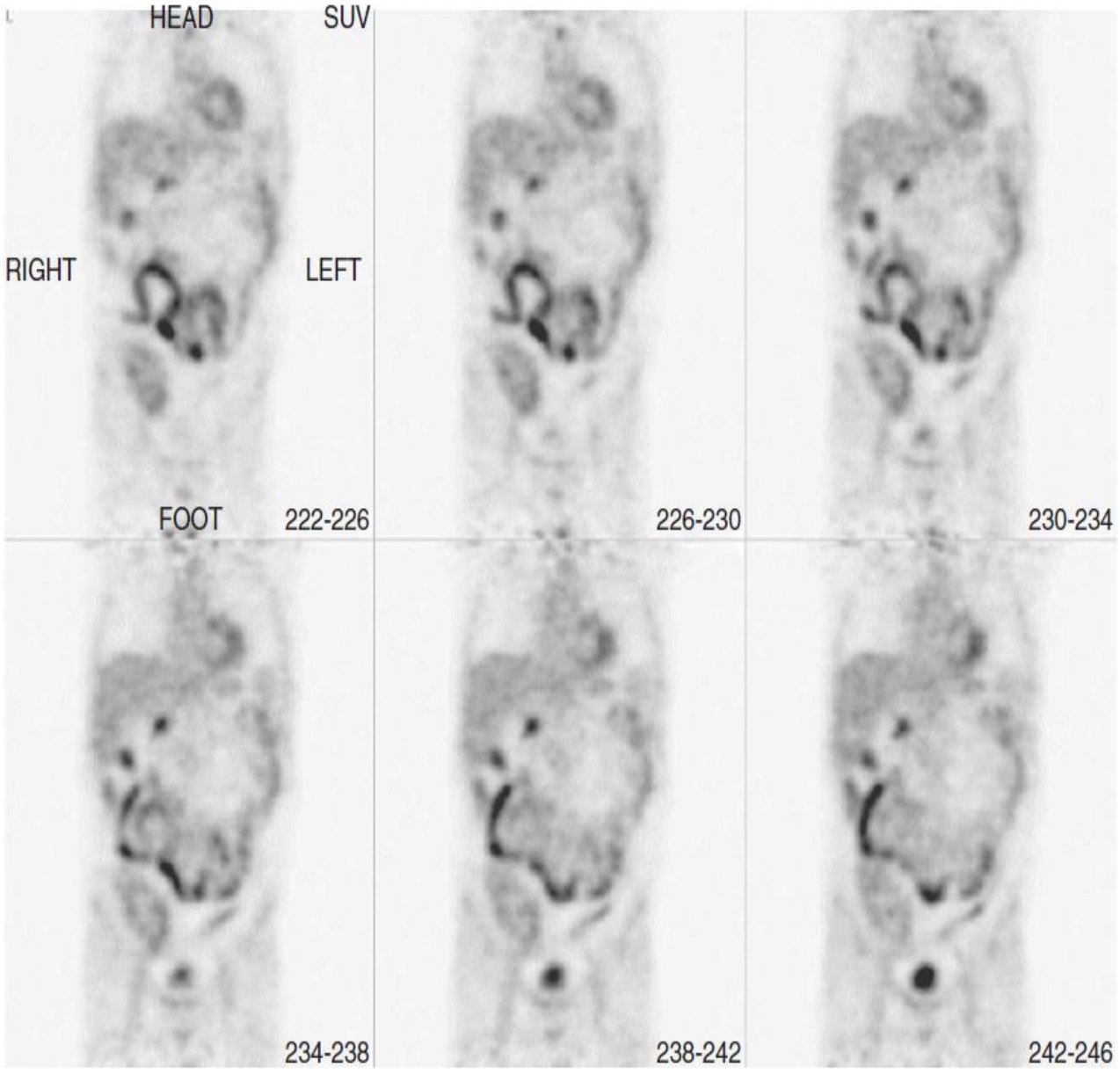

Figure 10. Diffuse FDG activity in the bowel. Although this pattern can be seen in normal adult patients, this finding was the only suspicious source of FUO in this patient, with a history of renal transplant. Subsequent colonoscopies and bone marrow biopsies were negative. The patient underwent a laparotomy; after segmental resection of the terminal ileum and cecum, he was diagnosed with Crohn's disease. (64)

Studies Regarding PET/CT and FUO :

In a study investigates the diagnostic value of ^{18}F-fluorodeoxyglucose positron emission tomography/computed tomography (^{18}F-FDG PET/CT) in patients with 109 classical fever of unknown origin (FUO). Of the 48 ^{18}F-FDG PET/CT scans, 41 (85.4%) were interpreted as abnormal, and 25 (52.1% of all scans) were considered clinically helpful. The final cause of fever was determined in 41 patients (85.4%); infection (25%), malignancy (12.5%), non-infectious inflammatory disease (16.7%) and miscellaneous causes (31.3%). ^{18}F-FDG PET/CT contributed to the final diagnosis of FUO in 65.8% (65).

In a 2-year retrospective cohort study at the Nîmes University Hospital, France, A total of 79 patients with FUO underwent ^{18}F-FDG-PET/CT. A final diagnosis was established in 61 (77.2 %) cases. Etiologies of FUO were determined using 18F-FDG-PET/CT findings in 45 (73.8 % of patients with diagnosis) cases. The sensibility and specificity value were 98 % and 87 %, respectively. The presence of adenopathy, low hemoglobin and increased C-reactive protein (CRP) were predictors of high-yield ^{18}F-FDG-PET/CT. ^{18}F-FDG-PET/CT may help to detect most causes of FUO. The predictors of high-yield ^{18}F-FDG-PET/CT found in this study can help identify patients likely to benefit from specific and early imaging techniques (66).

Role of FDG-PET IN Skeletal Inflammation

Diagnosis of Skeletal Infection

Diagnosis Using Morphologic Imaging Modalities:

Standard X-ray, although useful if they show the classic findings of bone destruction and periosteal reaction, may not show abnormalities until 10–21 days after the onset of infection. A 30–50% loss of bone density must occur before X-ray show any abnormalities, and radiographs are therefore relatively insensitive to the presence of acute bone infections (67).

Additionally, X-ray findings are unreliable in establishing the diagnosis of osteomyelitis among patients with violated bone. In these situations X-ray findings are non-specific, being diagnostic in as low as 3–5%of culture-positive cases.Nevertheless, X-ray should be the initial modality for the work-up of skeletal infection. Standard X-ray is relatively inexpensive, easily obtained, may determine that another underlying pathological condition exists, and frequently aid physicians in deciding what sort of additional imaging studies are required. Osteomyelitis in infants and children predominantly affects the growth intensive end regions of the long bones. This is because the inflammatory process commonly affects the articular regions adjacent to the metaphyseal and epiphyseal sites. Ultrasound accordingly may be of benefit in this group of patients and can be helpful in planning the management (68).

The common ultrasonography findings of osteomyelitis are intra-articular fluid collection and sub-periosteal abscess formation. These findings were found to precede any radiological changes by several days. Ultrasonography is also helpful in guiding aspiration for immediate microscopic and later bacteriological examinations (68).

The most helpful role of ultrasonography, however, is in the diagnosis and management of septic arthritis. In particular, ultrasonography is very

sensitive in detecting joint effusions and may clearly define the extent of septic arthritis, differentiate septic arthritis from soft tissue abscesses, or tenosynovitis, and help avoid unnecessary joint aspirations (68).

Following the highly successful introduction of MRI, CT has no major role in the diagnosis of osteomyelitis. However, it is a complementary procedure that is useful in sensitively detecting sequestra and can be useful in chronic osteomyelitis, in particular when determining the presence, or absence, of the sequestra is important for decision-making (regarding possible surgical intervention) (69).

MRI offers excellent depiction of both bone and soft tissue infection. Accordingly, MRI is often used instead of CT for the diagnosis of osteomyelitis. The results indicate that MRI is excellent in vertebral osteomyelitis and encouraging in diabetic foot osteomyelitis. The advantages of MRI over CT include improved soft-tissue contrast resolution, absence of beam-hardening artifacts from bone, and multiplanar capabilities. The sensitivity and specificity of MRI for osteomyelitis range from 60% to 100% and from 50% to 95% respectively (70).

Although the average overall accuracy of MRI for the diagnosis of osteomyelitis is approximately similar to that of multi-phase bone scans, it is not used routinely as it is more expensive and less available. It is used on an individual basis particularly when vertebral involvement is suspected; in complicated cases of chronic osteomyelitis when it is important to determine the extent of infection; in suspected diabetic foot osteomyelitis; and in situations when anatomical details are necessary for planning surgical intervention (70).

Diagnosis by Scintigraphic Methods :

Multi-phase bone scanning is the imaging modality of first choice for suspected osteomyelitis. These studies become positive within 24–48 h after the onset of symptoms (71).

The classic findings of osteomyelitis in the multiphase bone scan are increased regional perfusion as seen in flow and blood pool images and

a correspondingly increased uptake on delayed images. Bone scintigraphy is very sensitive in the early diagnosis of osteomyelitis. When the bone is not previously affected by other pathological conditions (non-violated), the bone scan has a high specificity as well and is an efficient and cost-effective modality in the diagnosis of osteomyelitis (72).

The overall sensitivity and specificity of bone scans for osteomyelitis in non-violated bone is 90–95%. When bone is violated the bone scan remains generally sensitive (90–95%) but is non-specific (30%). Four-phase bone scans improve the specificity which was demonstrated by Alazraki et al (73).

The bone scan alone may not establish the diagnosis, requiring a complementary radionuclide modality, such as ^{111}In leukocyte or ^{67}Ga; this improves the specificity. In this situation, the main benefit of the bone scan is to exclude the presence of osteomyelitis if it is unequivocally negative and to localize the abnormality better than other studies such as labeled leukocytes or gallium-67 (74).

Although the bone scan becomes positive very early in the course of the disease, it may not be useful in evaluating the response to treatment as it may remain positive for months after clinical resolution of the disease (75).

The gallium-67 scan also becomes positive in osteomyelitis 24–48 h after the onset of symptoms (74).

In the clinical setting of acute osteomyelitis, gallium-67 scans are 80–85% sensitive. On the other hand, positive gallium-67 scans are seen also with primary and metastatic neoplasms, chronic infections, and aseptic inflammatory and traumatic lesions. Specificity accordingly is approximately 70% (76).

To improve specificity, Tumeh et al. suggested that osteomyelitis is more likely to be present when ^{67}Ga uptake exceeds that of Tc-99m MDP or differs in distribution. If ^{67}Ga localization is less than Tc-99mMDP localization, infection is unlikely. If the two uptake patterns are equivalent, the findings may be indeterminate (77).

Combined ^{99m} Tc-MDP/^{67}Ga yielded higher specificity than Tc-99m MDP alone in the group of patients with violated bone: the specificity for Tc-99m MDP bone scan was 25% but, when combined with ^{67}Ga, it was 63%. Causes of ^{67}Ga false positives included fractures and juvenile rheumatoid arthritis (78).

Indium-111 oxime and Tc-99m HMPAO leukocyte studies are widely used in the diagnosis of osteomyelitis as specific agents for infection. Overall, In-111 leukocyte studies are sensitive (88%) as well as specific (91%) for osteomyelitis and are particularly useful in excluding infection in a previously violated site of bone such as post-traumatic, diabetic, and post-surgical conditions and in some patients with pressure sores (79).

Bone scintigraphy should be performed in conjunction with labeled leukocyte imaging for anatomical localization. Tc-99m HMPAO labeled leukocytes have been reported to yield an accuracy similar to that of In-111 leukocyte studies in the diagnosis of osteomyelitis but have the additional benefit of providing results on the same day. This technique may be particularly useful in children as the radiation dose is much lower than that of In-111 leukocyte technique (80).

Its disadvantage, however, is the inability to acquire dual Tc-99m-MDP and labeled WBC simultaneously. Indium-111 labeled leukocyte scans are not generally useful in the diagnosis of vertebral osteomyelitis as the images may show normal or decreased uptake and their accuracy is low (72).

Results of IgG immunoscintigraphy are encouraging in both acute and chronic osteomyelitis, including those cases associated with orthopedic appliances, with an average sensitivity of 95% and a specificity of 83%. It has been found to be as useful as labeled leukocytes in diagnosing infections and when it was compared directly to ^{67}Ga citrate it was found to be more sensitive and specific for infection than ^{67}Ga (81).

On the other hand, Tc-99m anti-granulocyte antibody which is reactive against NCA-90 antigen present on the surface of leukocytes was found

to be 84–93% sensitive and 72%specific for non-vertebral osteomyelitis. This agent is not useful in the diagnosis of vertebral osteomyelitis and hip replacement. In a manner similar to the patterns of labeled white blood cells, this agent also showed cold lesions in vertebral osteomyelitis (82).

A number of studies have evaluated the efficacy of Tc-99m nano-colloid imaging of infections including osteomyelitis. The sensitivity of this method ranges from 87% to 95%and specificity ranges from 77% to 100% (83) .

[^{18}F]-FDG PET appears to be especially helpful in those cases in which MRI cannot be performed or is non-diagnostic and as an adjunct in patients in whom the diagnosis is inconclusive (84).

Spinal infection:

[^{18}F]-FDG PET offers several potential advantages over conventional nuclear medicine tests in the evaluation of musculoskeletal and SI (Table 4) (84).

Advantages	Disadvantages
Early imaging and reporting	Currently not widely available
High-resolution images	Relatively high cost
High target-to-background ratio	Limited anatomic information
Low bone marrow uptake	Not infection specific
No significant uptake in degenerative bone disease/older vertebral fractures	
Not immunogenic	
Sensitive in chronic osteomyelitis	
High interobserver agreement	
Minimal labor intensity	
Acceptable radiation dose	

Table 4. Advantages and disadvantages of FDG PET in spinal infection as compared to conventional nuclear medicine techniques, such as bone scintigraphy, gallium scanning, and leukocyte scintigraphy (84).

Clinical studies :

Schmitz et al. and Bredella et al. investigated the FDG avidity in various types of vertebral compression fractures and concluded that, in general, benign fractures demonstrated significantly less FDG uptake than malignant fractures or SI and that recent and older fractures demonstrated, respectively, moderate and no or only mildly increased FDG uptake .It indicate that [^{18}F]-FDG PET is useful for diagnosing SI (Fig. 11) (85).

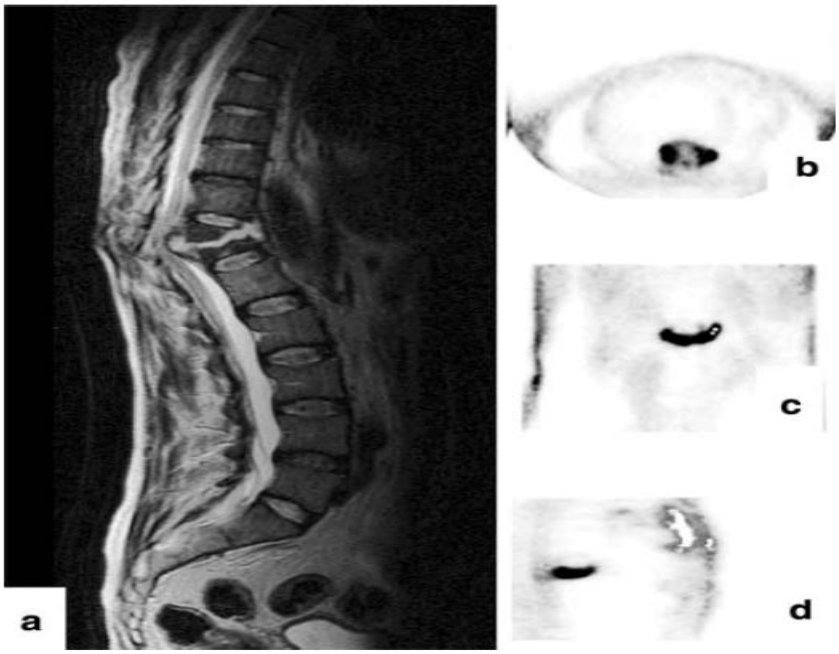

Fig. 11- Chronic hematogenous spondylodiscitis of the thoracic spine.
A 45-year-old man with multiple myeloma presents with severe back pain and prolonged fever in combination with increased inflammatory parameters. Sagittal T2-weighted MRI study (a) demonstrates abnormal signal at T11-12, but, nevertheless, the differential diagnosis with a vertebral compression fracture or even a spinal malignancy cannot reliably be made. Selected PET images (b transverse, c coronal, d sagittal view) demonstrate increased FDG uptake at the level of T11-12 vertebral disc, confirming a Staphylococcus aureus spondylodiscitis (85).

Guhlmann et al. studied 15 patients with suspected chronic osteomyelitis of the central skeleton, including the spine, and compared [^{18}F]-FDG PET to a radiolabeled anti-granulocyte antibody (AGA) (86). Two readers reviewed images independently. [^{18}F]-FDG PET was significantly more accurate than the AGA for reader 1 (93 vs. 70%) and reader 2 (100 vs. 80%) (86).

Schiesser et al. evaluated [^{18}F]-FDG PET in the diagnosis of metallic implant-associated infection in 22 patients (29 scans) with prior history of trauma (87). In a subgroup of six patients with clinically suspected spinal implant infection, [^{18}F]-FDG PET was true negative for implant infection in all six patients (including three patients with fracture non-union and one patient with osseous necrosis). One of the six patients had a soft tissue infection, correctly detected and localized with [^{18}F]-FDG PET. In this study the degree of overall inter-observer agreement was high (87).

Kalicke et al. evaluated the clinical usefulness of [^{18}F]-FDG PET in acute and chronic osteomyelitis in 21 patients; including 7 with spondylitis and reported that [^{18}F]-FDG PET yielded true-positive results in all 7 cases (88).

Stumpe et al. prospectively compared [^{18}F]-FDG PET to MRI for diagnosing SI in 30 patients with substantial vertebral end-plate abnormalities of the lumbar spine detected on MRI (89). A total of 38 sites were evaluated; there were 5 sites of infection in four patients. [^{18}F]-FDG PET was true-positive in all 5 foci of infection and true negative in all 33 uninfected sites (100% sensitivity and 100% specificity) (88). The sensitivity and specificity of MRI for detecting disc space infection were 50 and 96%, respectively (88).

They found [^{18}F]-FDG PET to be very helpful in the differentiation of severe degenerative changes of intervertebral discs from infective discitis (n = 5). These investigators concluded that [^{18}F]-FDG PET may be useful for differentiating degenerative from infectious end-plate abnormalities detected on MRI (89).

In perhaps the largest series reported to date, de Winter et al. investigated [^{18}F]-FDG PET in 73 patients (90). The overall accuracy of [^{18}F]-FDG PET in this prospective study was good (86%), and the negative predictive value (100%) was excellent. The authors concluded that chronic postoperative SI can be excluded when the PET study is negative. In the patient with spinal hardware, however, a positive study must be interpreted cautiously (Table 5) (91).

Benefits	Risks
No major metallic artifacts	FDG uptake in infection, inflammation (e.g. instability) and tumor
Postoperative FDG uptake in the spine for up to 4 months	Possible inflammatory reaction incited by spinal hardware
Faint or no FDG uptake in the degenerative spine	Limited anatomic information (co-registration with in-line CT needed)
Faint or no FDG uptake in older compression fractures	
High negative predictive value	

Table 5. Benefits and risks of FDG PET in spinal-fusion surgery patients (91)

A limitation of PET imaging in general is that despite a relatively high spatial resolution, the anatomic information available with PET images remains limited. To improve this, integrated in-line PET/CT systems (49, 87) (Fig. 12). offer excellent anatomic localization of the actual site of uptake, minimizing misinterpretation of localization from areas of clear-cut arthritic bony disease and infection, such as demonstrating the uptake to be associated with an arthritic facet joint rather than with the vertebral body or interspace (93).

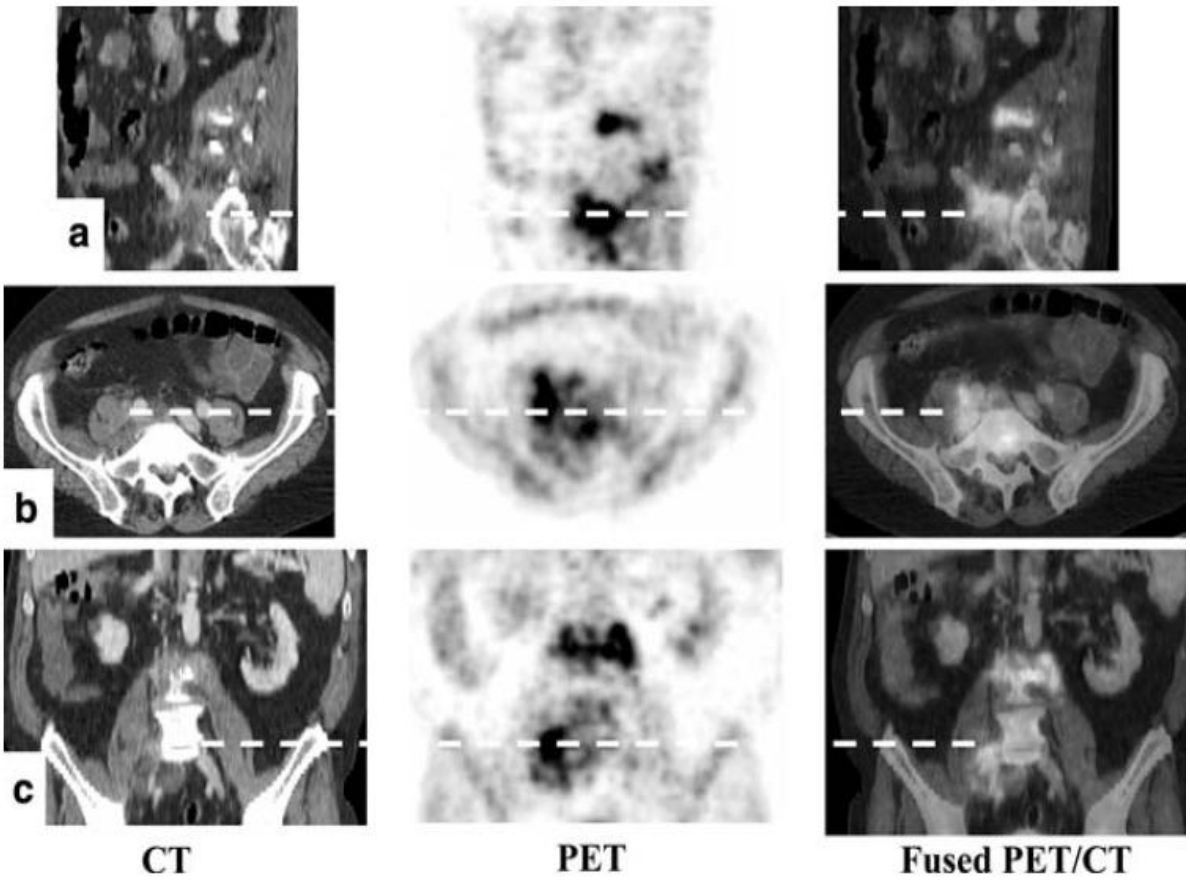

Fig. 12. high metabolic uptake localized in the right iliopsoas region (dashed lines, resp. a sagittal, b transverse, and c coronal CT, PET, and fused PET/CT images), indicating an occult spondylodiscitis complicated by a secondary psoas abscess; eventually the portal of entry was confirmed to be the urinary tract with a Staphylococcus aureus infection (49).

So, Hartmann et al. investigated the diagnostic value of [^{18}F]-FDG PET co-registered with in-line CT (PET/CT device) in patients with trauma and suspected chronic osteomyelitis in the axial and appendicular skeleton, including patients with metallic implants and prosthetic devices, at a minimum interval of 6 months after surgery (94).For the subgroup analysis of nine spinal regions (all of them involving the lumbar spine), [^{18}F]-FDG PET/CT was true positive in all seven cases of SI, and true negative in the two patients who did not have SI (100% accuracy). These investigators found that the precise anatomical localization provided by, and the extent of increased FDG uptake detected on, combined PET/CT were especially useful for planning surgical intervention, and, in the cases in which infection was limited to the soft tissues, for initiating antibiotic treatment (94).

Kim et al. performed dual time point [^{18}F]-FDG PET/CT in 22 consecutive patients with a high suspicion of spondylitis (based on clinic-radiography and bone scan findings), both pyogenic as well as tuberculosis (95). They imaged the patients, at 1 h and at 2 h after injection of FDG. Although the test was very sensitive for detecting SI, neither visual nor semi-quantitative analysis, using dual time point imaging, could reliably differentiate pyogenic from tuberculous infection (95).

In a retrospective study of 150 patients, Rosen et al. were the only one describing significant focal FDG uptake (of varying degree) in more than half of the patients, corresponding to degenerative spinal disease, primarily in the lumbosacral spine.

In a prospective study that made to determine whether ^{18}F-FDG PET/CT follow-up imaging after treatment in patients with spinal infection (SI) could provide useful prognostic information and determine the residual SI. It is found that The SUV_{max} and the SUV_{mean} were significantly declined after treatment in both of residual and non-residual ^{18}F- FDG PET/CT is useful for discrimination of residual and non-residual SI after treatment (92).

Overall, the results of [^{18}F]-FDG PET for diagnosing SI that have been reported by various investigators are very encouraging. PET studies, however, are dealing with a mixture of hematogenous and postoperative SI. Therefore, it is quite difficult to give sensitivity and specificity figures for the different types of SI (96).

There are, nevertheless, limitations to the test since FDG uptake reflects enhanced glucose metabolism in general, not infection specifically, while uptake is significantly higher in infection than in normal bone or benign compression fractures, there are few data comparing FDG uptake in SI to uptake in spinal tumors.

Infection and malignancy are not mutually exclusive and it is likely that the test will be less reliable for differentiating infection from tumor and detecting infection superimposed on tumor. Also in spinal-fusion surgery, especially in the presence of metallic implants, the test suffers from a

lower specificity. Increased FDG uptake, in the absence of infection, has been described in foreign body reactions, and aseptic loosening of orthopedic hardware (97).

Prosthetic joint infection:

Peri-prosthetic infection following total hip or knee arthroplasty is associated with significant morbidity and costs (98).The infection rates following primary implantation and revision surgery are approximately 1% and 3% for hip prostheses and 2% and 5% for knee prostheses, respectively. Differentiating prosthetic joint infection from aseptic loosening is of crucial importance for appropriate patient management; the treatment of an infected joint prosthesis generally involves both systemic antibiotics for an extended period and exchange arthroplasty in one or two stages, whereas aseptic loosening usually requires a single revision arthroplasty (98).

Diagnosing prosthetic joint infection is difficult; clinical signs and symptoms, laboratory tests, radiography, and joint aspiration are insensitive, nonspecific, or both. In addition, cross-sectional imaging modalities such as CT and MRI are hampered by artifacts produced by the prosthetic devices themselves (99).

Radionuclide imaging is less affected by metallic implants and may be more useful. Combined leukocyte–marrow scintigraphy has been reported to achieve a diagnostic accuracy of 90% or greater and is currently regarded as the imaging modality of choice for diagnosing prosthetic joint infection (99). However, combined leukocyte–marrow scintigraphy is labor-intensive, time-consuming, not widely available, and potentially hazardous because of direct handling of blood products (99).

FDG-PET enables visualization of hyper-glycolytic inflammatory cells (leukocytes, macrophages, and other immunologically active cells) during infection; it may be an attractive alternative to combined leukocyte–marrow scintigraphy because it requires only one injection and scan and is more widely available. Furthermore, treatment with antibiotics is not likely to affect the sensitivity of FDG-PET in delineating sites of infections

because FDG does not rely on leukocyte migration, in contrast to combined leukocyte–marrow scintigraphy (99).

Data on FDG-PET in patients with infected prosthetic devices are controversial. Zhuang et al. found PET to be more accurate in detecting infections in patients with hip replacements than in patients with knee replacements. There were ten false positive findings in 36 patients with total knee replacements using peri-prosthetic FDG uptake as a criterion. The sensitivity, specificity and accuracy of PET for detecting infection in patients with total knee replacements were 91%, 72% and 78%. The authors assumed that in addition to postsurgical changes, other factors must have contributed to the false positive results (100).

Love et al. showed that a peri-prosthetic FDG uptake pattern was neither sensitive nor specific for infection. Peri-prosthetic uptake was found both in infection and in aseptic loosening. One possible explanation for peri-prosthetic uptake in the absence of infection might be aberrant but otherwise normal bone marrow. Bone marrow distribution may be altered by an orthopedic device (101).

Van Acker et al. used focal FDG uptake at the bone–prosthesis interface as the criterion for infection. FDG-PET had a sensitivity of 100% and a specificity of 73% for the diagnosis of infection but offered no added benefit in comparison to white blood cell scintigraphy in combination with bone scintigraphy (102).

Apparently, the level of FDG uptake does not improve the performance of PET in diagnosing infection in patients with total knee replacement. FDG uptake has been shown to be even stronger in patients with aseptic prosthetic loosening (101).

Manthey et al. examined 28 patients with 14 hip and 14 knee prostheses with FDG-PET in order to differentiate different sources of pain in orthopedic prostheses. Nine of the 14 patients with painful knee prosthesis had synovitis diagnosed with PET. Synovitis was found more

frequently in patients with total knee replacement than in patients with total hip replacement (nine knees versus four hip prostheses) (103).

In another investigation with 21 consecutive patients with painful total knee replacements, diffusely increased FDG uptake in the synovial membrane was found. The authors reported that comparison of FDG-PET with bone scintigraphy facilitated the detection of focal FDG uptake at the bone–prosthesis interface, which is easily overlooked owing to intensified adjacent synovial uptake (102).

In Stumpe et al. study, 27 of 28 patients had increased synovial FDG uptake (Fig. 13) (104).

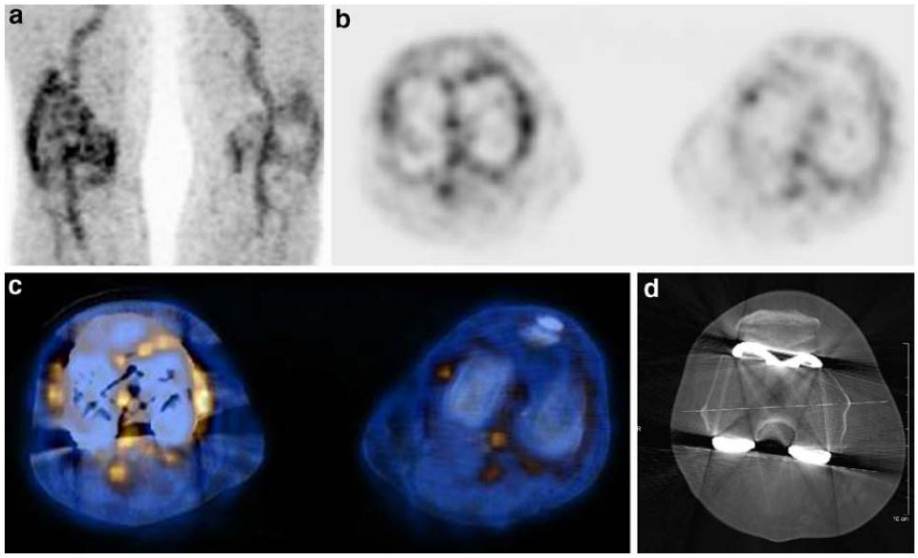

Fig. 13. Maximum intensity projection (MIP) PET (a), axial PET (b), axial PET/CT (c) and CT measurement of component rotation (d) in a 79-year-old man with knee replacement on the right. Pain at pes anserinus. There is strongly increased FDG accumulation in the synovial membrane of the right knee, including the suprapatellar recess. FDG accumulation is also seen in the contralateral left joint with painful osteoarthritis. Rotational CT demonstrates 10° internal rotation of the femoral component (104)

In addition, four of 12 patients in Stumpe et al. study showed granulomatous tissue with giant cells and macrophages at the knee prosthesis–bone interface. A foreign body reaction due to polyethylene and metal wear with shedding of particles was most likely to be responsible for this reaction (104) .

A study was done to identify the ability of ^{18}F-FDG-PET/CT to identify latent infections at the site of an interim hip spacer after resection arthroplasty for hip prosthesis infection. It was found that FDG-PET/CT is highly sensitive to detect latent infections in prosthetic hips and in interim hip spacers. The high negative predictive value of PET/CT scans is useful to rule out infections in patients with persistently elevated CRP levels. PET/CT might serve as an auxiliary tool to exclude latent infections in patients posing a clinical diagnostic dilemma (105).

Rheumatoid Arthritis:

RA is an autoimmune disease of unknown etiology which leads to chronic progressive systemic inflammation and synovial changes (106).

For a long time, RA has been a challenging disease for diagnosis. Current RA biomarkers have lacked sensitivity and specificity for diagnosis at an early stage of disease since many patients (up to 30%) may have no elevation in usual biomarkers such as rheumatoid factor (RF), anticyclic citrullinated peptide (anti-CCP), erythrocyte sedimentation rate (ESR), or C-reactive protein (CRP) (107).

The paradigm of RA treatment currently rests upon early detection and initiation of aggressive therapy which has shown to improve clinical outcomes and disease-associated morbidity (108).

Like MRI and diagnostic ultrasound (US) which are capable of detecting early synovitis prior to exam, FDG is able to detect it earlier in acute phase. PET is able to detect changes in synovium at the molecular level. This observation was made when RA patients with cancer, undergoing FDG PET scans for assessing disease activity, additional FDG uptake in the areas localized to their joint were noted. As a result, studies evaluating FDG PET for the diagnosis of RA have been performed (109).

A study by Lin and Sicuro recently demonstrated the diagnostic possibilities of FDG PET at a molecular level in RA. These investigators found that FDG uptake correlates well with synovial fluid TNF-alpha

concentration and provides an accurate means of detecting early disease in animal models of RA (110).

Likewise Matsui et al. demonstrated the ability of FDG-PET to detect early synovial inflammation using a collagen-induced arthritis model in rats. On day 14 when clinical signs of RA developed, the swollen joints were detected by FDG- PET as well. When histologic findings were compared with those of FDG PET, increased FDG uptake was seen to correspond with regions of bone destruction and pannus formation (111).

Disease burden assessment:

The quantitative evaluation of RA has always been very challenging. Detection based on changes seen on plain film radiography is not always sensitive and structural alterations such as osseous erosions in general lag behind clinical improvements. Use of semi-quantitative measures such as ESR and CRP are not always directly correlated with disease activity and are at best weak predictors of the clinical course of RA in any individual patient (112).

FDG-PET, however, may be very useful in the individual quantitative assessment of RA disease activity and its course. FDG PET also allows the use of soft tissue inflammation throughout the body as a direct evidence for disease activity. Numerous studies have highlighted the possibility of employing this technique for this purpose (112).

Beckers et al. compared FDG uptake in patients with RA to healthy control subjects and showed that SUV of the synovium in arthritic patients is correlated with US measurements of synovial thickness (Fig. 14) (53).

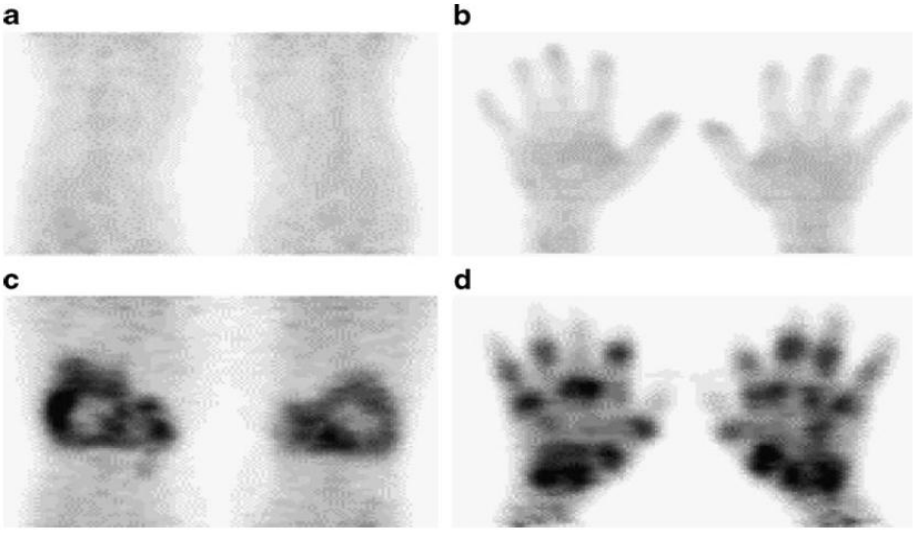

Fig. 14. ^{18}F-FDG PET images of healthy control subject (a and b) and RA patient with active disease (c and d). a 3-D projection image of normal tracer distribution in knee. b Normal distribution in hand and wrist. C Rheumatoid knee. d) Rheumatoid hand and wrist (53).

Twenty-one patients with RA as defined by the American Rheumatism Association (ARA) criteria, three healthy subjects and ten patients, who were being staged for melanoma, underwent FDG PET imaging. The maximum SUV (SUV_{max}) of joints of both the upper and lower extremities were measured. A significant linear correlation between the SUVs and synovial thickness was found for all affected joints investigated except for those of the metatarsophalangeal (MTP) joints. The cumulative SUV (defined as the sum of SUVs) of all PET-positive joints, as well as the number of positive joints in each patient, correlated significantly with clinical parameters as well (including the number of tender and swollen joints, the patient's and physician's global assessment scores, biologic measures such as ESR and CRP, US findings such as number of US-positive and Doppler-positive joints, and composite indices such as 28 joint counts and the simplified disease activity index) (53).

Likewise, Roivainen et al. conducted a study to examine the usefulness of PET imaging in the assessment of synovial inflammation and compared MRI measurements of synovial thickness with the degree of FDG uptake. Ten patients with established inflammatory joint disease and with clinical signs of joint inflammation (nine patients with knee joint involvement and one patient with ankle joint involvement) were studied. The SUVs in the inflamed synovia were measured and

then compared to synovial volumes measured on T1-weighted MR images. All patients showed a high accumulation of FDG at sites of clinically apparent arthritic change, and SUV correlated highly with synovial volume (54). This is an important point since MRI assesses vascularity and capillary permeability, whereas FDG PET measures glucose utilization and metabolic activity in the inflammatory cells (113).

RA is a disease which predominately affects small joints, and therefore Elzinga et al. examined FDG uptake in the hand and wrist joints in RA patients. A total of 25 patients were included (14 with RA, 6 with osteoarthritis, and 5 with fibromyalgia, which served as the control group since there are no associated anatomic abnormalities in this disorder). All RA patients had active synovial swelling at the time of scanning and all OA patients had at least one joint involved. They found that 29% of RA joints with clinical signs of inflammation demonstrated increased FDG uptake compared to 6% of the OA patients and 0% of the fibromyalgia controls (112).

In a more recent report, the inflammatory activity of the synovium in RA was assessed by FDG PET/CT, which was found to be superior in delineating inflammatory changes when compared to conventional radiographic techniques (114).This is especially important in RA when the FDG uptake by ligaments and tendenous attachments to bone must be discriminated from synovitis (115).

Lastly, FDG PET/CT may allow for highly accurate assessment of atlanto-axial instability in patients with RA. This is an important application since the cervical spine is a common site of synovitis in RA leading to nerve root compression and instability (116). FDG PET/CT can also be used to detect high-risk disease complications, such as atlanto-axial joint involvement, at an early stage (117).

Response assessment:

An important point has been raised by Brenner who stated if the cost-effectiveness of PET was high it would allow this modality to be translated to everyday clinical practice in rheumatology. PET, whish is

currently a relatively expensive modality, must provide additional critical information that is not attainable by the clinical or other laboratory based assessments for its routine clinical application and potential impact. The critical approach would require demonstrating that PET can serve as a tool to assess changes in disease activity in response to therapy (106).

One of the first studies to conclude that contrast-enhanced MRI and FDG-PET allow for comparison of efficacies of treatment was reported by Palmer et al. in 1995. Through performance of FDG PET of the wrist joints in 12 patients with inflammatory arthritis (9 of whom had RA), Clinical and imaging parameters were acquired before and after 2 weeks of no treatment, before and after 2 weeks of treatment with non-steroidal anti-inflammatory drugs (NSAIDS) or steroidal drugs, or before and after 12–14 weeks of treatment with methotrexate (MTX) (113).

FDG uptake and pannus volume decreased with therapy and were linearly correlated. In addition, both PET and MRI data were significantly correlated with improvement of clinical parameters in the wrist ($p < 0.002$). However, neither modality was associated with treatment success or failure as measured by the Paulus index (118).

Beckers et al. compared FDG PET (qualitatively and semi-quantitatively), dynamic contrast-enhanced MRI, and US in the assessment of RA synovitis before and after treatment with anti-TNF-alpha. In addition, CRP and matrix metalloproteinase (MMP) 3 were evaluated as markers of inflammation. They evaluated 16 knees in 16 patients at baseline and 4 weeks after initiation of anti-TNF-alpha treatment. FDG PET was positive in 69%, MRI in 9%, and US in 75% of knees. As expected, PET-positive knees had significantly higher Gd contrast enhancement and greater synovial thickness than PET-negatives knees. Importantly, changes in SUVs after 4 weeks were correlated with changes in MRI parameters and in serum CRP and MMP-3 levels, but not with changes in synovial thickness. Synovial tissues, in turn, took 6 weeks to decrease in thickness. This demonstrates the predictive capacity of molecular imaging with FDG PET which occurs earlier than morphologic changes and predicts the outcome (119).

In addition, Goerres et al. showed matched clinical and FDG PET results in 78% of joints of RA patients responding to infliximab therapy. Unlike other studies which used semi-quantitative methods of FDG assessment, this study developed a qualitative visual assessment scale between 0 and 4 and involved the assessment of multiple joints in each patient. In 12%of joints, PET was able to document a decrease of disease activity, whereas clinical evaluation did not, and in 16% the clinical evaluation revealed a decrease of disease activity, which was not detected by visual scoring of PET images (120).

Treatment outcomes as a whole are difficult to assess in RA and rely heavily on the definition of success. This difficulty, paired with a limited number of studies available, makes it challenging to truly assess the utility of PET for treatment assessment. Measuring one joint vs. overall joint activity in systemic diseases such as RA may provide greater insight into the impact of therapy (121).

Likewise, RA and other inflammatory processes have long suffered from a lack of objective criteria for response assessment. As a result, improvement in joint inflammation due to a therapeutic intervention may be masked by patients' reports of pain or stiffness, which may be responsible for disconnect between scales that involve patient reports of symptoms and objective PET findings. (121)

A recent study made to evaluate whether there is a correlation between the differences in joint uptake of 18F-FDG PET/CT and the improvement of clinical findings in RA patients undergoing anti-TNF therapies, it is found that the FDG uptake observed in the inflamed RA joints may reflect disease activity. The FDG-PET response was correlated with the clinical response to the biologic treatment of RA. (122).

Osteoarthritis:

The pathogenesis of OA is poorly understood. This disorder is thought to result from both mechanical and biochemical effects of aging and degenerative changes (123).

More recently, OA has been recognized as having an important inflammatory component. The disease process affects the entire joint structure, including the synovial membrane, subchondral bone, ligaments, and peri-articular muscles. It is thought, however, that the initiation of the process occurs at the chondrocyte level (124).

The synovium in OA is infiltrated with a mixed population of inflammatory cells and this leads to synovial hyperplasia and hypertrophy. This is reflected in certain clinical symptoms of OA, namely swelling and tenderness of the joints (125).

Currently, plain film radiography and clinical correlation serve as the standard practice for diagnosis and evaluation of the severity of OA, which is generally assessed by cartilage destruction. MRI is also able to accurately assess cartilage volume. However, as in RA, PET may provide a means of detecting early metabolic changes in OA as a result of the high concentrations of cartilage glycosaminoglycan's that are maintained by glucose metabolism in chondrocytes (115).

The theory that PET can detect metabolic changes in glucose metabolism at the chondrocyte level was first recognized when the PET portion of FDG-PET/CT scans of subjects referred for cancer imaging showed uptake at sites of OA that had been diagnosed on the CT portion of the examination as joints demonstrating OA. In addition, FDG PET has demonstrated increased radiotracer uptake in a wide variety of joints affected by OA including those of the spine (126).

Rosen et al. assessed the relationship between the severity of degenerative joint disease (DJD) and anatomic variations of the spine by comparing FDG PET and CT images. They noted that incidental findings suggesting DJD were common on FDG PET primarily in the lumbosacral area, and that the severity of disease as assessed by FDG PET corresponded with that of CT findings. More importantly, they were able to differentiate metastatic spinal lesions from degenerative changes using FDG PET/CT. Of note, the correlation of the degree of FDG uptake to the severity of CT findings although significant was weak, and therefore the authors hypothesized that this observation is related to the occurrence of

metabolic changes preceding structural changes, which are delayed for an extended period of time (127).

One of the first studies to show that the FDG PET findings precede symptomatic findings in OA was that of von Schulthess et al. The authors found a strong correlation of FDG uptake with age, and attributed this to subclinical chronic inflammation in the early stages of OA. Of note, FDG uptake did not correlate with joint symptoms, and the authors felt that this observation demonstrated the high sensitivity of PET in the detection of joint disease (128).

Wandler et al. took this one step further and identified FDG uptake patterns on PET for specific types of joint disease. They observed FDG uptake in 21 patients after a clinical diagnosis of shoulder disease had been established by clinical examination. Of these 21 patients, 14 had clinical findings consistent with a specific diagnosis in the abnormal shoulder. It was primarily shown that diffuse shoulder uptake on FDG PET was associated with OA, and in addition numerous other findings were made. For instance, two of four patients with focal greater tuberosity uptake of FDG had findings of rotator cuff injury, and two of four patients with focal glenoid uptake had findings of a frozen shoulder. This study thus raised the possibility that FDG uptake patterns may elucidate the type of joint disease (129).

One of the potential problems with using PET in the assessment of arthritis is that there are few studies that have scientifically analyzed age-matched controls. Thus, it is not clear how much the normal aging process may contribute to the appearance of OA-related uptake. This point is brought up by von Schulthess et al. who recognized that without histologic evidence, there was no way to confirm that the strong correlation of FDG uptake and age could be attributed to osteoarthritic changes alone (128).

Another problem of using FDG PET in the diagnosis of OA-related joint damage is a possible lack of specificity. The reason for this is that although the etiology of arthritis may be multifactorial, the degree of FDG uptake may be similar for many processes. This was reported in a study by Elzinga et al. By assessing smaller joints, they found that the number

of PET-positive joints in RA patients was significantly higher than that in OA patients (29 vs. 6%). These numbers reflect the incidence of pathologic uptake among all joints studied, including those with no clinical evidence of inflammation. In RA and OA patients, respectively, 76 and 100% of joints with clinical evidence of inflammation showed increased FDG uptake. Conversely, no increased uptake was found in the joints of control patients with fibromyalgia. The authors concluded that FDG uptake alone is difficult to use for differentiation between RA and OA since secondary OA or OA-induced synovitis may falsely contribute to joint uptake in RA (112).

Additionally, it is difficult to differentiate septic from aseptic inflammatory uptake. Some studies have even used FDG uptake as an indicator of infection and to exclude DJD in a given setting. For instance, Stumpe et al. concluded that FDG uptake was 100% sensitive and 100% specific for infection of a joint, and used this approach to differentiate between infectious and inflammatory processes (130).

Disease burden assessment:

Although there are only few studies which have assessed FDG PET as a means to measure the disease burden in OA, FDG PET has the potential to measure both disease burden and the extent of OA-related changes throughout joint structures in the body.

Nakamura et al. were one of the first groups to study FDG PET in the evaluation of OA. They established that FDG uptake is higher in knees involved by OA than in normal knees. They concluded that PET provides specific in vivo regional information about the inflammation associated with OA (131).

Despite the correlation of SUV with age and presumed osteoarthritic changes, there are few studies which have been able to show a correlation of SUV with clinical parameters. Parsons et al., examined patients with OA and painful knee joints. Of the 18 knees reported to be painful, 78% had knee joint space SUV_{max} which exceeded the average SUV_{max} of control knees. Similarly, 83% of painful knees had synovial

SUV_{max} that exceeded that of control knees. The difference between the two groups was found to be significant for both joint space and synovial uptake of FDG. The authors concluded that pain in the joint due to inflammation is associated with increased metabolic activity as seen on FDG PET (132).

Ankylosing spondylitis:

Ankylosing spondylitis (AS) is a chronic inflammatory joint disease which has a predilection for the spine, sacroiliac joints, and pelvic joints, leading eventually to spinal fusion. Aseptic spondylodiscitis is a classic complication of AS. This entity has been shown to correlate with FDG uptake (133).

Wendling et al. studied three patients with MRI documented lumbar aseptic spondylodiscitis requiring anti-TNF-alpha treatment. They were studied before and after 6 weeks of therapy using FDG PET in parallel with MRI and clinical evaluation. FDG uptake was evident at all sites of discitis in the three patients. Overall, PET was less capable of correctly identifying clinical response when compared to MRI, which was attributed to global FDG uptake in the red marrow of the lumbar spine (134).

A study included 15 patients with AS according to the modified New York criteria (AS group) and with active disease and 13 patients with mechanical low back pain (MLBP; control group) who were investigated with whole-body ^{18}F-PET/CT. The ratio of the uptake in the sacroiliac joint and that in the sacrum (SIJ/S) was calculated for every joint. It was found that quantitative ^{18}F-PET/CT may play a role in the diagnosis of sacroilitis in active AS and is an alternative to conventional bone scintigraphy in times of molybdenum shortage (135).

Juvenile idiopathic arthritis:

Juvenile idiopathic arthritis (JIA) is a childhood rheumatic disease defined as a clinically heterogeneous group of disease involving one or more joints with swelling, pain, or limited range of movement for at least 6 weeks, with age of onset younger than 16 years. It is the most common

form of arthritis that affects children and differs significantly from the types of arthritis seen in adults (136).

JIA can be divided into three categories: systemic, oligo-articular, and poly-articular. As implied by the name, the cause is unknown. However, with proper treatment, individuals can recover and lead normal lives. As with other arthritic assessments described above, therapy in JIA is currently guided by changes detected via structural imaging, even though radiography is insensitive to detect acute erosive changes in the cartilage. This suggests that FDG PET may be a promising modality for optimal patient management through earlier detection of JIA (136).

Tateishi et al. conducted a retrospective study to examine the clinical validity of FDG PET in JIA. They found that joint tenderness and swelling had a positive association with abnormal FDG uptake in the joint [odds ratio (OR) 5.37 and 7.12, respectively]. The SUV_{max} correlated with the neutrophil count, serum CRP and ESR. Joint erosion (OR 6.17), soft tissue swelling (OR 3.77), major joint involvement (OR 3.50), tenderness (OR 5.22), and serum CRP concentration (OR 1.81) were also associated with the FDG uptake as measured by SUV_{max} (137).

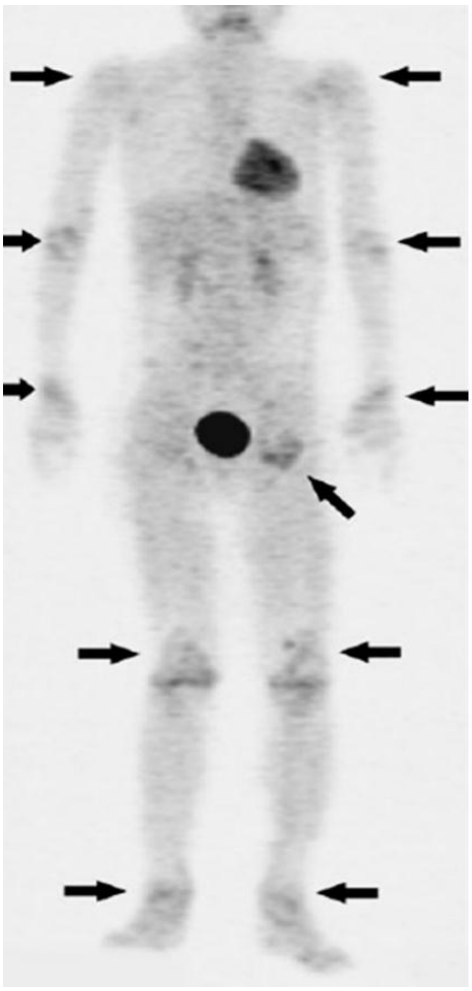

Fig. 15. A 9-year-old girl with polyarticular JIA. Whole-body 18F-FDG PET performed at presentation shows abnormal uptake of six major joints (arrows). The SUVmax of the involved joints ranged from 0.9 (left elbow) to 2.3 (left hip and right ankle). Physical examination revealed tenderness and swelling in elbows, wrists, knees, and ankles as well as limited range of motion in elbows (137).

Polymyalgia rheumatica:

Polymyalgia rheumatica (PMR) is a clinical syndrome characterized by stiffness and proximal muscle pain, usually afflicting patients over 50 years of age. PMR is often diagnosed by exclusion of other disorders that can cause similar complaints and by its rapid response to low-dose corticosteroids. The exact nature of PMR is unknown, but it is thought to either be due to vasculitis limited to the subclavian or axillary arteries or a synovitis of the shoulder and/or hip joints (138).

While many studies have documented increased FDG uptake in the major vessels, several studies and case reports have recently demonstrated more consistent uptake in the large joints in these patients (138).

In a prospective study by Blockmans et al., 35 patients with isolated PMR underwent FDG PET imaging before, 3 months after, and 6 months after treatment with corticosteroids. Total vascular score (TVS) was calculated as well as joint FDG uptake in the shoulders, hips, and spinous processes of the vertebrae. Overall, it was found that while mean TVS was low, FDG uptake in the shoulders, hips, and spinous processes was high (94, 89, and 51%, respectively) (139).

In another study, a similar finding was noted, although 32% of the control patients, who were matched for age and inflammatory parameters with 25 giant cell arteritis (GCA)/PMR patients, demonstrated increased FDG uptake. In retrospect, five of these control patients were found to actually suffer from RA, reactive arthritis, or psoriatic arthritis, and therefore may not be considered normal controls. It was concluded that FDG uptake in the shoulders or hips has a low specificity for PMR, but a high sensitivity (140).

In both of these studies, FDG uptake was not useful for monitoring response to corticosteroid therapy. Instead, after 3 and 6 months, laboratory tests such serum CRP and ESR decreased and provided the same amount of information as FDG uptake levels which also decreased. Thus, the authors concluded that repetitive PET scans in PMR patients offered no advantage for assessing response. Four patients with PMR were studied, ^{18}F- FDG PET/CT demonstrates uptake in the shoulder and hip joints and also interspinous and supraspinous focal and diffuse uptake. The authors propose that diffuse uptake may reflect ligament inflammation with focal uptake in adjacent interspinous bursitis (141).

Diabetic neuropathic arthropathy:

FDG PET appears to be of significant value in patients with complicated diabetic joint disease.

A study by Basu et al. demonstrated that FDG PET may help distinguish neuropathic osteo-arthropathy in the setting of the complicated diabetic foot, which is diagnostically challenging, by using clinical assessment and structural imaging techniques. This prospective study was designed to

investigate the usefulness of FDG PET in the complicated diabetic foot and specifically to determine if PET can show a difference between the uptake patterns in osteomyelitis vs. Charcot's neuropathy. In this study, 63 patients (17 patients with clinical diagnosis of Charcot's neuropathy, 21 patients with uncomplicated diabetic foot, 5 patients with osteomyelitis secondary to a complicated diabetic foot, and 20 non-diabetic patients with normal lower extremities) were examined with FDG PET and MRI consecutively. Abnormal uptake patterns were identified visually by comparison to the contralateral foot and by detecting areas of focal abnormality in the foot. Quantitative assessment was performed by measuring SUV_{max} of the affected sites. Imaging findings were compared with histopathologic results and clinical outcome when possible (Fig. 16). A low degree of FDG uptake was noted in Charcot joints which was greater than that in normal joints. SUV_{max} in osteomyelitis of the foot as a complication of diabetes mellitus was significantly higher than in Charcot joints. The SUV_{max} in Charcot joints ranged from 0.7 to 2.4 (mean 1.3± 0.4), whereas the SUV_{max} of normal mid-foot joints and of the uncomplicated diabetic foot ranged from 0.2 to 0.7 (Mean 0.42±0.12) and from 0.2 to 0.8 (mean 0.5±0.16), respectively (142).

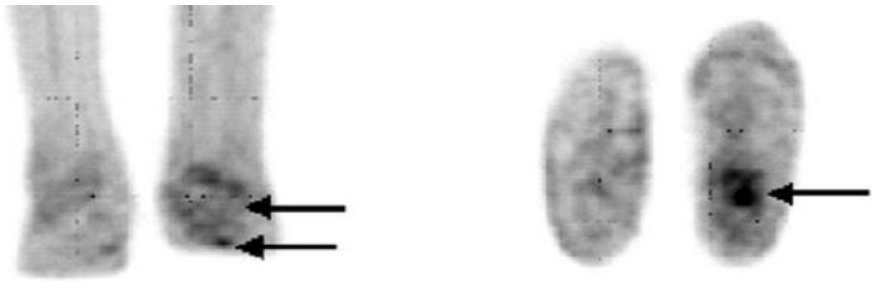

Fig.16. FDG PET in one patient with Charcot's neuro-arthropathy with foot ulcer. Note the focal uptake in the ulcer and the relatively low-grade diffuse uptake in the neuropathic osteo-arthropathy (arrows) (142).

Importantly, in the setting of a diabetic foot ulcer, PET was able to exclude the presence of osteomyelitis and had an overall accuracy and sensitivity for the diagnosis of Charcot foot greater than those of MRI. Overall sensitivity and accuracy in the diagnosis of Charcot foot were 100 and 93.8%, respectively, for FDG PET without co-registered CT and for MRI were 76.9 and 75%, respectively (142).

FDG PET also showed focal abnormalities which suggested soft tissue inflammation (n=7), which were proven histopatologically to be secondary to infection (142).

Role of FDG PET in Cardiovascular Inflammation

The underlying pathologic mechanism of most acute coronary syndromes is atherosclerotic plaque rupture. One cause of rupture is plaque inflammation, leading to fibrous cap destabilization (143).

Role of FDG PET in Atherosclerosis:

Atherosclerosis is the leading cause of death in developed countries in both men and women (143). A significant portion of health resources is placed to identify and treat those patients at high risk for developing cardiovascular events. The underlying pathologic mechanism of most acute unstable clinical syndromes is plaque rupture secondary to inflammatory cell infiltration (144).

Currently, imaging is generally used in patients who are symptomatic, although there is growing interest in identifying subjects at high risk before their first cardiovascular symptom. Imaging techniques used to identify atherosclerosis include x-ray coronary angiography, multi-detector CT, MRI, and ultrasound. These yield either a silhouette of the vessel lumen (angiography) or can image the artery wall directly (CT, MRI, and ultrasound) (145).

However, none of the above modalities give a direct noninvasive readout of plaque inflammation.

Biology of Atherosclerosis as It Relates to FDG PET:

Inflammation plays a key role in the initiation and progression of atherosclerosis and in triggering plaque rupture. It is believed that inflammation exerts its detrimental effects by degrading the fibrous cap, increasing apoptosis of the resident smooth muscle cells, and increasing the neovascularity of the plaque. The plaque type most associated with plaque rupture is the thin-cap fibroatheroma. These plaques are characterized by the presence of heavy macrophage infiltration. Patients

with acute ischemic events usually harbor multiple ruptured atherosclerotic plaques. Therefore, one approach to identify high-risk patients is noninvasive targeted inflammation imaging across several vascular beds. Quantifying such inflammation is useful for two reasons. First, it might allow refinement of current risk scores and target therapy to those most at risk. Second, serial noninvasive inflammation imaging would allow testing of novel anti-atherosclerotic drugs for efficacy (146).

For FDG PET to be able to image atherosclerosis there must be glucose usage by key cell types within the plaque. This seems to be the case, at least with inflammatory cells. Although macrophages can use fatty acids as fuel, an inflamed plaque has a macrophage-rich core that has a high metabolic rate, so it is often restricted to anaerobic metabolism. Given these anaerobic conditions, inflammatory cells favor production of adenosine triphosphate via the glycolytic pathway. Therefore, the greater the degree of inflammation in a plaque, the greater the rate of glucose consumption (147).

Atherosclerosis Imaging with FDG:

Atherosclerosis imaging with FDG PET has been demonstrated across multiple vascular beds, since the first prospective study. These include the carotid arteries, vertebral arteries, aorta, iliac, femoral, and popliteal arteries as well as the coronary circulation (148).

Generally, the degree of FDG uptake increases with the number of cardiovascular risk factors, including diabetes. The strongest predictors of FDG uptake appear to be male sex and advancing age, particularly if these are combined with the metabolic syndrome. Vascular FDG uptake appears to be linked with the presence of other high-risk imaging features of plaque instability, including echolucency on ultrasound, plaque hemorrhage or lipid-rich plaque on MRI, and the uptake of a macrophage-specific CT contrast agent (149).

Additionally, in a prospective study in subjects with recent transient ischemic attack, patients with micro-emboli on trans-cranial Doppler imaging had carotid plaques with significantly higher FDG uptake (150).

FDG uptake in vessels has been shown to correlate to quantitative gene expression of known markers of inflammation and plaque vulnerability (eg CD68) (151).

There are also positive associations with several pro-inflammatory biomarkers including matrix metalloproteinase 1, 3, and 9, along with negative correlations with the athero-protective adiponectin (152).

One study also reported a positive correlation with C-reactive protein levels (149).

Prognostic Implications of Vascular FDG Uptake:

In the absence of definitive prospective studies, information about the prognostic importance of arterial FDG uptake has been derived from cohort studies of patients undergoing imaging for oncological reasons.

In a study by Paulmier et al. arterial wall FDG uptake was compared in two patient groups matched for cardiovascular risk. In the high FDG uptake group, old cardiovascular events (>6 months before or after PET imaging) and recent cardiovascular events (<6 months before or after PET imaging) were significantly more frequent than in the low FDG uptake group (48% vs 15%, respectively [P=0.0006], and 30% vs 1.8%, respectively [P=0.0002]). In addition, high FDG uptake patients had a significantly higher calcification index than low FDG uptake patients. However, the localization of vascular calcifications and FDG hot spots did not match, with FDG hot spots often located between areas of calcification (153).

In a similar oncological prospective study by Rominger et al. the investigators excluded patients with known cardiovascular disease at baseline. During a 29-month follow-up of 900 subjects, there were 15 adjudicated cardiovascular events. When those subjects with events had their PET scans compared to the asymptomatic cohort, they had a significantly higher arterial FDG score. The authors established a cutoff of a target-to-background ratio of 1.7 for prediction of cardiovascular events. It was also suggested that the combination of arterial FDG uptake and calcification was the best predictor of future vascular events (154).

Arauz et al. suggested an SUV cut-off of 2.7 for predicting adverse events in the carotid circulation, when FDG imaging was performed prior to carotid intervention (155).

A study was done for quantification of FDG uptake in atherosclerotic plaque involves measurement of the standardized uptake value (SUV) of an artery of interest and of the venous blood pool in order to calculate a target to background ratio (TBR), which is calculated by dividing the arterial SUV by the venous blood pool SUV. This method has shown to represent a stable, reproducible phenotype over time, has a high sensitivity for detection of vascular inflammation, and also has high inter- and intra-reader reliability (156).

Reproducibility of FDG PET Atherosclerosis Imaging:

Reproducibility statistics for FDG PET compare favorably with those published for MRI and ultrasound measures of plaque burden. In the longer term, there seems to be a degree of progression of FDG uptake in arterial segments, with smaller changes noted in calcified segments in the same patients. This situation may be due to active, FDG-avid plaques becoming burned out, with calcification a manifestation of this late phase of atherosclerosis (157).

Tracking Vascular Inflammation with Therapy Using FDG PET:

After publication of an intriguing preclinical intervention study using probucol (158), Tahara et al. (159) investigated whether low-dose simvastatin attenuated plaque inflammation. They studied 43 consecutive subjects undergoing FDG PET imaging for cancer work-up. Subjects were randomized with half receiving simvastatin (n=21) and the other half receiving dietary management without medication (n=22). Simvastatin significantly attenuated plaque FDG uptake by around 10% in this statin-naive population. Of interest, the decrease in FDG uptake correlated with high density lipoprotein (HDL) cholesterol elevation, and not with the degree of low-density lipoprotein cholesterol reduction (160).

In a similar study of 60 healthy (non-oncology) patients, Lee et al. demonstrated that baseline vascular FDG uptake correlated with several

atherogenic risk factors, and could be significantly lowered by intensive lifestyle modification alone. Once again, the magnitude of inflammation reduction closely correlated with the extent of increase in plasma HDL (161).

FDG PET and Coronary Atherosclerosis:

Given the previous data, it is logical to expect that FDG PET imaging might generate useful data about inflamed plaques within the coronary arteries. However, there are several challenges. The coronary arteries are small and constantly in motion, especially their distal portions. In addition, the respiratory cycle can mean mismatch between CT and PET data sets, which are acquired asynchronously (162).

The myocardial muscle itself can use glucose as a fuel, and it therefore accumulates FDG, swamping any such uptake within the coronary artery unless attempts are made to switch myocardial metabolism to fatty acids. This can be achieved, at least in some subjects, by administration of a high-fat, low-carbohydrate diet to suppress glycolysis and thereby decrease myocardial FDG uptake (162).

Despite these obstacles, coronary artery plaque imaging with FDG has been reported by several groups.

Dunphy et al. showed that FDG PET imaging was possible within the proximal coronaries. In addition, they found that patients with coronary FDG uptake were four times more likely to have documented coronary artery disease and also noted a correlation between an abnormal myocardial perfusion scan and coronary artery FDG uptake (163).

In a prospective study in a non-oncology cohort of patients, Rogers et al. demonstrated that plaque activity within recently stented culprit lesions in acute coronary syndrome patients was significantly higher than within recently stented plaques in stable patients. Importantly, they also noted that ascending aorta FDG uptake correlated with coronary artery FDG uptake this finding may negate the need to attempt coronary artery imaging if substantiated by other studies (148).

Wykrzykowska et al. observed a correlation between the presence of angiographic disease and FDG uptake signal in the coronary arteries (P=0.07; 80 vessels examined) (162).

Saam et al. (164) conducted a retrospective analysis of almost 300 cancer patients and measured FDG uptake in the coronary arteries. The authors reported that they could evaluate coronary artery FDG uptake in about half of the subjects; the others had myocardial FDG uptake that precluded this. In those with coronary FDG uptake, there was a correlation between the number of several cardiovascular risk factors, the pericardial fat volume, and the quantity of calcified plaque present in the coronary arteries (164).

Aortic inflammation & FDG-PET/CT :

Aortic pulse wave velocity (PWV) is the velocity by which the arterial pulse wave travels along the aorta. It mainly depends on the elasticity of the arterial walls, which leads to a dilation at the time of inflow. This precise index of aortic stiffness has also been established as a strong indicator of the risk of cardiovascular events in various study populations (165). It has additionally been shown to be related:

- To the amount of aortic calcifications, giving evidence of the role of arterial structural damages (166).
- To biological signs of inflammation, especially CRP plasma levels (167), another indicator of cardiovascular risk. It may be questioned therefore whether aortic stiffness may also be influenced by inflammation of the aortic walls (168).

Presently, aortic inflammation can be detected and monitored in vivo by using hybrid imaging systems, where CT imaging of FDG. It is not known, however, whether this sign of inflammatory infiltrate is associated with an enhancement in arterial stiffness.

In a population of patients routinely referred for hybrid PET/CT imaging, A pilot study was planned in order to analyze the relationship between arterial stiffness, assessed by PWV, and the respective amounts of aortic calcification and inflammation in patients routinely referred for oncologic causes (169).

It's showed that aortic stiffness is also influenced by aortic inflammation, identified by hybrid FDG-PET/CT imaging, even if this influence appeared to be limited compared with that related to aortic calcifications. The rationale of the use of PET imaging in this setting is that FDG is actively trapped by activated inflammatory cells. This point was previously established in cell cultures and in studies where the results of vascular FDG-PET imaging could be correlated with histological analyses of atherosclerotic lesions (170).In that study (169), the best prediction of the central aortic PWV was achieved by averaging the SUV_{max} of each artery slice over the first half of thoracic aorta (ascending portion and arch), in addition to the determination of the calcium volume on the same aortic segments. Under normal conditions, indeed, the initial part of aorta shows higher elasticity because of the higher density of elastin fibers. It is therefore in this initial part that the parietal damage is likely to have the most deleterious effects on global compliance and elasticity of the aorta (171).

In previous human studies, FDG activity in the aorta has generally been quantified using mean or maximal SUV values expressed in absolute values or relative to the activity from a venous blood region. All these parameters were tested in the present pilot study and the best relationship with central PWV was achieved with maximal SUV values. This remains to be assessed in a much larger series, but it may be hypothesized that such maximal values might better reflect the activity achieved within the thin parietal foci of FDG, as documented in the examples in (Fig. 17) (172, 173).

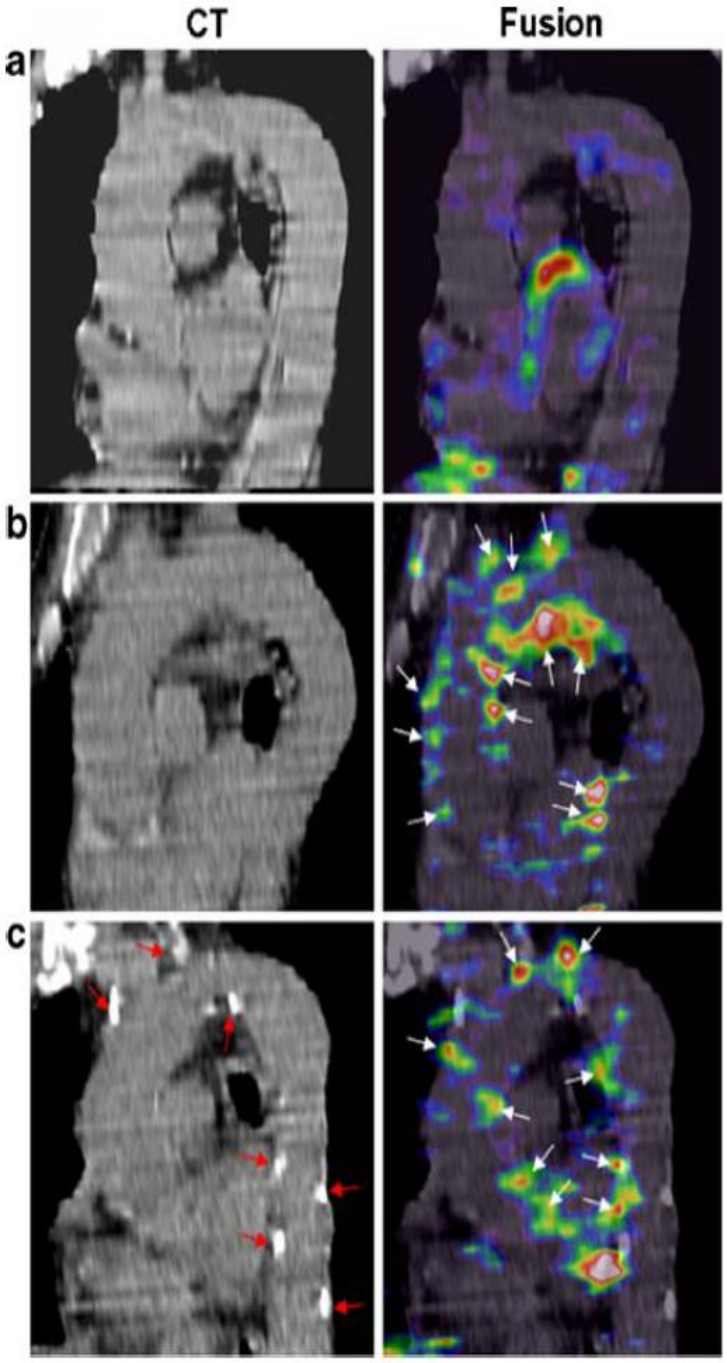

Fig. 17. Representative CT images (left) and fusion of CT and PET images (right) obtained in the same slices, orientated in a sagittal oblique direction and including the aortic arch:
a) a 56-year-old patient with low aortic PWV (8 m.s−1), no aortic calcifications and a low level of FDG activity (average SUVmax on initial half of thoracic aorta 1.5); **b)** a 66-year-old patient with a higher aortic PWV (13 m.s−1), a high level of FDG activity (average SUVmax 2.5) but a low amount of calcifications;
c) a 67-year-old patient with an even higher aortic PWV (20 m.s−1) and both a high amount of calcifications (red arrows) and a high level of FDG activity (average SUVmax 2.5). FDG activity is represented with a colour scale starting just upon the aortic blood activity and with a maximum set to 200% of this blood activity. In this way, parietal foci of FDG can be seen in the two patients who exhibited high levels of aortic activity (white arrows) (173).

In agreement with the previous studies, which were conducted in comparable populations of patients referred for an oncological PET investigation (163, 174-176), it's found that aortic FDG activity was related to age and to the number of cardiovascular risk factors. The original observation of a relationship between aortic stiffness, assessed by aortic PWV, and aortic FDG activity is not surprising since inflammation is commonly involved in the active stages of atherosclerosis development (177). Moreover, this inflammation is known to induce functional and structural changes, which are likely to enhance arterial stiffness. These changes include impairment in the nitric oxide dependent

endothelial relaxation (178) and an increased activity of certain matrix metalloproteinase leading to breakdown of the elastin network (179).

Such mechanisms might be expected to significantly enhance aortic stiffness, but not at the level reached by the massive arterial calcifications that are detected by CT. This is presumably the reason why VCa was a much stronger predictor of aortic PWV than aortic FDG activity. A strong relationship between PWV and arterial calcifications has already been documented in experimental animal models, as well as in particular populations of patients showing high rates of vascular calcification, in patients with diabetes or end-stage renal disease, i.e. in subjects at very high cardiovascular risk (166).

This relationship has never been previously assessed in patients not belonging to these specific high-risk groups

In a multivariate stepwise model, SUV_{max} was an important determinant of central aortic PWV adding 11% of the variability of the central aortic PWV. Interestingly, contrary to the fixed areas of aortic calcifications, a high level of aortic FDG activity is likely to give evidence of a still ongoing parietal process involving activated inflammatory cells (169).

Further follow-up studies are required to assess the effects on aortic stiffness of a subsequent healing process which might involve arterial fibrosis and calcification.

Calcifications are indeed generally considered to occur at a final and relatively stable stage of arteriosclerosis, whereas FDG trapping by inflammatory cells may provide evidence of a much more transient and earlier stage (174).

In a previous FDG-PET/ CT study, certain aortic foci with high levels of FDG activity were shown evolving through a calcification process, which was detectable by CT imaging at a median time of only 13 months. Such a relationship might offer new opportunities for preventing subsequent aortic stiffening, especially by statins, which have recently been shown to lower the arterial FDG uptake in humans (159).

Large vessel vasculitis & FDG PET(/CT):

Two forms of primary large vessel vasculitis (LVV) were distinguished: giant cell arteritis (GCA) and Takayasu arteritis (TA) (180).

GCA is the most common form and has an incidence of 20 per 100,000 in the population aged over 50 years. Women are affected twice as often as men (181). Characteristically, it affects the temporal artery, resulting in temporal arteritis as a synonym for GCA. Temporal arteritis does not cover the whole clinical spectrum however; since the entire aorta and all its branches can be affected .The clinical presentation is variable and includes typical signs of temporal arteritis (e.g., headache, jaw claudication, and scalp tenderness) but also several nonspecific symptoms, such as fever, malaise, fatigue, and myalgia (182).

The diagnostic reference method for GCA is a temporal artery biopsy, but the test results can be false negative. A false negative rate of 15–70% is reported; therefore, the incidence of GCA might be underestimated (183).

TA is the second form of primary LVV and primarily affects the aorta and its main branches as well as the coronary and pulmonary arteries. It has an incidence of only 2 per 1,000,000. The mean age of onset is 35 years and the prevalence in women is 2 to 25 times higher than in men, depending on the series considered (184). The clinical picture is somewhat similar to that of giant cell arteritis (185), but many of the typical signs of temporal arteritis are not commonly found in TA (186). TA can have a quite devastating course, reflected in a mortality rate as high as 35% at 5 years, similar to that seen in malignancies (187).

Several findings however, suggest that GCA and TA may be two processes within the spectrum of the same single disease (185). Despite that in the course of the disease stenosis, occlusions, and aneurysms may occur, it is reported that early diagnosis and monitoring of TA are both hampered as serological and inflammation parameters are unreliable (188).

Both fluorodeoxyglucose positron emission tomography (^{18}F-FDG PET) and pathology studies revealed that the inflammation of TA affects mainly the aorta and its branches, but in a more focal and localized, inhomogeneous pattern than seen in GCA and with more intense FDG uptake than GCA. TA may also present as isolated involvement of renal arteries, pulmonary arteries, vertebral arteries, or coronary arteries (189).

Imaging studies play an important role in diagnosing and monitoring LVV. Angiography, ultrasonography, CT, and MRI used to be the most commonly employed imaging techniques. The differential diagnosis with accompanied atherosclerotic development can be very difficult however. Even if vasculitis can be diagnosed by angiography, differentiation between active vasculitic lesions and plaque formation is difficult.

In more recent years ^{18}F-FDG PET has become an increasingly important diagnostic tool for diagnosing LVV (190). Because the morphological changes in the vessel wall are preceded by inflammatory activity, LVV can be diagnosed in an earlier stage than with the conventional imaging techniques (191). ^{18}F-FDG PET also identifies more regions of the aorta and its branches involved in the inflammatory process than MRI (192). Hybrid ^{18}F-FDG PET/CT seems to be superior to ^{18}F-FDG PET alone in this; by fusing the functional images of the ^{18}F-FDG PET with the anatomical images of the CT, it is easier to localize regional ^{18} F-FDG uptake (Figs. 18) (193).

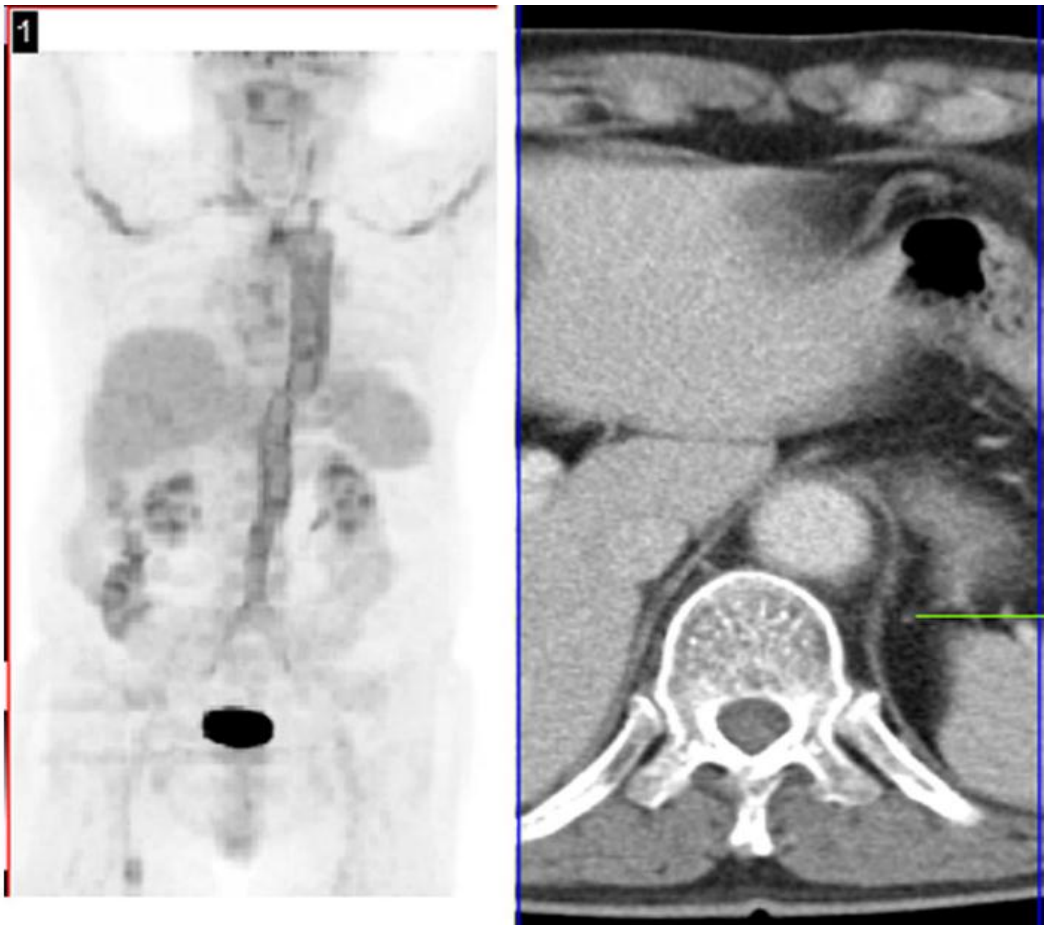

Fig. 18. Left image is a maximum intensity projection of the PET investigation showing pathological activity in aortic arch and abdominal aorta until the bifurcation, and in both subclavian arteries and art. brachialis on both sides. SUV $_{max}$ 4.3. Right image is a transverse CT slice showing wall thickening of the aorta at the level of the crus of the diaphragm (193).

Hybrid ^{18}F-FDG PET/CT is able to identify focal vascular inflammation and focal vascular calcification as different phases of atherosclerosis in order to exclude this as the cause of the increased ^{18}F-FDG uptake As a result, the number of false positive test results will be reduced, thereby increasing the specificity of the technique (194).

On the other hand, due to the low incidence, a high proportion of negative test results of ^{18}F-FDG-PET/CT for LVV can be expected. This is undesirable from cost-effectiveness point of view, although a negative test result for LVV can still be of use, if it provides clues to other diagnoses (e.g., lymphoma, infection).

Few studies have been published to identify clinical and analytical parameters that may improve the effectiveness of the use of ^{18}F-FDG PET (/CT) scans vs. biopsies of the temporal artery for diagnosing GCA.

The results of the ^{18}F-FDG PET scans were compared to biochemical markers of inflammation; the intensity of ^{18}F-FDG uptake appeared to be significantly correlated with CRP, ESR, and thrombocytes (195). On the contrary, it has also been reported that the levels of biochemical markers of inflammation do not always correlate with the results of the ^{18}F-FDG PET scan (196).

In Hooisma et al. study (197) which identify clinical and analytical parameters that may improve the effectiveness of the use of ^{18}F-FDG PET(/CT) scans for diagnosing LVV , something similar is seen all patients with a positive test result for LVV had an elevated CRP, only one of the patients had a normal ESR. The aorta and its main branches are not suitable for routine histological examination; direct proof of vascular inflammation is therefore not possible. However, the hypothesis that a homogeneous/smooth linear pattern of ^{18}F-FDG uptake in the aorta and its main branches, with intensity higher than the liver uptake, is highly suggestive for GCA has considerable indirect evidence:

-There is an established close association between polymyalgia rheumatica and GCA; cytokine mRNA levels (mainly IL-2) are almost identical in specimens (198). Interestingly; moderately increased ^{18}F-FDG uptake in the large vessel walls as a sign of vasculitis in patients with active PMR is reported (139).

Role of FDG PET in hemorrhoids:

Hemorrhoids are present in healthy individuals. The main observations of hemorrhoids are hemorrhage, thrombosis, and prolapse. Several theories have been proposed for the mechanisms of hemorrhoidal development including the varicose vein theory, the sliding anallining theory and the vascular hyperplasia theory, and the neovascularization theory (199).

These pathological changes result in prolapsed anovascular cushions, which subsequently interfere with venous return. Decreased venous

return, thought to be the mechanism of action, induces dilation of the venous plexus, venous stasis, and/or thrombosis (200).

Thrombosis in the venous plexus may elicit an inflammatory response. Moreover, vascular proliferation has been reported to cause an important pathologic change in hemorrhoids, which might be due to thrombosis formation. Therefore, thrombosis, inflammation, and vascular proliferation should be considered in the pathogenesis of hemorrhoids (200).

In a study, eight (5.1%) subjects with hemorrhoids had SUV_{max} higher than 4.1, which was the highest SUV_{max} for the anal region in the normal group. The highest SUV_{max} in the hemorrhoid was 8.3 which was similar to the case reported by Lu et al. In their report, the SUV_{max} in the hemorrhoids was 8.0 (201).

In 2004, Kikuchi et al. found marked accumulation of FDG in internal and external jugular vein thrombosis (202).

In addition, Miceli et al. reported that FDG–PET may be useful in evaluating response to treatment (203).

In 2010, Khosa et al. (204) reported an increased FDG uptake not only within the vein but also the thrombus itself and concluded FDG–PET/CT appropriately shows venous thrombosis and might play a prominent role in the future. Recently, the relationship between angiogenesis and FDG uptake has been discussed (205).

In an animal study, Calcagno et al. found a positive correlation between neovessel count in atherosclerotic plaques and ^{18}F-FDG uptake. They concluded that FDG–PET could be used as a clinical tool in the evaluation of lesion prognosis and monitoring of anti-angiogenic therapies (205).

Role of FDG PET in GIT inflammation

Imaging Abdominal Inflammation:

Abdominal Abscess:

Rapid and accurate diagnosis of an abdominal abscess is crucial. The mortality from untreated abscesses approaches 40% and may reach 100% in some series. The mortality among patients treated reaches. Delayed diagnosis is associated with higher mortality in spite of treatment. If localizing signs suggest abdominal infection, morphological modalities, predominantly ultrasound and CT may be used first, depending on the location of suspected infection in the abdomen. Standard radiographs have low sensitivity, although when seen, findings are specific (206).

The advantages of these modalities are numerous, but most importantly they provide quick results and adequate anatomical details. These studies can be used to guide needle aspiration and abscess drainage. Ultrasound can be used portably for critically ill patients. (206)

One of the major limitations of these modalities is the inability to differentiate infected from non-infected tissue abnormalities, particularly in early stages of infection (phlegmon) before formation of abscesses. (206)

When the results of the morphological modalities are inconclusive, nuclear medicine techniques may be used to detect abdominal infections (206)

In one study, 16% of patients suspected of having abdominal infection in fact had extra-abdominal infections as seen on ^{111}In leukocyte scans (207). Accordingly, negative morphological modalities, when used first, may be followed by whole-body nuclear imaging. Labeled WBC studies are the most specific for acute infections. Ga-67 is more suitable for infection of longer duration.

^{99m}TcHMPAO-labeled WBCs frequently used in critically ill patients after US and/or CT have yielded inconclusive results (208).

It is worthy of note that ^{99m}Tc HMPAO-labeled WBCs provide quicker results than 67Ga- or ^{111}In-labeled WBCs. Minoja et al. (209) reported a sensitivity of 95%, a specificity of 91%, and an accuracy of 94% for ^{99m}Tc-labeled WBC scanning in intensive care unit patients with occult infections. The gallium-67 scan has been reported to have a better diagnostic specificity than the C-reactive protein test for abdominal infections (210).

Role of FDG PET in Inflammatory Bowel Disease IBD:

Upright chest radiography and abdominal series, barium enema and upper GI, CT scanning, MRI and ultrasonography are the main imaging modalities used for the diagnosis. The assessment of the intestinal lumen has traditionally been done by conventional barium studies including barium meal follow through and small bowel enteroclysis. While enteroclysis provides information on the size and site of intestinal strictures, it fails to provide information on the activity of the strictures and surrounding structure (211).

Much interest has been focused on computerized tomography (CT) enteroclysis and magnetic resonance (MR) enteroclysis in recent times to overcome the individual deficiencies of CT/MRI (no distention of the small intestine) and conventional enteroclysis (no extra-luminal information) (211).

Both the CT enteroclysis and MR Enteroclysis are reported to be highly accurate in depicting mucosal abnormalities and extra-intestinal complications in patients with inflammatory diseases of the intestine CT scanning and ultrasonography are best for demonstrating complications such as intra-abdominal abscesses and fistulas. Evaluation of the extent of the disease and disease activity is often difficult. Although these techniques provide excellent anatomical information, they fail to show the metabolic status of the disease activity (211).

Small intestinal endoscopic techniques such as capsule endoscopy and double balloon enteroscopy hold a lot of promise for evaluation of the intestinal lumen; however, they fail to provide information on the intestinal wall and surrounding structures. Therefore, they are combined with a cross-sectional imaging technique such as CT enteroclysis or more often MR enteroclysis (212).

Conventional tracers like radiolabelled leukocytes have been well-established noninvasive scintigraphy techniques and are still widely used for evaluation of the extent and activity of the disease in patients with IBD (213). Leukocyte scintigraphy demonstrated sensitivity of 80% to 98% and specificity of 90% to 100% for the detection of IBD in untreated patients (214).

Scintigraphy using autologous leukocytes, labeled with ^{111}In or ^{99m}Tc, is still considered the “gold standard” nuclear medicine technique for the imaging of infection and inflammation, including evaluation of IBD activity. However, leukocyte scintigraphy suffers from substantial shortcomings of the tedious, time-consuming cell labeling procedure. In addition, this technique has false positive results in patients with mesenteric ischemia, carcinoma of the colon and intestinal bleeding (214).

PET has been used for assessment of various inflammatory disorders and has shown encouraging results (215). The interpretation of abdominal PET images is often difficult due to physiologic uptake of FDG in a variety of abdominal/pelvic organs, which makes it difficult to distinguish normal from abnormal uptake. As the intestine remains in a collapsed state, the resolution of the intestine remains very poor on PET/CT. Therefore, distension of the intestine is required for better resolution on imaging.Combining PET with CT enteroclysis, we proposed to evaluate the intestine after its inflation with negative contrast, a technique called PET-CT enteroclysis(216).

In Chandan et al. pilot study (217) including 17 patients with inflammatory diseases of the intestine, the feasibility and diagnostic yield of PET/CT enteroclysis is assessed. In this study, PET/CT enteroclysis as a single test showed significantly more lesions in the intestine in

comparison to those seen by conventional barium studies and colonoscopic examination in combination. In this study (217), reported the feasibility of PET/CT enteroclysis. The feasibility and accuracy of CT enteroclysis in patients with Crohn's disease has been well documented in the literature (211) .

At times, it may be difficult to differentiate malignant lesions from inflammatory diseases based on the activity seen on PET/CT. For such a differentiation, using dual point FDG-PET imaging, Zhuang et al. observed that the SUVs of delayed images increased significantly over time in malignant lesions, whereas the SUV of inflammatory lesions decreased significantly over time(218).

Segmental pattern of FDG uptake has been reported in patients with proctitis, infectious colitis, lymphocytic colitis and hemorrhagic colitis, whereas a nodular focal or multifocal pattern is seen in polyps, adenoma, and colonic cancer (219).

Diffusely increased FDG uptake has been described in patients with inflammatory enterocolitis (220). FDG uptake has even detected in histologically confirmed mildly inflamed lesions in patients with Crohn's disease where colonoscopic examination appeared normal (220).

A combination of typical patterns of intestinal wall enhancement as seen at contrast-enhanced CT and a diffuse FDG uptake within the small intestine at PET suggests the presence of an inflammatory or an infectious disease with greater certainty (221).

PET has been used in the evaluation and monitoring of children patients with IBD in whom a colonoscopic examination is difficult to carry out.

In a study including 38 patients with Crohn's disease (17 ileal, 12 ileo-colic, 5 pan-colonic, 3 left-sided disease, 1 right-sided disease) and 17 with ulcerative colitis (15 pancolitis, 2 left-sided colitis), Lemberg et al. assessed the value of PET in identifying active intestinal inflammation and compared the results with those seen on conventional endoscopic and radiological studies. PET correctly identified active inflammatory

diseases in 80% of children with IBD (81.5% with Crohn's disease, 76.4% with ulcerative colitis) and correctly showed no evidence of inflammation in children with recurrent abdominal pain. FDG accumulation corresponded with sites of active disease at colonoscopy in 83.8% and with small bowel follow-through with pneumo-colon in 75% of patients (222).

In a retrospective study, Loffler et al. using histology as the standard of reference, reported sensitivity, specificity and accuracy of 98%, 68% 83% with PET-CT as compared that with endoscopic examination (90%, 75%, 82%). For small intestinal lesions, FDG-PET was more reliable (223).

In the evaluation of inflammation in the colon and terminal ileum in patients with Crohn's disease, Neurath et al. reported a sensitivity of 85%, 67% and 41%, respectively, and specificity of 89%, 93% and 100%, respectively, of PET, hydro-MRI and granulocyte scintigraphy with labeled antibodies in a comparative study(224).

Pio and colleagues reported a good correlation between the intensity of activity as quantified by FDG-labeled WBCs PET and histo-pathologic grading of the degree of inflammation (52).

One of the main advantages of PET/CT enteroclysis in the evaluation of intestine is the ability to acquire CT enteroclysis scans during the same scanning session as PET scans. It is a non-invasive test that can evaluate both small and large intestine in the same sitting. This test has a potential to differentiate the active form of disease from the fibrostenotic form, especially in Crohn's disease, and therefore can guide treatment. One major issue with the use of PET/CT enteroclysis is radiation exposure where patients are subjected to the ionizing radiation of the CT-scan along with the radioactivity of FDG. However, radiation exposure to a patient undergoing complete intestinal evaluation (enteroclysis and CT-scan of the abdomen) is 12–15 mSV (enteroclysis 3 mSV and CT abdomen 10 mSV), which is more than that given by PET/CT enteroclysis alone (225).

The major limitation of this study is the lack of an endoscopic evaluation of the small intestine for comparison. There was however a correlation

between the lesions seen at colonoscopy and PET/CT enteroclysis. Secondly, there is a lack of follow-up in this study.

Role of FDG PET in post treatment follow up:

Bret et al study evaluates resolution of the appropriate FDG-PET determination after clinical improvement in IBD, showed that PET scanning did show reduced activity following induction of remission in IBD (fig. 19). In this study, patients have active segments on PET scan with no clinical symptoms. Thus, PET can show residual active inflammation in patients who are otherwise in clinical remission, there was no correlation between persistent areas of the appropriate FDG-PET determination and risk for relapse of the disease (i.e., presence of inflammation just below the threshold of clinical symptoms), although this was a small pilot study (226).

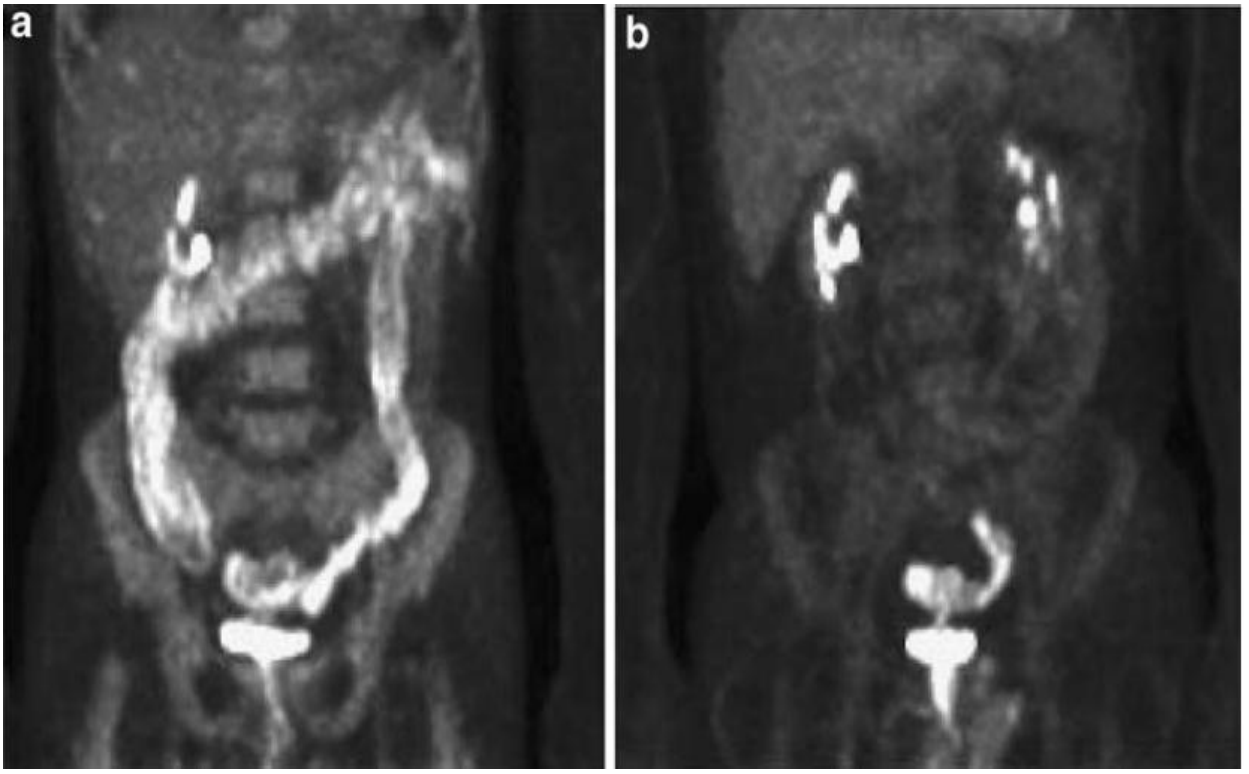

Fig. 19. PET/FDG scan: Anterior view of the MIP image of a patient with ulcerative colitis before (a) and after (b) therapy. The rectosigmoid area continues to be abnormal, but the ascending, transverse and descending colon are now normal. (226)

The time course for reduction of the appropriate FDG/PET determination has also not been studied, criteria for repeat PET scan was

based on improvement of symptoms and not a specified time period after the initial scan.

Duration to repeat PET scan ranged from 77 to 807 days, and in this timeframe, there was no difference in PET results.

Role of FDG PET in autoimmune pancreatitis (AIP) :

Autoimmune pancreatitis (AIP) is a unique form of chronic pancreatitis with a pathogenesis which may involve an autoimmune mechanism (227). It has been reported that AIP is occasionally associated with other autoimmune diseases (228). It is characterized by irregular narrowing of the main pancreatic duct, enlargement of the pancreas, increased levels of serum γ-globulin, IgG or IgG4, the presence of autoantibodies and responsiveness to steroid therapy (229).

The histological features of AIP include a dense lymphoplasmacytic infiltrate of the pancreatic parenchyma and secondary fibrosis. AIP patients frequently have various extra pancreatic lesions EPLs. (230).

Nakamoto et al. carried out FDG-PET studies on six patients with AIP and reported that AIP caused intense uptake of FDG in the pancreas. They also reported that the follow-up PET scans of three patients who had received steroid therapy showed the disappearance of this intense uptake in the pancreas. These researchers performed early (1 h) and delayed (2 h) dual time point imaging to examine the changes in SUV in AIP and found that the SUVs increased with time in three of four patients with AIP. They therefore concluded that the addition of delayed scanning would not help in differentiating malignant tumors from AIP. However, they did not study FDG uptake features of EPLs in AIP (231).

In Nakajo et al. Study, the initial PET scan revealed that all six patients with AIP had intense FDG uptake (grade 3) in the pancreas, which disappeared during and following steroid therapy or spontaneously (232).

A recent study concluded that FDG-PET/CT may be helpful to differentiate AIP from PC (pancreatic cancer) by assessing FDG-uptake

patterns in the pancreas and extra-pancreatic lesions, it may have the potential to assess the disease activity of AIP and its extra-pancreatic lesions, and it may be useful as a monitoring marker for tapering or stopping steroid therapy. (233)

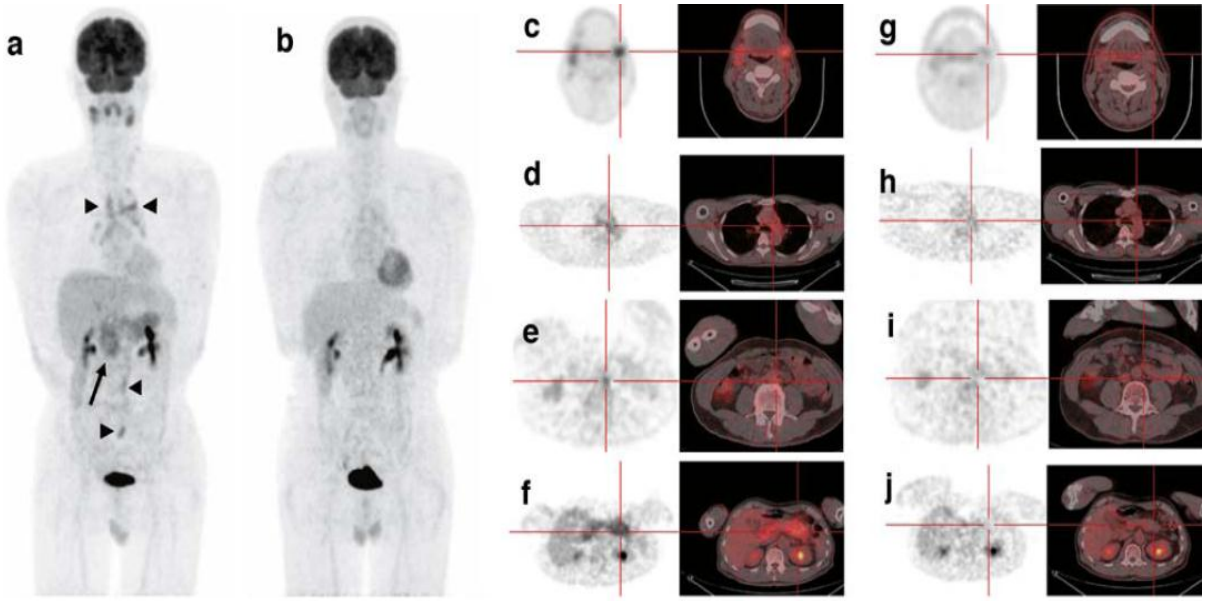

Fig. 20. FDG-PET/CT images of a 53-year-old man with AIP, sclerosing sialadentitis and lymphadenopathy prior to and following steroid therapy (Patient 5). The early whole-body FDG-PET coronal MIP image prior to steroid therapy (a) shows abnormal FDG uptake not only in the entire pancreas (arrow), but also in the bilateral submandibular glands and mediastinal, bilateral hilar and abdominal lymph nodes (arrowheads).The early whole-body FDG-PET coronal MIP image taken during steroid therapy (b) shows no abnormal FDG uptake in the pancreas, submandibular glands and lymph nodes. The early PET/CT images taken prior to(c–f) and during (g–j) steroid therapy show more clearly these changes(c–j). The bilateral submandibular glands, mediastinal lymph nodes and pancreas are reduced in size on CT scans taken during steroid therapy (234)

The value of two-point imaging in the assessment of inflammatory status in AIP and EPLs remains to be elucidated.

When the FDG uptake is noted in the systemic organs or tissues of a patient who has abnormal FDG uptake in the pancreas, AIP should be included in the differential diagnosis of pancreatic diseases. Indeed, in three, the morphological or serological examinations were performed after the initial PET scan, and the diagnosis of AIP was then made. Thus, whole-body FDG PET or PET/CT may be a useful approach for detecting AIP and associated EPLs and for monitoring their disease activity following steroid therapy (234).

Role of FDG PET in pulmonary inflammatory diseases

The role of the chest X-ray cannot be overemphasized. The chest X-ray should be used as the initial imaging modality for most chest pathologies. In many instances, however, an additional modality is needed to evaluate certain chest conditions including infections.

Although CT often clearly depicts chest pathology including infections, ^{67}Ga still is commonly used in such cases. ^{111}In leukocytes have limited utility for chest infections. Siemon et al. studied ^{67}Ga imaging in a variety of pulmonary disorders and found excellent sensitivity and specificity (235).

Gallium-67 has also been widely used in AIDS patients to detect PCP. It is highly sensitive and correlates with the response to therapy. In a study comparing ^{67}Ga, bronchial washing, and trans-bronchial biopsy in 19 patients with PCP and AIDS, ^{67}Ga and bronchial washing were 100% sensitive compared with 81% for trans-bronchial biopsy (236). ^{67}Ga is also valuable in idiopathic pulmonary fibrosis, sarcoidosis and amiodarone toxicity (237).

It is also useful in monitoring response to therapy of other infections including tuberculosis. ^{111}In WBC imaging is less helpful, as the specificity of abnormal pulmonary uptake (either focal or diffuse) is very low.

Non-infectious problems that cause abnormal uptake include congestive heart failure, atelectasis, pulmonary embolism, ARDS, and idiopathic conditions (238).

FDG–PET is a non-invasive imaging technique that has significant potential to quantify pulmonary inflammation with high sensitivity. Pulmonary FDG–PET imaging has demonstrated enhanced FDG uptake in chronic obstructive pulmonary disease (239) and acute lung injury Also, high pulmonary uptake of FDG has been observed in patients with

head injury, who are at risk of developing acute respiratory distress syndrome, but who had no lung symptoms at the time of the scan. It is suggested that FDG–PET imaging can be successfully exploited to study various inflammatory pulmonary disorders and is likely to provide objective means to assess alveolar inflammation in a wide variety of diffuse lung diseases. The feasibility to monitor the extent and activity of the alveolitis during the course of the disease can be utilized for follow-up evaluation to therapy and also can be employed as a biomarker in new drug development (240).

FDG–PET Characteristics Indicating Inflammatory Etiology in Non-specific Mediastinal and Hilar Foci:

Several investigators have examined the variables for determining benign or malignant nature of non-specific uptake in the mediastinum and hilar nodes on FDG–PET scan .The parameters or factors that have been utilized include:

(a) The maximum standard uptake value (SUV_{max}), especially after partial volume correction of the measured value,

(b) dual-time-point PET imaging,

(c) Symmetry,

(d) Site of the primary tumor,

(e)Node size and characteristics as revealed by the computed tomography

(f) absence/presence of FDG-avid foci in non-hilar and hilar mediastinal nodes, and

(g) The degree of stability of uptake between the scans in those who participated in more than two studies in their disease course (240).

Role of FDG PET in Tuberculosis:

Tuberculoma is discrete nodule, usually less than 3 cm in diameter, in which repeated infection has caused a core of caseous necrosis surrounded by zone of epithelioid cells and collagen with peripheral round cell infiltration. Small, discrete shadows in the vicinity of the main lesion, known as “satellite lesions”, are observed in as many as 80% of cases (241).

The promising features of FDG–PET imaging in the management of patients with this disorder are

(a) Its potential role for assessing therapeutic response,

(b) Its ability to detect unsuspected distant sites of infection because of the whole body nature of this imaging technique,

(c) Its role in guiding for a biopsy site (combined PET/CT, in particular, may be very useful for this purpose), and

(d) Diagnosis of suspected recurrence and residual disease following successful therapy (241).

It is important to note that this role for FDG–PET has a geographical relevance as developing countries have high prevalence of tuberculosis and, therefore, the probability of false-positive FDG–PET results are high in the Asian population compared to that of the Europeans or North Americans (241).

In a study aimed to evaluate the diagnostic value of dual time point imaging (DTPI) of ^{18}F-FDG/CT for detecting the infective lesions in patients with extra-pulmonary tuberculosis (EPTB), it was found that early whole body PET/CT imaging may be sufficient for the detection of the EPTB lesions and DTPI of PET/CT may also not be a useful technique in differentiating between EPTB and non-EPTB lesions. (242)

Another study was made to describe patterns of pulmonary tuberculosis on FDG-PET/CT. It identified two distinct patterns of pulmonary TB on FDG-PET/CT. The lung pattern related to a restricted and slight hyper-metabolic infection and the lymphatic pattern related to a systemic and intense infection. Combined interpretation of PET and CT findings improves the specificity of images, especially for the lung pattern. (243)

Role of FDG PET in Sarcoidosis:

Sarcoidosis is a chronic granulomatous multiorgan disease of unknown etiology that most frequently involves the lungs which is the major cause of morbidity in these patients. The disease is characterized in affected organs by an accumulation of T lymphocytes and mononuclear phagocytes, non-caseating epithelioid granulomas, and derangements of the normal tissue architecture.

Disease activity in sarcoidosis can be best assessed by detecting and quantifying the degree of inflammatory and granulomatous reactions that occur in the lungs. Since both sarcoidosis and lymphomas affect lymphoid systems throughout the body, the pattern noted on the FDG–PET images is non-specific and cannot differentiate between the two distinct entities (Fig. 21) (244).

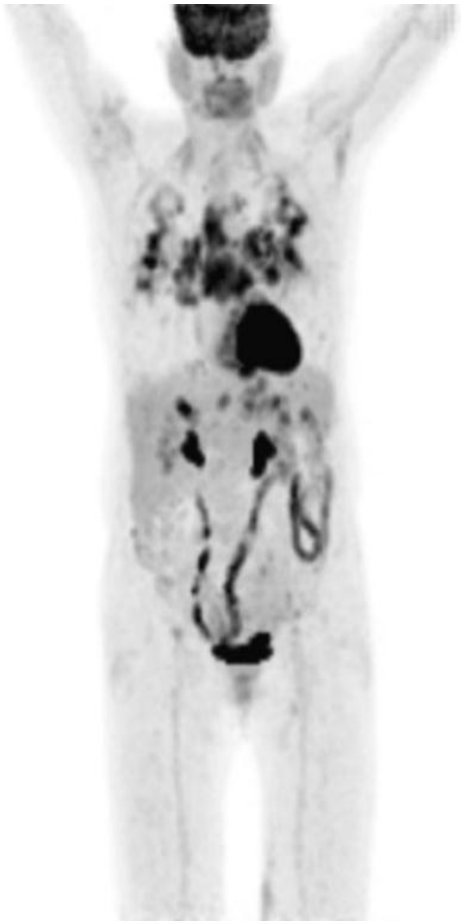

Fig. 21. Whole-body FDG–PET demonstrating avid FDG uptake in the mediastinal nodes and bilateral lungs in a proven case of sarcoidosis. (244)

To evaluate the role of FDG–PET/CT in sarcoidosis, Braun et al. retrospectively assessed 20 consecutive patients with biopsy-proven sarcoidosis. For thoracic, sinonasal, and pharyngo-laryngeal localizations, the sensitivity of FDG–PET/CT was 100%, 100%, and 80%, respectively, for these sites. Overall sensitivity for all 36 biopsy-proven localizations improved from 78% to 87% after excluding skin involvement. When ^{67}Ga scintigraphy and ^{18}F-FDG PET/CT were compared for the 12 patients who underwent both examinations, the overall sensitivity of ^{67}Ga

scintigraphy was 58% and 79%, and by using FDG–PET improved to 67% and 86% after excluding all sites of skin involvement (244).

A study was done to develop a prediction rule that can be used to identify symptomatic sarcoidosis patients who have a high probability of PET-positivity. It concluded that ^{18}F-FDG PET/CT is a useful adjunct to other diagnostic methods for detecting active inflammatory sites in chronic sarcoidosis patients with persistent symptoms, especially those with normal ACE levels. ^{18}F-FDG PET/CT proved advantageous for determining the spread of active disease throughout the body and influenced the decision to adjust the therapy (245).

Another study done to develop a prediction rule that can be used to identify symptomatic sarcoidosis patients who have a high probability of PET-positivity. It concluded that the derived and internally validated clinical prediction rule, based on sIL-2R levels and HRCT scoring results, appeared to be useful to identify sarcoidosis patients with a high probability of inflammatory activity. Using this rule may enable a more effective use of PET scan for assessment of inflammatory activity in sarcoidosis (246).

Role of FDG PET in Occupational Pleuropulmonary Disorders:

Pneumoconiosis includes coal worker's pneumoconiosis, silicosis, and asbestosis of which silicosis and asbestosis are the two major types. Data on the PET appearance of pneumoconiosis has been reported in the literature. FDG uptake has been observed in pneumoconiosis and progressive massive fibrosis. This uptake may be related to the presence of inflammatory cells such as macrophages, as well as fibroblasts (247).

In a prospective evaluation study. 55 consecutive patients referred for the evaluation of suspected malignant pleural mesothelioma (MPM) and recurrence of MPM underwent two sequential PET scans (dual-time-point imaging). The mean ±SD of the $SUV_{max}1$, $SUV_{max}2$, and Δ% SUV_{max} in both newly diagnosed and recurrent MPM were significantly higher than those of benign pleural disease group (PG0.0001). It was also observed that there is increasing uptake of ^{18}F-FDG over time in pleural

malignancies, whereas the uptake in benign pleural disease generally stays stable or decreases over time. The study results indicated that the dual-time-point imaging may help in differentiating benign from malignant pleural disease by increasing the sensitivity and is also helpful for guiding the biopsy site for diagnosis (248).

FDG-PET in the idiopathic interstitial pneumonias (IIPs):

The idiopathic interstitial pneumonias (IIPs) are a heterogeneous group of disorders resulting from damage to the lung parenchyma due to varying patterns of inflammation and fibrosis. Idiopathic pulmonary fibrosis (IPF), nonspecific interstitial pneumonia (NSIP) and cryptogenic organizing pneumonia (COP) comprise the majority of IIP cases. Distinguishing different types of IIP is important because COP is known to show a better prognosis than IPF and NSIP.

In Umeda et al study of 50 patients with IIP, It is found that the early SUV (cut-off: 1.5) in COP was significantly higher than that in IPF and NSIP with reasonable sensitivity and specificity, although no significant difference between IPF and NSIP was observed. On the other hand, a positive value of RI-SUV (cut-off: 0%) predicts the deterioration of pulmonary function within a 1-year observation period in patients with IIP. However, early SUV was not a significant predictor of disease progression. With regard to image diagnosis of IIPs, the early SUV level of ^{18}F-FDG PET could be useful for distinguishing COP from IPF and NSIP. The main histopathologic feature of COP is a patchy process characterized primarily by organizing pneumonia involving variable numbers of inflammatory cells, such as lymphocytes, macrophages and neutrophils, with a lower degree of interstitial fibrosis, as compared to IPF and NSIP (249).

Nagai et al. noted that increased cell recovery and percentage of lymphocytes in BAL fluid were found in patients with COP compared to those with IPF These findings suggest that the degree of inflammatory cell infiltrates has an effect on early SUV in IIP (250).

The results of Umeda et al also indicate that RI-SUV is useful for determining disease activity as a predictor of disease progression.

Since RI-SUV could predict the deterioration of pulmonary function after 12 months of follow-up examinations, it has potential as a predictor of survival in IPF and NSIP patients at the time of diagnosis (fig. 22, 23) (249).

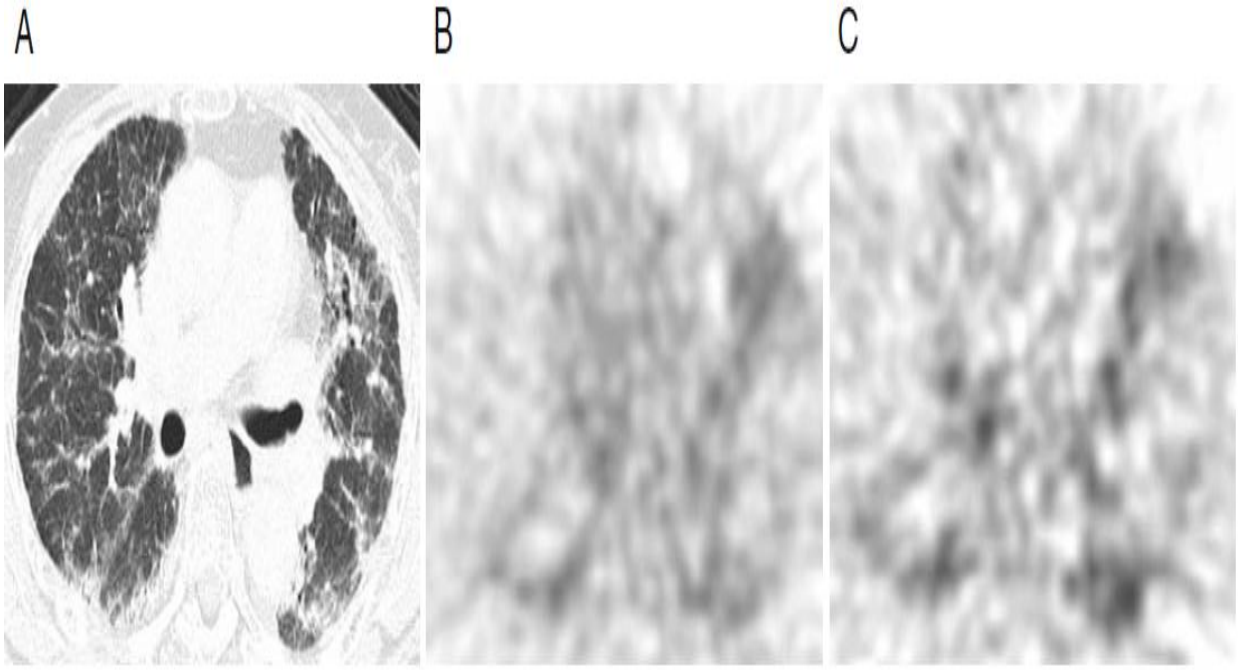

Fig. 22. A 70-year-old woman with pathologically diagnosed NSIP. Deterioration of pulmonary function was seen at 3 months after ^{18}FFDG PET scanning and she died 3 years after the initial diagnosis because of respiratory dysfunction. a Chest HRCT showing ground-glass opacities and reticular shadows in both lung fields. b Trans axial ^{18}F-FDG PET (early imaging) showing ^{18}F-FDG accumulation in lesions with abnormal shadows on corresponding CT images. c ^{18}FFDG PET (delayed imaging) showing increased 18F-FDG accumulation compared to early imaging (RI-SUV=24.3%) (251)

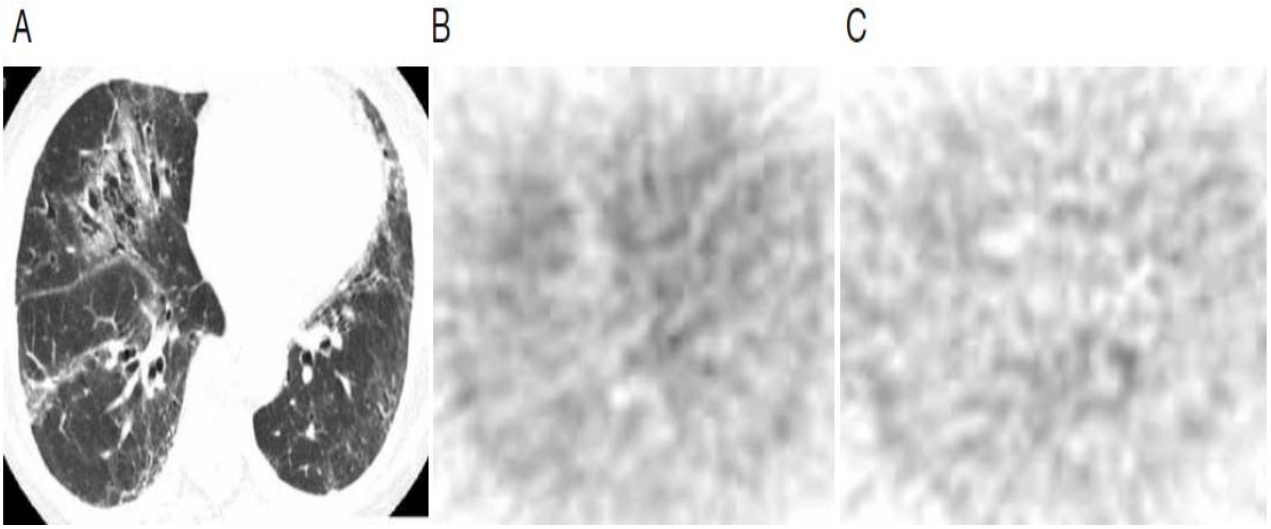

Fig. 23. A 73-year-old woman with pathologically diagnosed NSIP. No deterioration of pulmonary function was seen 1 year after ^{18}F-FDG PET scanning. a Chest HRCT showing ground-glass opacities and reticular shadows in both lung fields. b Transaxial ^{18}F-FDG PET (early imaging) showing ^{18}F-FDG accumulation in lesions with abnormal shadows on corresponding CT images. c ^{18}F-FDG PET (delayed imaging) showing decreased ^{18}F-FDG accumulation compared to early imaging (RI-SUV=−22.0%) (251)

Although malignant FDG uptake does not reach its maximum value until 5 h after administration (251), whereas benign inflammatory lesions and physiological FDG uptake lesions show a stable pattern or a slight decline (252). Activation of inflammatory cells causes a sustained increase in FDG accumulation over time. These findings suggest that inflammatory cell activity is associated with sustained FDG uptake (positive RI-SUV value) in progressive IIP lung (fig. 31, 32)(254).

Based on the data presented, it might be possible to use dual-time-point ^{18}F-FDG PET imaging to classify IIPs into four groups, and for management of IIPs , as follows:

(1) High early SUV level (> 1.5) and positive RI-SUV (> 0%) correspond to progressive COP patients. Since it is predicted that patients will have deterioration of pulmonary function in the short term and good response to corticosteroid therapy, corticosteroid therapy is required.

(2) High early SUV level (> 1.5) and negative RI-SUV (< 0%) could correspond to stable COP patients, and patients could be expected to show improvement within a 1-year observation period.

(3) Low early SUV level (< 1.5) and positive RI-SUV (> 0%) are progressive IPF and NSIP patients. Since it is predicted that patients will

have deterioration of pulmonary function within 12 months and poor to moderate response to corticosteroid therapy, other treatment options may be required (e.g. immunosuppressant).

(4) Low early SUV level (< 1.5) and negative RI-SUV (< 0%) are stable IPF and NSIP patients. Since it is predicted that patients will not show deterioration of pulmonary function within 12 months and usually have poor response to corticosteroid treatment, immediate corticosteroid therapy may not be required.

FDG-PET in Bleomycin-induced pneumonitis (BIP):

Bleomycin-induced pneumonitis (BIP) has emerged as one of the leading causes of death in Hodgkin lymphoma (HL) treated with adriamycin, bleomycin, vinblastine, and dacarbazine (ABVD) (255).

BIP is related to the lack of bleomycin in activating enzyme (bleomycin hydrolase) in the lungs. The central event in the development of BIP is endothelial damage due to bleomycin-induced release of cytokines and free radicals, followed by recruitment of inflammatory cells into lung parenchyma, and subsequently of fibroblasts leading to fibrosis (256).

With clinical BIP, Buchler et al. also suggested that FDG-PET imaging could monitor the inflammatory phase of BIP, independently of conventional CT scanning (257).

In Connerotte et al study the researchers extend these findings by reporting two patients with HL treated with ABVD, in which early interim PET showed pulmonary FDG uptake, in the absence of pulmonary symptoms. PET alterations resolved after cessation of bleomycin as the only intervening process. These cases illustrate the potential of FDG-PET to detect BIP at an early preclinical stage (258).

Promising Future Role of FDG–PET in the Assessment of Lung and Airway Inflammation:

FDG–PET is a non-invasive imaging technique that has significant potential to quantify pulmonary inflammation with high sensitivity. Pulmonary FDG–PET imaging has demonstrated enhanced FDG uptake

in chronic obstructive pulmonary disease (239) and acute lung injury. Also, high pulmonary uptake of FDG has been observed in patients with head injury, who are at risk of developing acute respiratory distress syndrome, but who had no lung symptoms at the time of the scan. It is suggested that FDG–PET imaging can be successfully exploited to study various inflammatory pulmonary disorders and is likely to provide objective means to assess alveolar inflammation in a wide variety of diffuse lung diseases. The feasibility to monitor the extent and activity of the alveolitis during the course of the disease can be utilized for follow-up evaluation to therapy and also can be employed as a biomarker in new drug development (240).

Therapeutic Response Monitoring:

As in malignancies, FDG–PET holds great promise for determining the effects of therapy for a variety of benign disorders. Hence, in several reports, FDG–PET has been proposed as an effective tool in the evaluation of the therapeutic efficacy in infectious disease (259).

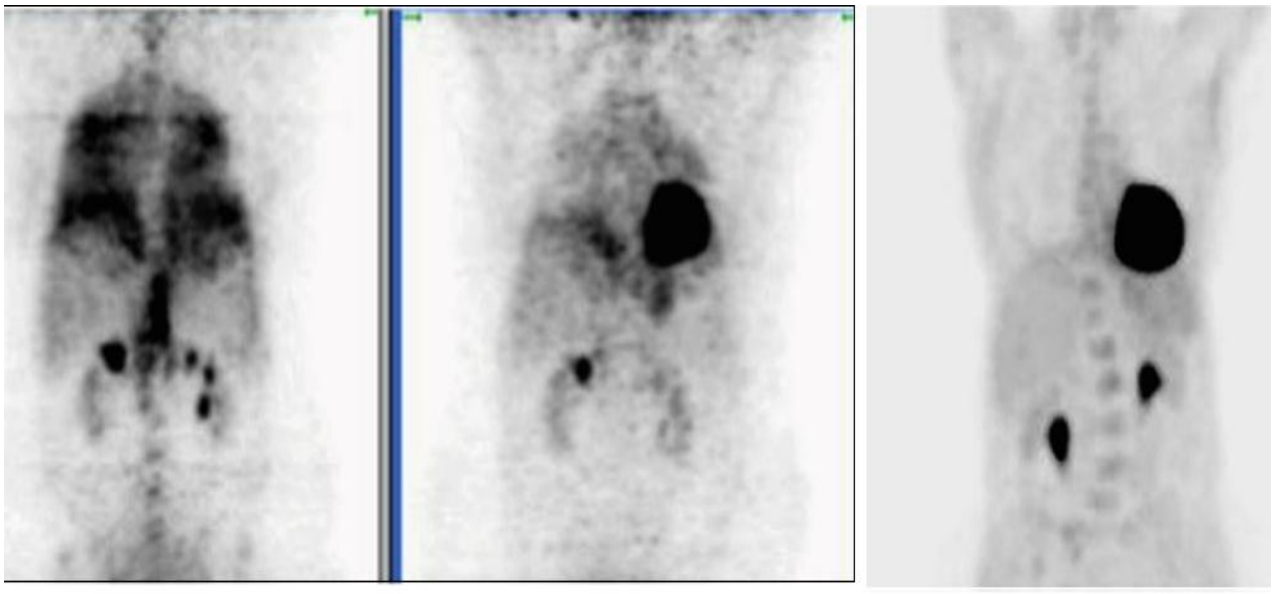

Fig. 24. FDG–PET maximum intensity projection images (antero-posterior view) demonstrating the FDG uptake during the treatment course in a patient with Mycobacterium avium–intercellulare (MAI) infection. (259)

The change of FDG activity following antibiotics has been postulated as an effective way to determine the efficacy of the anti-tuberculosis therapy (Fig. 24). (259).

Chamilos et al. (260) examined the utility of this modality in 16 non-neutropenic patients with invasive mold infections. The results indicated the importance of FDG–PET in guiding the duration of treatment in most patients (n=8). The role of FDG–PET in monitoring therapeutic efficacy has also been described in the setting of invasive aspergillosis (261), candidal lung abscess following antifungal therapy (262), and Pneumocystis carinii pneumonia (263).

Role of FDG-PET in Renal Inflammation

Imaging Renal Infections:

The CT scan has good sensitivity and specificity in the diagnosis of renal infections.

IVP has a very limited value when the question is urinary tract infection, with a sensitivity of only 25% (264).

Ultrasound has been used frequently to evaluate the kidneys with suspected infections.The sensitivity of US has been shown to be 40%–55%, which is inferior to the result for cortical scintigraphy (sensitivity of 86%, specificity of 81% using 99mTc-glucoheptonate) (265).

Positive ultrasonography can obviate the need for DMSA; however, because of a large number of false negative results with reported sensitivities of 42%–58%and underestimation of the pyelonephritis lesions, ultrasonography cannot replace ^{99m}Tc-DMSA (266).

In a comparative study with IVP and US (24% and 42% sensitivity, respectively) (267), cortical scintigraphy was the modality of choice for detecting and following pyelonephritis. Renal ultrasonography is not sensitive for detecting renal parenchymal infections (268).

To date ^{99m}Tc-DMSA is considered the most sensitive method for the detection of acute pyelonephritis in children. Furthermore it permits the photopenic area to be calculated as the inflammatory volume which correlates with the severity of infection and the possibility of scar formation (269) although some of the defects detected might be too small to be clinically significant (270).

The pathophysiologic basis of the ability of Doppler sonography in detecting acute pyelonephritis is the fact that the acute phase of pyelonephritis is the focal decrease of renal perfusion due to edema,

which causes vascular compression, intravascular granulocyte aggregation or both, leading to capillary and arteriolar occlusion facilitating the detection of these hypo-vascular areas (271).

Spiral CT and MRI with contrast have been found to be sensitive in detecting acute pyelonephritis (272). MRI is not practical because of the cost and the need for sedation for the longer periods required for imaging (266).

Autosomal Dominant Polycystic Kidney Disease (ADPKD) is the most common monogenic severe kidney disease, with an average incidence of 1 in 800 live births (273).

In spite of its high frequency, its clinical management is still controversial and even some of the most common clinical threats, such as intracystic infection, may represent an unmet challenge (274).

Conventional imaging methods, including ultrasounds, CT and MR scans, are valuable in discriminating between non-complicated and complicated cysts, but are often unable to clearly discriminate between bleeding and infection or, in particular in acquired cystic disease, neoplasia (275). The concomitance of renal function impairment limits the potential of CT or MR scans, due to the relative or absolute contraindications for contrast media. Furthermore, the presence of several “complicated” cysts is common in severely enlarged liver or kidneys in ADPKD, and a complex structural derangement is usual in “acquired uremic cysts”, often impairing the precise localization of the infectious process (273).

The use of scintigraphy with leucocytes labeled with indium or gallium has been reported as a promising diagnostic tool (276). The limits of this technique are the lack of prompt availability, the high costs and the relatively poor spatial discrimination (277). The first two limits are partly shared by FDG-PET and PET/CT, able to identify metabolically active tissues, including infection, vasculitis and several types of neoplasia (278).

Several recent case reports and two larger case series have suggested that FDG-PET is a very promising tool in the diagnosis of the infected kidney and liver cysts in ADPKD, probably superior to DMSA scan on account of its better spatial discrimination, particularly when combined with CT scanning. In spite of the high potential interest, few studies have investigated the use of FDG-PET/CT in the diagnosis and follow-up of infected kidney cysts (275).

In Piccoli et al ,a case series study, the researcher report on 10 consecutive patients with suspected cystic infection (6 with ADPKD and 4 affected by multiple kidney cysts), in which the diagnosis was based and the clinical management was tailored upon the results of FDG-PET. FDG-PET was positive in 6 cases (5 kidney and 1 liver cyst), was repeated during follow-up in 4 patients and was negative in 4 cases. In the positive cases, FDG-PET guided the therapeutic choices; in particular, the duration of therapy was supported by imaging data in the 4 cases with multiple scans. No relapse was recorded after discontinuation of antibiotic therapy in the treated patients. The negative cases did not develop clinical signs of cystic infection over follow-up (279).

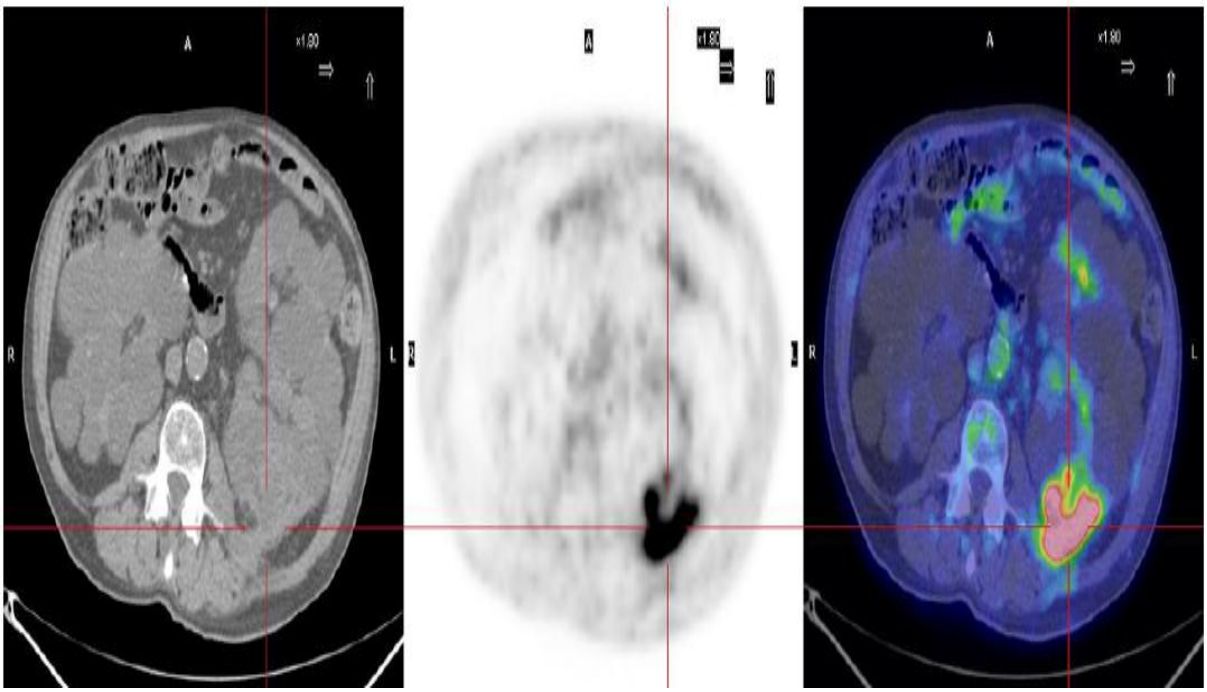

Figure 25. FDG-PET scan: intracystic kidney infection in ADPKD. (275)

Summary and Conclusion

Inflammation is part of the non-specific immune response that occurs in reaction to any type of bodily injury and that the cardinal signs of inflammation can be explained by increased blood flow, elevated cellular metabolism, vasodilatation, release of soluble mediators, extravasation of fluids and cellular influx. In some disorders the inflammatory process, which under normal conditions is self-limiting, becomes continuous and chronic inflammatory disease Inflammation has very specific characteristics, whether acute or chronic, and the innate immune system plays a pivotal role, as it mediates the first response. Infiltration of innate immune system cells, specifically neutrophils and macrophages, characterizes the acute inflammation, while infiltration of T lymphocytes and plasma cells are features of chronic inflammation. Monocytes/macrophages play a central role in both, contributing to the final consequence of chronic inflammation which is represented by the loss of tissue function due to fibrosis develops subsequently.

Timely identification and localization of infectious and inflammatory process are of critical importance in the treatment of patients presenting with suspicion of infection and inflammation. Whilst other radiological techniques (CT, MRI, US) are used for the localization of infectious foci, they rely merely on anatomical changes. Therefore, there has to be a reasonable elapse of time before the infection is diagnosed. In contrast, scintigraphic detection of infection and inflammation is a non-invasive method of whole-body scanning based on functional tissue changes. Several radiopharmaceuticals are currently employed for the scintigraphic imaging of infection and inflammation.

Fluorine 18 fluorodeoxyglucose (FDG) is a readily available radiotracer that offers rapid, exquisitely sensitive high-resolution tomography. FDG PET can also help localize the source of fever of undetermined origin (FUO), thereby guiding additional testing. In the musculoskeletal system, FDG PET accurately helps diagnose spinal osteomyelitis, and in inflammatory conditions such as sarcoidosis and vasculitis, it appears to be useful for defining the extent of disease and monitoring response to treatment. FDG PET may be of limited usefulness in postoperative

patients and in patients with a failed joint prosthesis or a tumor. Nevertheless, this relatively new imaging technique promises to be helpful in the diagnosis of infection and inflammation. FDG PET will likely assume increasing importance in assessing FUO, spinal osteomyelitis, vasculitis, and sarcoidosis and may even become the radionuclide imaging procedure of choice in the evaluation of some or all of these pathologic conditions.

In patients with acquired immunodeficiency syndrome, FDG positron emission tomography (PET) accurately helps localize foci of infection and is particularly useful for differentiating central nervous system lymphoma from toxoplasmosis.

Conclusion:

Advantages of FDG-PET as compared with the other conventional radiologic and scintigraphic methods for the imaging of inflammation and infection include the ability to provide a result as early as 11/2 to 2 hours after tracer injection, the relatively low radiation dose, and the excellent spatial resolution and lesion-to-background contrast. These advantages contribute to the superior accuracy of FDG-PET for the diagnosis or exclusion of infections.

PET and PET/CT in FUO:

FDG-PET is a valuable new imaging technique that has the potential for a major role in patients with FUO. It can detect malignancies as well as infectious and noninfectious inflammatory processes at an early stage of the disease. It has proven its superiority to other currently used conventional nuclear medicine imaging techniques.

When ordered early in the diagnostic workup, FDG-PET has the potential to identify the area of abnormal activity where the cause of fever is likely to be found. This adds valuable information that can be used to focus the investigation and to eliminate unnecessary procedures, resulting in better management of the patients.

PET and PET/CT in Skeletal Infection:

-While FDG uptake in uninfected fractures may normalize more rapidly than gallium or bisphosphonate uptake, differentiating infection from tumor may still be problematic.

-Also, PET/CT has an expanding role in diagnosing osseous infection, especially in patients with MRI contraindications and in the postoperative spine.

-In prosthetic joint infection and spinal infection PET/CT may be an attractive alternative to combined leukocyte–marrow scintigraphy because it requires only one injection Furthermore, treatment with antibiotics is not likely to affect the sensitivity of FDG-PET/CT in delineating sites of infections because FDG does not rely on leukocyte migration, in contrast to combined leukocyte–marrow scintigraphy.

-In rheumatoid arthritis FDG is able to detect early synovitis earlier in acute phase. PET is able to detect changes in synovium at the molecular level. PET/CT may be very useful in the individual quantitative assessment of RA disease activity and its course.

-It was found that quantitative ^{18}F-PET/CT may play a role in the diagnosis of sacroilitis in active AS and is an alternative to conventional bone scintigraphy.

- PET/CT may be a promising modality for optimal patient management through earlier detection of JIA.

- In case of a diabetic foot ulcer, PET was able to exclude the presence of osteomyelitis and had an overall accuracy and sensitivity for the diagnosis of Charcot foot greater than those of MRI.

PET and PET/CT in Cardiovascular Inflammation:

^{18}F-FDG PET (/CT) is increasingly used in patients with elevated inflammatory parameters and clinical characteristics compatible with LVV. In a certain amount of these cases, ^{18}F-FDG PET (/CT) will directly point to LVV, thereby avoiding several time-consuming and sometimes unpleasant tests. On the other hand, due to the low incidence, a high proportion of negative test results of ^{18}F-FDG PET (/CT) for LVV can be

expected. This is undesirable from cost-effectiveness point of view, although a negative test result for LVV can still be of use, if it provides clues to other diagnoses (e.g., lymphoma, infection).

-In atherosclerosis of large vessels and coronaries, it was suggested that the combination of arterial FDG uptake and calcification was the best predictor of future vascular events because baseline vascular FDG uptake correlated with several atherogenic risk factors.

PET and PET/CT in GIT Inflammation:

-PET-CT enteroclysis detects a significantly higher number of lesions both in small and large intestine in comparison to that detected by conventional barium and colonoscopy combined together. This technique is non-invasive, feasible and very promising.

- PET/CT may be a useful approach for detecting AIP and associated EPLs and for monitoring their disease activity following steroid therapy

PET and PET/CT in pulmonary Inflammation:

$^{-18}$F-FDG PET can provide noninvasive information for characterization of IIP as well as a prediction of disease progression and responsiveness to treatment with corticosteroids at the time of initial presentation.

-In TB it was found that early whole body PET/CT imaging may be sufficient for the detection of the EPTB lesions and DTPI of PET/CT may also not be a useful technique in differentiating between EPTB and non-EPTB lesions.

-In sarcoidosis ^{18}F-FDG PET/CT proved advantageous for determining the spread of active disease throughout the body and influenced the decision to adjust the therapy, especially in patients with normal ACE levels.

-In pneumoconiosis dual-time-point PET /CT imaging may help in differentiating benign from malignant pleural disease by increasing the sensitivity and is also helpful for guiding the biopsy site for diagnosis

PET and PET/CT in Renal Infection:

FDG-PET is confirmed as a promising diagnostic tool for detecting intracystic infection in ADPKD and in multiple kidney cysts, and a potential guide for tailoring therapy.

الملخص العربي

الالتهاب هو جزء من استجابة الجهاز المناعي ويحدث كرد فعل على أي نوع من الإصابة الجسدية
وتتكون العناصر الرئيسية للالتهاب من زيادة تدفق الدم، ارتفاع الأيض الخلوي ، وتوسع الأوعية، وإطلاق سراح وسطاء الذوبان، تسرب سوائل و تدفق خلايا الدم البيضاء في المكان المصاب.
في بعض حالات الاتهاب ، والتي في ظل الظروف الطبيعية تصبح تلقائية الشفاء، يستمرالالتهاب ويصبح مزمنا
الأمراض الالتهابية لها خصائص مميزة سواء كانت حادة أو مزمنة، و يلعب نظام المناعة الفطري دورا محوريا، حيث أنه تمثل أول استجابة للأصابة.
ويعتبر وجود الخلايا المناعية المتمثلة في كرلت الدم البيضاء (العدلات الضامة)، هي ما يميز الالتهاب الحاد، في حين وجود الخلايا اللمفية تي وخلايا البلازما هي ملامح من الأتهاب المزمن.
خلايا الدم البيضاء (العدلات الضامة) تلعب دورا محوريا في كلا النوعين من الألتهاب، وتساهم التليف الذي يحدث في وقت لاحق في الألتهابات المزمنة والذي يمكن أن يسبب فقدان جزئي لوظيفة الأنسجة المصابة .
تحديد الوقت المناسب وموقع الألتهاب ذو أهمية حاسمة في العلاج.
وبينما تستخدم بعض التقنيات الإشعاعية التشخيصية (الأشعة المقطعية، الرنين المغناطيسي، والسونار) لتحديد موقع البؤر المعدية، الا انها تعتمد فقط على التغيرات التشريحية. لذا، لا بد أن يكون هناك مرور فترة كافية من الوقت قبل أن يتم التغيير التشريحي وتشخيص العدوى.
بينما في المقابل، التشخيص بواسطة المسح البوزيتروني الطبقي هو طريقة غيرغازية للجسم وتتم على أساس التغيرات النسيجية الوظيفية مما يمكن من التشخيص المبكر والدقيق للألتهب وتحديد مكانة قبل حدوث تغييرات تشريحية

FDG هي مادة مشعة متاحة تقدم بشكل سريع، حساس وعالي الدقة التصوير المقطعي للأماكن ذات الأيض الخلوي المرتفع متضمنة أماكن حدوث الألتهاب

يساعد التصوير المقطعي بالإصدار البوزيتروني على تحديد مكان بؤر العدوى بدقة في المرضى الذين يعانون من متلازمة نقص المناعة المكتسب (الأيدز)

كما أنها مفيدة بشكل خاص للتمييز بين سرطان الغدد الليمفاوية في الجهاز العصبي المركزي من داء المقوسات (Toxoplasmosis)

ويمكن للماسح البوزيتروني الطبقي أن يساعد أيضا في تحديد مصدر حمى المنشأ غير محدد

وفي الجهاز الحركي يمكن لأشعة المسح البوزيتروني الطبقي أن تساعد على التشخيص الدقيق لألتهاب العمود الفقري

ويبدو أنها أيضا مفيدة لتحديد مدى انتشار المرض ورصد استجابة للعلاج في حالات الالتهابات الأخرى مثل ساركويد والتهاب الأوعية الدموية وتصلب الشرايين

قد تكون أشعة المس البوزيتروني الطبقي ذات فائدة محدودة في المرضى بعد العملية الجراحية والمرضى الذين يعانون من فشل بعد عملية زراعة المفاصل الصناعية. ولكنها ذات مستقبل واعد في تشخيص العدوى والالتهابات.

الخلاصة:

مزايا أشعة الماسح ابوزيتروني الطبقي بالمقارنة مع الوسائل الشعاعية التقليدية وأساليب المسح الذري الأخرى في تشخيص الالتهابات والعدوى تشمل القدرة على تقديم نتيجة لذلك في أقرب وقت من2 الى 6 ساعة بعد حقن المادة المشعة ، وكذلك فإن الجرعة الإشعاعية منخفضة نسبيا، ودقة وجودة صورة الأشعة. مما يساهم ويزيد من دقة تشخيص مكان العدوى

دور الماسح البوزيتروني الطبقي في الحمى الغير معلومة المنشأ:

للماسح البوزيتروني الطبقي دور رئيسي في المرضى الذين يعانون من الحمى غير معلومة المنشأ. حيث يمكنه الكشف عن الأورام الخبيثة وكذلك عن الالتهابات المعدية وغير المعدية في مرحلة مبكرة من المرض. وقد ثبت تفوقه على غيره من الوسائل التقليدية المستخدمة للتصوير في الطب النووي.
فعندما يتم عمل تلك الأشعة في مرحلة مبكرة من عملية التشخيص يتم تحديد مكان نشاط أيضي غير طبيعي في الجسم يمكن أن يكون سببا للحمى غير معلومة المنشأ مما يضيف معلومات قيمة يمكن استخدامها لأجراء المزيد من الخطوات تشخيصية الأكثر دقة والأستغناء عن الوسائل التشخيصية الغير ضرورية.

دور الماسح البوزيتروني الطبقي في التهاب الهيكل العظمي:

بعد شفاء الأصابة تعود أشعة المسح البوزيتروني الطبقي الى الصورة الطبيعية بشكل أسرع من أشعة المسح الذري على العظام سواء كانت بالجاليوم أو التقليدية (بمادة ثنائي الفسفونات) ،وبذلك يمكنها التمييز بين الألتهابات والأورام.

كما أن الماسح البوزيتروني الطبقي المدمج بالأشعة المقطعية له دور هام في تشخيصالتهاب العظام

وخاصة بعد العمليات الجراحية في العمود الفقري وفي المرضى المحظور عملهم أشعة الرنين المغناطيسي.
وفي حالات تلوث المفاصل الصناعية وحالات التهاب العمود الفقري يمثل الماسح البوزيتروني الطبقي المدمج بالأشعة المقطعية بديل جيد للمسح الذري على نخاع العظام والمسح الذري باستخدام كرات الدم البيضاء المشعة حيث يتم الحقن بالمادة المشعة مرة واحدة فقط كما أن العلاج بالمضادات الحيوية لا يؤثر على حساسيته على عكس المسح بكرات الدم البيضاء المشعة

وفي مرض الروماتويد يقوم الماسح البوزيتروني الطبقي بالتشخيص المبكر للتغيرات التي تحدث في الغشاء الزلالي. كما أنه يمكنه التنبؤ بتطور المرض.

كما وجد أن الماسح البوزيتروني الطبقي المدمج بلأشعة المقطعية الكمي يلعب دورا هاما في تشخيص التهاب المفصل بين عظام العجز وعظام الحوض في مرض تيبس العمود الفقري النشط كبديل للمسح الذري التقليدي على العظام.

ويمثل الماسح الطبقي البوزيتروني وسيلة واعدة للتشخيص المبكر لمرض التهاب المفاصل مجهول المنشأ في الصغار.

وفي حالات قرحة القدم السكري يستطيع الماسح الطبقي البوزيتروني الطبقي استبعاد اصابة العظام كما انه اعلى في الحساسية والدقة من الرنين المغناطيسي في تشخيص مرض شاركو المفصلي.

دور الماسح البوزيتروني الطبقي في التهاب القلب والأوعية الدموية:

يستخدم الماسح البوزيتروني الطبقي بشكل متزايد في المرضى الذين يعانون من العلامات الأكلينيكية الدالة على مرض التهاب الأوعية الدموية الكبرى. وفي عدد من هذه الحالات، يوجه الماسح البوزيتروني المقطعي التشخيص مباشرة الى المرض وبالتالي تجنب العديد من الاختبارات التي تستغرق وقتا طويلا.ومن ناحية أخرى نتيجة لانخفاض معدل الأصابة بذلك المرض فأننا نحصل على نسبة عالية من النتائج السلبية لأشعة المسح البوزيتروني الطبقي لمرض التهاب الأوعية الدموية الكبرى وهذا أمر غير مرغوب فيه من حيث التكلفة. وعلى الرغم من ذلك فانه يمكن أن تكون نتيجة الفحص السلبية لمرض التهاب الأوعية الدموية الكبرى مفيدة، إذا كانت توفر دلالات تشخيصية لأمراض أخرى (على سبيل المثال، الأورام الليمفاوية، والعدوي).

وفي تصلب الشرايين الكبيرة والتاجية يفترض أن تركيز ماة الفلورين ثنائي الفوسفات مع التكلس في الأوعية الدموية المصابة يمثلان أحسن وسيلة للتنبؤ بأي اصابات مستقبلية للأوعية حيث يتناسب التركيز المبدئي للفلورين ثنائي الفوسفات في الأصابة مع عدة عوامل مسببة لتصلب الشرايين.

دور الماسح البوزيتروني الطبقي في التهاب الجهاز الهضمي:

يقوم الماسح البوزيتروني الطبقي المدمج بالأشعة المقطعية مع الحقن المعوي حقنة معوية بالكشف عن عدد أكبر بكثير من الأصابات بالقياس إلى الكشف عنها بواسطة تنظير القولون ووالأشعة التقليدية بالباريوم مجتمعة معا سواء في الأمعاء الدقيقة أو الغليظة. مما يشكل أسلوبا واعدا للتشخيص.

كما أن اجراء المسح البوزيتروني الطبقي المدمج بالأشعة المقطعية للمرضى المصابون بمرض التهاب البنكرياس المناعي يكشف عن اصابات خارج البنكرياس (EPLs) في خمسة من ستة مرضى، كما يتغير امتصاص المادة المشعة المستخدمة بالتزامن مع نشاط المرض سواء في التهاب البنكرياس المناعي أو في الأصابات خارج البنكرياس وفقا للتقييم بالوسائل الأخرى المورفولوجية والمصلية.

دور الماسح البوزيتروني الطبقي في التهاب الرئة:

يوفر الماسح البوزيتروني الطبقي معلومات لتوصيف امرض الألتهاب الرئوي الخلالي مجهول السبب فضلا عن التنبؤ بتطور المرض واستجابته للعلاج بالكورتيزون.

وفي حالات الدرن وجد أن اجراء الماسح البوزيتروني الطبقي المدمج بالأشعة المقطعية مبكرا على الجسم كله قد يكون كافيا لتشخيص الأصابات خارج الرئتين .

أما في مرض ساركويد فقد ثبت أن الماسح البوزيتروني الطبقي المدمج بالأشعة المقطعية مميز جدا في تحديد انتشار المرض في الجسم كله وقد يؤثر على قرارنا في تعديل العلاج وخاصة في المرضى ذوي المستويات الطبيعية لل ACE.

و قد يساعد الماسح البوزيتروني الطبقي ثنائي التوقيت في التمييز بين أورام الغشاء البلوري الخبيثة وبين تليف الرئة الغباري (pneumoconiosis) . كما يساعد على تحديد مكان الأصابة لأخذ عينة.

دور الماسح البوزيتروني الطبقي في التهاب الكلى:

تم تأكيد الماسح البوزيتروني الطبقي كوسيلة تشخيصية واعدة للخراريج الكيسية في مرض تكيس الكليتين الوراثي ذو الجين السائد كما يمكن أن يستخدم للدلالة على امكانية الأستجابة للعلاج.

References:

.1 Ferrero-Miliani L, Nielsen OH, Andersen PS, Girardin SE. Chronic inflammation: importance of NOD2 and NALP3 in interleukin-1beta generation. Clinical and experimental immunology. 2007;147:227-35.

.2 Fritz JH, Girardin SE. How Toll-like receptors and Nod-like receptors contribute to innate immunity in mammals. Journal of endotoxin research. 2005;11:390-4.

.3 Delbeke D, Coleman RE, Guiberteau MJ, Brown ML, Royal HD, Siegel BA, et al. Procedure guideline for tumor imaging with 18F-FDG PET/CT 1.0. Journal of nuclear medicine. 2006;47:885-95.

.4 Jass JR. Understanding pathology : from disease mechanisms to clinical practice. Amsterdam, The Netherlands: Harwood Academic Publishers; 1999.228 p.

.5 Ogata T. The role of inflammatory chemotactic factor (leukoegresin) and permeability factor (vasoexin) in acute inflammation: an electron microscopic observation of biologic action of these natural mediators. The Kumamoto medical journal. 1971;24:103-23.

.6 Kumar V, Abbas AK, Fausto N, Robbins SL, Cotran RS. Pathologic basis of disease. 7th ed. Philadelphia: Elsevier Saunders; 2005. 1525p.

.7 Athens JW ,Raab SO, Haab OP, Mauer AM, Ashenbrucker H, Cartwright GE, et al. Leukokinetic studies. III. The distribution of granulocytes in the blood of normal subjects . The Journal of clinical investigation. 1961;40:159-64.

.8 Rote NSV. Inflammation Pathophysiology. edit. McCance K. L., Huether S. E..St. Louis: Mosby; 1998; 205-236.

.9 Fischman AJ, Babich JW, Strauss HW. A ticket to ride: peptide radiopharmaceuticals. Journal of nuclear medicine. 1993;34:2253-63.

.10 Boerman OC, Oyen WJ, Corstens FH, Storm G. Liposomes for scintigraphic imaging: optimization of in vivo behavior. Q J Nucl Med. 1998;42:271-9.

.11 De Winter F, Gemmel F, Van Laere K, De Winter O, Poffijn B, Dierckx RA, et al. 99mTc-ciprofloxacin planar and tomographic imaging for the diagnosis of infection in the postoperative spine: experience in 48 patients. European journal of nuclear medicine and molecular imaging. 2004;31:233-9.

.12 Vallabhajosula S. Technetium99-m-labeled chemotactic peptides: specific for imaging infection? Journal of nuclear medicine. 1997;38:1322-6.

.13 Humm JL, Rosenfeld A, Del Guerra A. From PET detectors to PET scanners. European journal of nuclear medicine and molecular imaging. 2003;30:1574-97.

.14 Knoll GF. Radiation detection and measurement . 3rd ed. New York: J. Wiley; 2000. 802 p.

.15 Daube-Witherspoon ME, Karp JS ,Casey ME, DiFilippo FP, Hines H, Muehllehner G, et al. PET performance measurements using the NEMA NU 2-2001 standard. Journal of nuclear medicine. 2002;43:1398-409.

.16 Sugawara Y ,Zasadny KR, Neuhoff AW, Wahl RL. Reevaluation of the standardized uptake value for FDG: variations with body weight and methods for correction. Radiology. 1999;213:521-5.

.17 Zaidi H, Koral KF. Scatter modelling and compensation in emission tomography. European journal of nuclear medicine and molecular imaging. 2004;31:761-82.

.18 Bendriem B, Townsend DW. The theory and practice of 3D PET. Dordrecht in Developments in nuclear medicine; Boston: Kluwer Academic; 1998. vol32, 167 p.
.19 Kak AC, Slaney M, IEEE Engineering in Medicine and Biology Society. Principles of computerized tomographic imaging. New York. IEEE Press; 1988. 329 p.
.20 Lange K, Carson R. EM reconstruction algorithms for emission and transmission tomography. J Comput Assist Tomogr. 1984;8:306–16.
.21 Hudson HM, Larkin RS. Accelerated image reconstruction using ordered subsets of projection data. IEEE transactions on medical imaging. 1994;13:601-9.
.22 Sheline YI, Mintun MA, Barch DM, Wilkins C, Snyder AZ, Moerlein SM. Decreased hippocampal 5-HT(2A) receptor binding in older depressed patients using [18F]altanserin positron emission tomography. Neuropsychopharmacology. 2004;29:2235-4.
.23 Autio A, Henttinen T, Sipila HJ, Jalkanen S, Roivainen A. Mini-PEG spacering of VAP-1-targeting 68Ga-DOTAVAP-P1 peptide improves PET imaging of inflammation. EJNMMI research. 2011;1:10.
.24 Tolor A, Tolor B, Blumin SS. Self-concept and lous of control in primarygrade children identified as requiring special educational programing. Psychological reports. 1977;40:43-9.
.25 Koch TR, Carney JA, Morris VA, Go VL. Somatostatin in the idiopathic inflammatory bowel diseases. Diseases of the colon and rectum. 1988;3:198-203.
.26 Cook GJ, Wegner EA, Fogelman I. Pitfalls and artifacts in 18FDG PET and PET/CT oncologic imaging. Seminars in nuclear medicine. 2004;34:122-33.
.27 Poeppel TD, Krause BJ, Heusner TA, Boy C, Bockisch A, Antoch G. PET/CT for the staging and follow-up of patients with malignancies. European journal of radiology. 2009;70:382-92.
.28 von Schulthess GK, Steinert HC, Hany TF. Integrated PET/CT: current applications and future directions. Radiology. 2006;238:405-22.
.29 Lin E., Alavi A. Patient presentation in PET and PET/CT, a clinical guide : Thieme Medical; 2009.37-33
.30 Lin E, Kinahan P, Alavi A. The value of PET/CT in PET and PET/CT, a clinical guide: Thieme Medical Publishers; 2009.88-98
.31 Chi PC, Mawlawi O, Luo D, Liao Z, Macapinlac HA, Pan T. Effects of respiration-averaged computed tomography on positron emission tomography/computed tomography quantification and its potential impact on gross tumor volume delineation. International journal of radiation oncology, biology, physics. 2008;71:890-9.
.32 Ak I, Stokkel MP, Pauwels EK. Positron emission tomography with 2-[18F]fluoro-2-deoxy-D-glucose in oncology. Part II. The clinical value in detecting and staging primary tumours. Journal of cancer research and clinical oncology. 2000;126:560-74.
.33 Som P, Atkins HL, Bandoypadhyay D, Fowler JS, MacGregor RR, Matsui K, et al. A fluorinated glucose analog, 2-fluoro-2-deoxy-D-glucose (F-18): nontoxic tracer for rapid tumor detection. Journal of nuclear medicine. 1980;21:670-5.
.34 Stumpe KD, Dazzi H, Schaffner A, von Schulthess GK. Infection imaging using whole-body FDG-PET. European journal of nuclear medicine. 2000;27:822-32.
.35 Brown RS, Leung JY, Fisher SJ, Frey KA, Ethier SP, Wahl RL. Intratumoral distribution of tritiated fluorodeoxyglucose in breast carcinoma: I. Are inflammatory cells important? Journal of nuclear medicine. 1995;36:1854-61.

.36 Yamada S, Kubota K, Kubota R, Ido T, Tamahashi N. High accumulation of fluorine-18-fluorodeoxyglucose in turpentine-induced inflammatory tissue. Journal of nuclear medicine. 1995;36:1301-6.
.37 Sugawara Y, Gutowski TD, Fisher SJ, Brown RS, Wahl RL. Uptake of positron emission tomography tracers in experimental bacterial infections: a comparative biodistribution study of radiolabeled FDG, thymidine, L-methionine, ^{67}Ga-citrate, and 125I-HSA. European journal of nuclear medicine. 1999;26:333-41.
.38 Meller J, Sahlmann CO, Scheel AK. ^{18}F-FDG PET and PET/CT in fever of unknown origin. Journal of nuclear medicine. 2007;48:35-45.
.39 Mourad O, Palda V, Detsky AS. A comprehensive evidence-based approach to fever of unknown origin. Archives of internal medicine. 2003;163:545-51.
.40 Lohr JA, Hendley JO. Prolonged fever of unknown origin: a record of experiences with 54 childhood patients. Clinical pediatrics. 1977;16:768-73.
.41 Iikuni Y, Okada J, Kondo H, Kashiwazaki S. Current fever of unknown origin 1982-1992. Intern Med. 1994;33:67-73.
.42 AbuRahma AF, Saiedy S, Robinson PA, Boland JP, Cottrell DJt, Stuart C. Role of venous duplex imaging of the lower extremities in patients with fever of unknown origin. Surgery. 1997;121:366-71.
.43 Bluman EM, Palumbo MA, Lucas PR. Spinal epidural abscess in adults. The Journal of the American Academy of Orthopaedic Surgeons. 2004;12:155-63.
.44 Ozaras R, Celik AD, Zengin K, Mert A, Ozturk KR, Cicek Y, et al. Is laparotomy necessary in the diagnosis of fever of unknown origin? .Acta chirurgica Belgica. 2005;105:89-92.
.45 Kjaer A, Lebech AM. Diagnostic value of ^{111}In-granulocyte scintigraphy in patients with fever of unknown origin. Journal of nuclear medicine. 2002;43:140-4.
.46 Maugeri D, Santangelo A, Abbate S, Rizza I, Calanna A ,Lentini A, et al. A new method for diagnosing fever of unknown origin (FUO) due to infection of muscular-skeletal system in elderly people: leukoscan Tc-99m labelled scintigraphy. European review for medical and pharmacological sciences. 2001;5:123-6.
.47 El-Haddad G, Zhuang H, Gupta N, Alavi A. Evolving role of positron emission tomography in the management of patients with inflammatory and other benign disorders. Seminars in nuclear medicine. 2004;34:313-29.
.48 Zhuang H, Duarte PS, Pourdehnad M, Maes A, Van Acker F, Shnier D, et al. The promising role of ^{18}F-FDG PET in detecting infected lower limb prosthesis implants. Journal of nuclear medicine. 2001;8:44-41.
.49 Keidar Z, Militianu D, Melamed E, Bar-Shalom R, Israel O. The diabetic foot: initial experience with ^{18}F-FDG PET/CT. Journal of nuclear medicine. 2005;46:444-9.
.50 Heald AE, Hoffman JM, Bartlett JA, Waskin HA. Differentiation of central nervous system lesions in AIDS patients using positron emission tomography (PET). International journal of STD & AIDS. 1996;7:337-46.
.51 Milman N, Mortensen J, Sloth C. Fluorodeoxyglucose PET scan in pulmonary sarcoidosis during treatment with inhaled and oral corticosteroids. Respiration; international review of thoracic diseases. 2003;70:408-13.
.52 Pio BS, Byrne FR, Aranda R, Boulay G ,Spicher K, Song MH, et al. Noninvasive quantification of bowel inflammation through positron emission tomography imaging of 2-

deoxy-2-[^{18}F]fluoro-D-glucose-labeled white blood cells. Molecular imaging and biology. 2003;5:271-7.
.53 Beckers C, Ribbens C, Andre B, Marcelis S, Kaye O, Mathy L, et al. Assessment of disease activity in rheumatoid arthritis with ^{18}F-FDG PET. Journal of nuclear medicine. 2004;45:956-64.
.54 Roivainen A, Parkkola R, Yli-Kerttula T, Lehikoinen P, Viljanen T, Mottonen T, et al. Use of positron emission tomography with methyl-^{11}C-choline and 2-^{18}F-fluoro-2-deoxy-D-glucose in comparison with magnetic resonance imaging for the assessment of inflammatory proliferation of synovium. Arthritis and rheumatism. 2003;48:3077-84.
.55 Duysinx B, Nguyen D, Louis R, Cataldo D, Belhocine T, Bartsch P, et al. Evaluation of pleural disease with 18-fluorodeoxyglucose positron emission tomography imaging. Chest. 2004;125:489-93.
.56 Yap JT, Carney JP, Hall NC, Townsend DW. Image-guided cancer therapy using PET/CT. Cancer J. 2004;10:221-33.
.57 Porceddu SV, Jarmolowski E, Hicks RJ, Ware R, Weih L, Rischin D, et al. Utility of positron emission tomography for the detection of disease in residual neck nodes after (chemo)radiotherapy in head and neck cancer. Head & neck. 2005;27:175-81
.58 Dadparvar S, Anderson GS, Bhargava P, Guan L, Reich P, Alavi A, et al. Paraneoplastic encephalitis associated with cystic teratoma is detected by fluorodeoxyglucose positron emission tomography with negative magnetic resonance image findings. Clinical nuclear medicine. 2003;28:893-6.
.59 Knockaert DC, Mortelmans LA, De Roo MC, Bobbaers HJ. Clinical value of gallium-67 scintigraphy in evaluation of fever of unknown origin. Clinical infectious diseases. 1994;18:601-5.
.60 Lorenzen J, Buchert R, Bohuslavizki KH. Value of FDG PET in patients with fever of unknown origin. Nuclear medicine communications. 2001;22:779-8.
.61 de Winter F, van de Wiele C, Vogelaers D, de Smet K, Verdonk R, Dierckx RA. Fluorine-18 fluorodeoxyglucose-position emission tomography: a highly accurate imaging modality for the diagnosis of chronic musculoskeletal infections. The Journal of bone and joint surgery American volume. 2001;83:651-60.
.62 Xiu Y, Yu JQ, Cheng E, Kumar R, Alavi A, Zhuang H. Sarcoidosis demonstrated by FDG PET imaging with negative findings on gallium scintigraphy. Clinical nuclear medicine. 2005;30:193-5.
.63 Kjaer A, Lebech AM, Eigtved A, Hojgaard L. Fever of unknown origin: prospective comparison of diagnostic value of 18F-FDG PET and 111In-granulocyte scintigraphy. European journal of nuclear medicine and molecular imaging. 2004;31:622-6.
.64 Jasper N, Dabritz J, Frosch M, Loeffler M, Weckesser M, Foell D. Diagnostic value of [^{18}F]-FDG PET/CT in children with fever of unknown origin or unexplained signs of inflammation. European journal of nuclear medicine and molecular imaging. 2010;37:136-45.
.65 Kim YJ, Kim SI, Hong KW, Kang MW. Diagnostic value of 18 F-FDG PET/CT in patients with fever of unknown origin. Internal medicine journal. 2012;42:834-7.
.66 Crouzet J, Boudousq V, Lechiche C, Pouget JP, Kotzki PO, Collombier L, et al. Place of ^{18}F-FDG-PET with computed tomography in the diagnostic algorithm of patients with fever of unknown origin. European journal of clinical microbiology & infectious diseases : official publication of the European Society of Clinical Microbiology. 2012;31:1727-33.

.67 Bonakdar-pour A, Gaines VD. The radiology of osteomyelitis. The Orthopedic clinics of North America. 1983;14:21-37.
.68 Riebel TW, Nasir R, Nazarenko O. The value of sonography in the detection of osteomyelitis. Pediatr Radiol. 1996;26:291-7.
.69 Tumeh SS, Aliabadi P, Seltzer SE, Weissman BN, McNeil BJ. Chronic osteomyelitis: the relative roles of scintigrams, plain radiographs, and transmission computed tomography. Clinical nuclear medicine. 1988;13:710-5.
.70 Beltran J, Campanini DS, Knight C, McCalla M. The diabetic foot: magnetic resonance imaging evaluation. Skeletal radiology. 1990;19:37-41.
.71 Handmaker H, Leonards R. The bone scan in inflammatory osseous disease. Seminars in nuclear medicine. 1976;6:95-105.
.72 Schauwecker DS. The scintigraphic diagnosis of osteomyelitis. AJR American journal of roentgenology. 1992;158:9-18.
.73 Alazraki N, Dries D, Datz F, Lawrence P, Greenberg E, Taylor A, Jr. Value of a 24-hour image (four-phase bone scan) in assessing osteomyelitis in patients with peripheral vascular disease. Journal of nuclear medicine. 1985;26:711-7.
.74 Rosenthall L, Lisbona R, Banerjee K. A nucleographic and radioangiographic study of a patient with torsion of the spleen. Radiology. 1974;110:427-8.
.75 Scoles PV, Hilty MD, Sfakianakis GN. Bone scan patterns in acute osteomyelitis. Clinical orthopaedics and related research. 1980:210-7.
.76 Rosenthall L, Kloiber R, Damtew B, Al-Majid H .Sequential use of radiophosphate and radiogallium imaging in the differential diagnosis of bone, joint and soft tissue infection: quantitative analysis. Diagnostic imaging. 1982;51:249-58.
.77 Tumeh SS, Aliabadi P, Weissman BN, McNeil BJ. Chronic osteomyelitis: bone and gallium scan patterns associated with active disease. Radiology. 1986;158:685-8.
.78 Knight D, Gray HW, McKillop JH, Bessent RG. Imaging for infection: caution required with the Charcot joint. European journal of nuclear medicine. 1988;13:523-6.
.79 McCarthy K, Velchik MG, Alavi A, Mandell GA, Esterhai JL, Goll S. Indium-111-labeled white blood cells in the detection of osteomyelitis complicated by a pre-existing condition. Journal of nuclear medicine. 1988;29:1015-21.
.80 Seabold JE, Ferlic RJ, Marsh JL, Nepola JV. Periarticular bone sites associated with traumatic injury: false-positive findings with ^{111}In-labeled white blood cell and Tc-99m MDP scintigraphy. Radiology. 1993;186:845-9.
.81 Rubin RH, Fischman AJ. The use of radiolabeled nonspecific immunoglobulin in the detection of focal inflammation. Seminars in nuclear medicine. 1994;169:79-24.
.82 Gratz S, Braun HG, Behr TM, Meller J, Herrmann A, Conrad M, et al. Photopenia in chronic vertebral osteomyelitis with technetium-99m-antigranulocyte antibody. Journal of nuclear medicine 1997;38:211-6.
.83 Flivik G, Sloth M, Rydholm U, Herrlin K, Lidgren L. Technetium-99m-nanocolloid scintigraphy in orthopedic infections: a comparison with indium-111-labeled leukocytes. Journal of nuclear medicine. 1993;34:1646-50.
.84 Kumar R, Basu S, Torigian D, Anand V, Zhuang H, Alavi A. Role of modern imaging techniques for diagnosis of infection in the era of 18F-fluorodeoxyglucose positron emission tomography. Clinical microbiology reviews. 2008;21:209-24.

.85 Walker RC, Jones-Jackson LB, Martin W, Habibian MR, Delbeke D. New imaging tools for the diagnosis of infection. Future microbiology. 2007;2: 54-27
.86 Guhlmann A, Brecht-Krauss D, Suger G, Glatting G, Kotzerke J, Kinzl L, et al. Fluorine-18-FDG PET and technetium-99m antigranulocyte antibody scintigraphy in chronic osteomyelitis. Journal of nuclear medicine. 1998;39:2145-52.
.87 Schiesser M, Stumpe KD, Trentz O, Kossmann T, Von Schulthess GK. Detection of metallic implant-associated infections with FDG PET in patients with trauma: correlation with microbiologic results. Radiology. 2003;226:391-8.
.88 Kalicke T, Schmitz A, Risse JH, Arens S, Keller E, Hansis M, et al. Fluorine-18 fluorodeoxyglucose PET in infectious bone diseases: results of histologically confirmed cases. European journal of nuclear medicine. 2000;27:524-8.
.89 Stumpe KD, Zanetti M, Weishaupt D, Hodler J, Boos N, Von Schulthess GK. FDG positron emission tomography for differentiation of degenerative and infectious endplate abnormalities in the lumbar spine detected on MR imaging. AJR American journal of roentgenology. 2002;179:1151-7.
.90 De Winter F, Gemmel F, Van De Wiele C, Poffijn B, Uyttendaele D, Dierckx R. 18-Fluorine fluorodeoxyglucose positron emission tomography for the diagnosis of infection in the postoperative spine. Spine. 2003;28:1314-9.
.91 de Winter F, Dierckx R, de Bondt P, Vogelaers D, Verdonk R, Van de Wiele C. FDG PET as a single technique is more accurate than the combination bone scan/white blood cell scan in chronic orthopedic infections (COI). Journal of nuclear medicine. 2000;41:16.
.92 Kim SJ, Kim IJ, Suh KT, Kim YK, Lee JS. Prediction of residual disease of spine infection using F-18 FDG PET/CT. Spine. 2009;34:2424-30.
.93 Palestro CJ, Love C, Miller TT. Diagnostic imaging tests and microbial infections. Cellular microbiology. 2007;9:2323-33.
.94 Hartmann A, Eid K, Dora C, Trentz O, von Schulthess GK, Stumpe KD. Diagnostic value of ^{18}F-FDG PET/CT in trauma patients with suspected chronic osteomyelitis. European journal of nuclear medicine and molecular imaging. 2007;34:704-14.
.95 Schmitz A, Risse JH, Textor J, Zander D, Biersack HJ, Schmitt O, et al. FDG-PET findings of vertebral compression fractures in osteoporosis: preliminary results. Osteoporosis international : a journal established as result of cooperation between the European Foundation for Osteoporosis and the National Osteoporosis Foundation of the USA. 2002;13:755-61. Epub 2002/08/27.
.96 Rosen RS, Fayad L, Wahl RL. Increased 18F-FDG uptake in degenerative disease of the spine: characterization with 18FFDG PET/CT. Journal of nuclear medicine technology . .2006;80:47-1274
.97 Gravius S, Gebhard M, Ackermann D, Bull U, Hermanns-Sachweh B, Mumme T. [Analysis of ^{18}F-FDG uptake pattern in PET for diagnosis of aseptic loosening versus prosthesis infection after total knee arthroplasty. A prospective pilot study .[Nuklearmedizin Nuclear medicine. 2010;49:115-23.
.98 Toms AD, Davidson D, Masri BA, Duncan CP. The management of peri-prosthetic infection in total joint arthroplasty. The Journal of bone and joint surgery British volume. 2006;88:149-55.
.99 Love C, Tomas MB, Marwin SE, Pugliese PV, Palestro CJ. Role of nuclear medicine in diagnosis of the infected joint replacement. Radiographics. 2001;21:1229-38.

.100 Stumpe KD, Notzli HP, Zanetti M, Kamel EM, Hany TF, Gorres GW, et al. FDG PET for differentiation of infection and aseptic loosening in total hip replacements: comparison with conventional radiography and three-phase bone scintigraphy. Radiology. 2004;231:333-41.
.101 Love C, Marwin SE, Tomas MB, Krauss ES, Tronco GG, Bhargava KK, et al. Diagnosing infection in the failed joint replacement: a comparison of coincidence detection ^{18}F-FDG and 111In-labeled leukocyte/99mTc-sulfur colloid marrow imaging. Journal of nuclear medicine. 2004;45:1864-71.
.102 Van Acker F, Nuyts J, Maes A, Vanquickenborne B, Stuyck J, Bellemans J, et al. FDG-PET, 99mTc-HMPAO white blood cell SPET and bone scintigraphy in the evaluation of painful total knee arthroplasties. European journal of nuclear medicine. 2001;28:1496-504.
.103 Manthey N, Reinhard P, Moog F, Knesewitsch P, Hahn K, Tatsch K. The use of [^{18} F]fluorodeoxyglucose positron emission tomography to differentiate between synovitis, loosening and infection of hip and knee prostheses. Nuclear medicine communications. 2002;23:645-53.
.104 Stumpe KD, Romero J, Ziegler O, Kamel EM, von Schulthess GK, Strobel K, et al. The value of FDG-PET in patients with painful total knee arthroplasty. European journal of nuclear medicine and molecular imaging. 2006;33:1218-25.
.105 Chen SH, Ho KC, Hsieh PH, Lee MS, Yen TC. Potential clinical role of ^{18}F FDG-PET/CT in detecting hip prosthesis infection: a study in patients undergoing two-stage revision arthroplasty with an interim spacer. Q J Nucl Med Mol Imaging. 2010;54:429-35.
.106 Brenner W. 18F-FDG PET in rheumatoid arthritis: there still is a long way to go. Journal of nuclear medicine. 2004;45:927-9.
.107 Sokolove J, Strand V. Rheumatoid arthritis classification criteria -It's finally time to move on! .Bull NYU Hosp Jt Dis. 2010;8:68:232.
.108 Goekoop-Ruiterman YP, de Vries-Bouwstra JK, Allaart CF, van Zeben D, Kerstens PJ, Hazes JM, et al. Clinical and radiographic outcomes of four different treatment strategies in patients with early rheumatoid arthritis: a randomized, controlled trial. Arthritis and rheumatism. 2005;52:3381-90.
.109 Bakheet SM, Powe J. Fluorine-18-fluorodeoxyglucose uptake in rheumatoid arthritis-associated lung disease in a patient with thyroid cancer. Journal of nuclear medicine. 1998;39:234-6.
.110 Lin E, Sicuro P. FDG uptake in cervical facet subchondral cysts demonstrated by PET/CT. Clinical nuclear medicine. 2008;33:268-70.
.111 Matsui T, Nakata N, Nagai S, Nakatani A, Takahashi M, Momose T, et al. Inflammatory cytokines and hypoxia contribute to ^{18}F-FDG uptake by cells involved in pannus formation in rheumatoid arthritis. 2009;50:920-6.
.112 Elzinga EH, van der Laken CJ, Comans EF, Lammertsma AA, Dijkmans BA, Voskuyl AE. 2-Deoxy-2-[F-18]fluoro-D-glucose joint uptake on positron emission tomography images: rheumatoid arthritis versus osteoarthritis. Molecular imaging and biology. 2007;9:357-60.
.113 Palmer WE, Rosenthal DI, Schoenberg OI, Fischman AJ, Simon LS, Rubin RH, et al. Quantification of inflammation in the wrist with gadolinium-enhanced MR imaging and PET with 2-[F-18]-fluoro-2-deoxy-D-glucose. Radiology. 1995;196:647-55.
.114 Ju JH, Kang KY, Kim IJ, Yoon JU, Kim HS, Park SH, et al. Visualization and localization of rheumatoid knee synovitis with FDG-PET/CT images. Clinical rheumatology. 2008;27:39-41.

.115 Altman R, Asch E, Bloch D, Bole G, Borenstein D, Brandt K, et al. Development of criteria for the classification and reporting of osteoarthritis. Classification of osteoarthritis of the knee. Diagnostic and Therapeutic Criteria Committee of the American Rheumatism Association. Arthritis and rheumatism. 1986;29:1039-49.
.116 Kaneta T, Hakamatsuka T, Yamada T, Takase K, Sato A, Higano S, et al. Atlantoaxial osteoarthritis in rheumatoid arthritis: FDG PET/CT findings. Clinical nuclear medicine. 2006;31:209.
.117 Kubota K, Ito K, Morooka M, Minamimoto R, Miyata Y, Yamashita H, et al. FDG PET for rheumatoid arthritis :basic considerations and whole-body PET/CT. Annals of the New York Academy of Sciences. 2011;1228:29-38.
.118 Paulus HE, Egger MJ, Ward JR, Williams HJ. Analysis of improvement in individual rheumatoid arthritis patients treated with disease-modifying antirheumatic drugs, based on the findings in patients treated with placebo. The Cooperative Systematic Studies of Rheumatic Diseases Group. Arthritis and rheumatism. 1990;33:477-84.
.119 Beckers C, Jeukens X, Ribbens C ,Andre B, Marcelis S, Leclercq P, et al. ^{18}F-FDG PET imaging of rheumatoid knee synovitis correlates with dynamic magnetic resonance and sonographic assessments as well as with the serum level of metalloproteinase-3. European journal of nuclear medicine and molecular imaging. 2006;33:275-80.
.120 Goerres GW, Forster A, Uebelhart D, Seifert B, Treyer V, Michel B, et al. ^{18}F- FDG whole-body PET for the assessment of disease activity in patients with rheumatoid arthritis. Clinical nuclear medicine. 2006;31:386-90.
.121 Wunder A, Straub RH, Gay S, Funk J, Muller-Ladner U. Molecular imaging: novel tools in visualizing rheumatoid arthritis. Rheumatology (Oxford). 2005;44:1341-9.
.122 Okamura K, Yonemoto Y, Arisaka Y, Takeuchi K, Kobayashi T, Oriuchi N, et al. The assessment of biologic treatment in patients with rheumatoid arthritis using FDG-PET/CT. Rheumatology (Oxford). 2012;51:1484-91.
.123 Pelletier JP, Martel-Pelletier J ,Abramson SB. Osteoarthritis, an inflammatory disease: potential implication for the selection of new therapeutic targets. Arthritis and rheumatism. 2001;44:1237-47.
.124 Conaghan PG, Felson D, Gold G, Lohmander S, Totterman S, Altman R .MRI and non-cartilaginous structures in knee osteoarthritis. Osteoarthritis and cartilage / OARS, Osteoarthritis Research Society. 2006;14:87-94.
.125 Nakamura H, Masuko K, Yudoh K, Kato T, Nishioka K, Sugihara T, et al. Positron emission tomography with 18F-FDG in osteoarthritic knee. Osteoarthritis and cartilage / OARS, Osteoarthritis Research Society. 2007;15:673-81.
.126 Omoumi P, Mercier GA, Lecouvet F, Simoni P, Vande Berg BC. CT arthrography, MR arthrography, PET, and scintigraphy in osteoarthritis. Radiologic clinics of North America. 2009;47:595-615.
.127 Rosen RS, Fayad L, Wahl RL. Increased 18F-FDG uptake in degenerative disease of the spine: Characterization with ^{18}F-FDG PET/CT. Journal of nuclear medicine. 2006;47:1274-80.
.128 von Schulthess GK, Meier N, Stumpe KD. Joint accumulations of FDG in whole body PET scans. Nuklearmedizin Nuclear medicine. 2001;40:7-193
.129 Wandler E, Kramer EL, Sherman O, Babb J, Scarola J, Rafii M. Diffuse FDG shoulder uptake on PET is associated with clinical findings of osteoarthritis. AJR American journal of roentgenology. 2005;185:797-803.

.130 Basu S, Zhuang H, Torigian DA, Rosenbaum J, Chen W, Alavi A. Functional imaging of inflammatory diseases using nuclear medicine techniques. Seminars in nuclear medicine. 2009;39:124-45.
.131 Nakamura J, Yamada K, Mitsugi N, Saito T. A case of SAPHO syndrome with destructive spondylodiscitis suspicious of tuberculous spondylitis. Modern rheumatology / the Japan Rheumatism Association. 2010;20:93-7.
.132 Parsons MD, Torigian, Alavi A. Metabolic activity in the painful knee joint as measured on FDG-PET. Society of NuclearMedicine Annual Meeting Abstracts. 2008;49:270.
.133 Mathur T, Manadan AM, Hota B, Block JA. Pseudo-septic hip arthritis as the presenting symptom of ankylosing spondylitis: a case series and review of the literature. Clinical and experimental rheumatology. 2010;28:416-8.
.134 Wendling D, Blagosklonov O, Streit G, Lehuede G, Toussirot E, Cardot JC. FDG-PET/CT scan of inflammatory spondylodiscitis lesions in ankylosing spondylitis, and short term evolution during anti-tumour necrosis factor treatment. Annals of the rheumatic diseases. 2005;64:1663-5.
.135 Strobel K, Fischer DR, Tamborrini G, Kyburz D, Stumpe KD, Hesselmann RG, et al. ^{18}F-fluoride PET/CT for detection of sacroiliitis in ankylosing spondylitis. European journal of nuclear medicine and molecular imaging. 2010;37:1760-5.
.136 Dannecker GE, Quartier P. Juvenile idiopathic arthritis: classification, clinical presentation and current treatments. Hormone research. 2009;72:4-12.
.137 Tateishi U, Imagawa T, Kanezawa N, Okabe T, Shizukuishi K, Inoue T, et al. PET assessment of disease activity in children with juvenile idiopathic arthritis. Pediatr Radiol. 2010;40:1781-8.
.138 Toriihara A, Seto Y, Yoshida K, Umehara I, Nakagawa T, Liu R, et al. F-18 FDG PET/CT of polymyalgia rheumatica. Clinical nuclear medicine. 2009;34:305-6.
.139 Blockmans D, De Ceuninck L, Vanderschueren S, Knockaert D, Mortelmans L, Bobbaers H. Repetitive 18-fluorodeoxyglucose positron emission tomography in isolated polymyalgia rheumatica: a prospective study in 35 patients. Rheumatology (Oxford). 2007;46:672-7.
.140 Blockmans D, Stroobants S, Maes A, Mortelmans L. Positron emission tomography in giant cell arteritis and polymyalgia rheumatica: evidence for inflammation of the aortic arch. The American journal of medicine. 2000;108:246-9.
.141 Adams H, Raijmakers P, Smulders Y. Polymyalgia rheumatica and interspinous FDG uptake on PET/CT. Clinical nuclear medicine. 2012;37:502-5.
.142 Basu S, Chryssikos T, Houseni M, Scot Malay D, Shah J, Zhuang H, et al. Potential role of FDG PET in the setting of diabetic neuro-osteoarthropathy: can it differentiate uncomplicated Charcot's neuroarthropathy from osteomyelitis and soft-tissue infection? .Nuclear medicine communications. 2007;28:465-72.
.143 Rosamond W, Flegal K, Friday G, Furie K, Go A, Greenlund K, et al. Heart disease and stroke statistics--2007 update: a report from the American Heart Association Statistics Committee and Stroke Statistics Subcommittee. Circulation. 2007;115: 69-171.
.144 Shaw LJ, Narula J. Risk assessment and predictive value of coronary artery disease testing. Journal of nuclear medicine. 2009;50:1296-306.
.145 Shah PK. Screening asymptomatic subjects for subclinical atherosclerosis: can we, does it matter, and should we?. J Am Coll Cardiol 2010;56:98–105.

.146 Newby DE. Triggering of acute myocardial infarction: beyond the vulnerable plaque. Heart. 2010;96:1247-51.
.147 Sluimer JC, Daemen MJ. Novel concepts in atherogenesis: angiogenesis and hypoxia in atherosclerosis. The Journal of pathology. 2009;218:7-29.
.148 Rogers IS, Nasir K, Figueroa AL, Cury RC, Hoffmann U, Vermylen DA, et al. Feasibility of FDG imaging of the coronary arteries: comparison between acute coronary syndrome and stable angina. JACC Cardiovascular imaging. 2010;3:388-97.
.149 Kim TN, Kim S, Yang SJ, Yoo HJ, Seo JA, Kim SG, et al. Vascular inflammation in patients with impaired glucose tolerance and type 2 diabetes: analysis with ^{18}F-fluorodeoxyglucose positron emission tomography. Circulation Cardiovascular imaging. 2010;3:142-8.
.150 Moustafa RR, Izquierdo-Garcia D, Fryer TD, Graves MJ, Rudd JH, Gillard JH, et al. Carotid plaque inflammation is associated with cerebral microembolism in patients with recent transient ischemic attack or stroke: a pilot study. Circulation Cardiovascular imaging. 2010;3:536-41.
.151 Pedersen SF ,Graebe M, Fisker Hag AM, Hojgaard L, Sillesen H, Kjaer A. Gene expression and ^{18}FDG uptake in atherosclerotic carotid plaques. Nuclear medicine communications. 2010;31:423-9.
.152 Rudd JH, Myers KS, Bansilal S, Machac J, Woodward M ,Fuster V, et al. Relationships among regional arterial inflammation, calcification, risk factors, and biomarkers: a prospective fluorodeoxyglucose positron-emission tomography/computed tomography imaging study. Circulation Cardiovascular imaging. 2009;2:15-107.
.153 Paulmier B, Duet M, Khayat R, Pierquet-Ghazzar N, Laissy JP, Maunoury C, et al. Arterial wall uptake of fluorodeoxyglucose on PET imaging in stable cancer disease patients indicates higher risk for cardiovascular events. Journal of nuclear cardiology.2008;15:209-17.
.154 Rominger A, Saam T, Wolpers S, Cyran CC, Schmidt M, Foerster S, et al. ^{18}F-FDG PET/CT identifies patients at risk for future vascular events in an otherwise asymptomatic cohort with neoplastic disease. Journal of nuclear medicine. 2009;50:1611-20.
.155 Arauz A, Hoyos L, Zenteno M, Mendoza R, Alexanderson E. Carotid plaque inflammation detected by 18F-fluorodeoxyglucose-positron emission tomography. Pilot study. Clinical neurology and neurosurgery. 2007;109:409-12.
.156 Mehta NN, Torigian DA, Gelfand JM, Saboury B, Alavi A. Quantification of atherosclerotic plaque activity and vascular inflammation using [^{18}F] fluorodeoxyglucose positron emission tomography/computed tomography (FDG-PET/CT). Journal of visualized experiments. 2012;63:e3777.
.157 Varghese A, Crowe LA, Mohiaddin RH, Gatehouse PD, Yang GZ, Firmin DN, et al. Inter-study reproducibility of 3D volume selective fast spin echo sequence for quantifying carotid artery wall volume in asymptomatic subjects. Atherosclerosis. 2005;183:361-6.
.158 Ogawa M, Magata Y, Kato T, Hatano K, Ishino S, Mukai T, et al. Application of ^{18}F-FDG PET for monitoring the therapeutic effect of antiinflammatory drugs on stabilization of vulnerable atherosclerotic plaques. Journal of nuclear medicine: . 2006;47:1845-50.
.159 Tahara N, Kai H, Ishibashi M, Nakaura H, Kaida H, Baba K, et al. Simvastatin attenuates plaque inflammation: evaluation by fluorodeoxyglucose positron emission tomography. J Am Coll Cardiol. 2006;48:1825-31.
.160 Rudd JH, Machac J, Fayad ZA. Simvastatin and plaque inflammation. J Am Coll Cardiol. 2007;49:1991

.161 Lee SJ, On YK, Lee EJ, Choi JY, Kim BT ,Lee KH. Reversal of vascular 18F-FDG uptake with plasma high-density lipoprotein elevation by atherogenic risk reduction. Journal of nuclear medicine. 2008;49:1277-82.
.162 Wykrzykowska J, Lehman S, Williams G, Parker JA, Palmer MR, Varkey S, et al. Imaging of inflamed and vulnerable plaque in coronary arteries with ^{18}F-FDG PET/CT in patients with suppression of myocardial uptake using a low-carbohydrate, high-fat preparation. Journal of nuclear medicine. 2009;50:563-8.
.163 Dunphy MP, Freiman A, Larson SM, Strauss HW. Association of vascular ^{18}F-FDG uptake with vascular calcification. Journal of nuclear medicine: . 2005;46:1278-84.
.164 Saam T, Rominger A, Wolpers S, Nikolaou K, Rist C, Greif M, et al. Association of inflammation of the left anterior descending coronary artery with cardiovascular risk factors, plaque burden and pericardial fat volume: a PET/CT study. European journal of nuclear medicine and molecular imaging. 2010;37:1203-12.
.165 Willum-Hansen T, Staessen JA, Torp-Pedersen C, Rasmussen S, Thijs L, Ibsen H ,et al. Prognostic value of aortic pulse wave velocity as index of arterial stiffness in the general population. Circulation. 2006;113:664-70.
.166 Mackey RH, Venkitachalam L, Sutton-Tyrrell K. Calcifications, arterial stiffness and atherosclerosis. Advances in cardiology. 2007;44:234-44.
.167 Schnabel R, Larson MG, Dupuis J, Lunetta KL, Lipinska I, Meigs JB, et al. Relations of inflammatory biomarkers and common genetic variants with arterial stiffness and wave reflection. Hypertension. 2008;51:1651-7.
.168 Paffen E, DeMaat MP. C-reactive protein in atherosclerosis: A causal factor?. Cardiovascular research. 2006;71:30-9.
.169 Joly L, Djaballah W, Koehl G, Mandry D, Dolivet G, Marie PY, et al. Aortic inflammation, as assessed by hybrid FDG-PET/CT imaging, is associated with enhanced aortic stiffness in addition to concurrent calcification. European journal of nuclear medicine and molecular imaging. 2009;36:979-85.
.170 Tawakol A, Migrino RQ, Bashian GG, Bedri S, Vermylen D, Cury RC, et al. In vivo 18F-fluorodeoxyglucose positron emission tomography imaging provides a noninvasive measure of carotid plaque inflammation in patients. J Am Coll Cardiol. 2006;48: 24-818
.171 Lederman RJ, Raylman RR, Fisher SJ, Kison PV, San H, Nabel EG, et al. Detection of atherosclerosis using a novel positron-sensitive probe and 18-fluorodeoxyglucose (FDG). Nuclear medicine communications. 2001;22:747-53.
.172 Zhang Z, Machac J, Helft G, Worthley SG, Tang C, Zaman AG, et al. Non-invasive imaging of atherosclerotic plaque macrophage in a rabbit model with F-18 FDG PET: a histopathological correlation. BMC nuclear medicine. 2006;6:3.
.173 Rudd JH, Myers KS, Bansilal S, Machac J, Rafique A, Farkouh M, et al. (18)Fluorodeoxyglucose positron emission tomography imaging of atherosclerotic plaque inflammation is highly reproducible: implications for atherosclerosis therapy trials .J Am Coll Cardiol. 2007;50:892-6.
.174 Bural GG, Torigian DA, Chamroonrat W, Houseni M, Chen W, Basu S, et al. FDG-PET is an effective imaging modality to detect and quantify age-related atherosclerosis in large arteries. European journal of nuclear medicine and molecular imaging. 2008;35:562-9.

.175 Tahara N, Kai H, Yamagishi S, Mizoguchi M, Nakaura H, Ishibashi M, et al. Vascular inflammation evaluated by [18F]-fluorodeoxyglucose positron emission tomography is associated with the metabolic syndrome. J Am Coll Cardiol. 2007;49:1533-9.
.176 Ben-Haim S, Kupzov E, Tamir A, Frenkel A, Israel O. Changing patterns of abnormal vascular wall F-18 fluorodeoxyglucose uptake on follow-up PET/CT studies .Journal of nuclear cardiology. 2006;13:791-800.
.177 Avolio A. Genetic and environmental factors in the function and structure of the arterial wall. Hypertension. 199 .7-26:34;5.
.178 Rudd JH, Myers KS, Bansilal S, Machac J, Pinto CA, Tong C, et al. Atherosclerosis inflammation imaging with 18F-FDG PET: carotid, iliac, and femoral uptake reproducibility, quantification methods, and recommendations. Journal of nuclear medicine. 2008;49:871-8.
.179 Packard RR, Libby P. Inflammation in atherosclerosis: from vascular biology to biomarker discovery and risk prediction. Clinical chemistry. 2008;54:24-38.
.180 Jennette JC, Falk RJ, Andrassy K, Bacon PA, Churg J, Gross WL, et al. Nomenclature of systemic vasculitides. Proposal of an international consensus conference. Arthritis and rheumatism. 1994;37:187-92.
.181 Salvarani C, Cantini F, Hunder GG. Polymyalgia rheumatica and giant-cell arteritis. Lancet. 2008;372:234-45.
.182 Janssen SP, Comans EH, Voskuyl AE, Wisselink W, Smulders YM. Giant cell arteritis: heterogeneity in clinical presentation and imaging results. Journal of vascular surgery : official publication, the Society for Vascular Surgery [and] International Society for Cardiovascular Surgery, North American Chapter. 2008;48:1025-31.
.183 Mari B ,Monteagudo M, Bustamante E, Perez J, Casanovas A, Jordana R, et al. Analysis of temporal artery biopsies in an 18-year period at a community hospital. European journal of internal medicine. 2009;20:533-6.
.184 Gornik HL, Creager MA .Aortitis. Circulation. 2008;117:3039-51.
.185 Maksimowicz-McKinnon K, Clark TM, Hoffman GS. Takayasu arteritis and giant cell arteritis: a spectrum within the same disease?. Medicine. 2009;88:221-6.
.186 Mwipatayi BP, Jeffery PC, Beningfield SJ, Matley PJ, Naidoo NG, Kalla AA, et al. Takayasu arteritis: clinical features and management: report of 272 cases. ANZ journal of surgery. 2005;75:110-7.
.187 Kissin EY, Merkel PA. Diagnostic imaging in Takayasu arteritis. Current opinion in rheumatology. 2004;16:31-7.
.188 Ahmadi-Simab K, Hellmich B, Holl-Ulrich K, Fleischmann C, Dourvos O, Gross WL. Acute coronary syndrome in Takayasu arteritis without elevation of acute phase parameters. Rheumatology (Oxford). 2007;46:554–5.
.189 Bartels AL, Zeebregts CJ, Bijl M, Tio RA, Slart RH. Fused FDG-PET and MRI imaging of Takayasu arteritis in vertebral arteries. Annals of nuclear medicine. 2009;23:753-6.
.190 Zerizer I, Tan K, Khan S, Barwick T, Marzola MC, Rubello D, et al. Role of FDG-PET and PET/CT in the diagnosis and management of vasculitis. European journal of radiology. 2010;73:504-9.
.191 Meller J, Strutz F, Siefker U, Scheel A, Sahlmann CO, Lehmann K, et al. Early diagnosis and follow-up of aortitis with [^{18}F]FDG PET and MRI. European journal of nuclear medicine and molecular imaging. 2003;30:730-6.

.192 Henes JC, Muller M, Krieger J, Balletshofer B, Pfannenberg AC, Kanz L, et al. [^{18}F] FDG-PET/CT as a new and sensitive imaging method for the diagnosis of large vessel vasculitis. Clinical and experimental rheumatology. 2008;2647-52.
.193 EII PJ. The contribution of PET/CT to improved patient management. The British journal of radiology. 2006;79:32-6.
.194 Hautzel H, Sander O, Heinzel A, Schneider M, Muller HW. Assessment of large-vessel involvement in giant cell arteritis with ^{18}F-FDG PET: introducing an ROC-analysis-based cutoff ratio. Journal of nuclear medicine. 2008;49:1107-13.
.195 Moosig F, Czech N, Mehl C, Henze E, Zeuner RA, Kneba M, et al. Correlation between 18-fluorodeoxyglucose accumulation in large vessels and serological markers of inflammation in polymyalgia rheumatica: a quantitative PET study. Annals of the rheumatic diseases. 2004;63:870-3.
.196 Arnaud L, Haroche J, Malek Z, Archambaud F, Gambotti L, Grimon G, et al. Is ^{18}F-fluorodeoxyglucose positron emission tomography scanning a reliable way to assess disease activity in Takayasu arteritis? Arthritis and rheumatism. 2009;60:1193-200.
.197 Hooisma GA, Balink H, Houtman PM, Slart RH, Lensen KD. Parameters related to a positive test result for FDG PET(/CT) for large vessel vasculitis: a multicenter retrospective study. Clinical rheumatology. 2012;31:861-71.
.198 Weyand CM, Tetzlaff N, Bjornsson J, Brack A, Younge B, Goronzy JJ. Disease patterns and tissue cytokine profiles in giant cell arteritis. Arthritis and rheumatism. 1997;40:19-26.
.199 Aigner F, Bodner G, Gruber H, Conrad F, Fritsch H, Margreiter R, et al. The vascular nature of hemorrhoids. Journal of gastrointestinal surgery : official journal of the Society for Surgery of the Alimentary Tract. 2006;10:1044-50.
.200 Nisar PJ, Scholefield JH. Managing haemorrhoids. BMJ. 2003;327:847-51.
.201 Lu YY, Lin WY. Hemorrhoids: a possible cause of high FDG uptake in the rectum. Ann Nucl Med Sci. 2006;19:213–7.
.202 Kikuchi M, Yamamoto E, Shiomi Y, Nakamoto Y, Fujiwara K, Watanabe F, et al. Case report: internal and external jugular vein thrombosis with marked accumulation of FDG. The British journal of radiology. 2004;77:888-90.
.203 Miceli M, Atoui R, Walker R, Mahfouz T, Mirza N, Diaz J, et al. Diagnosis of deep septic thrombophlebitis in cancer patients by fluorine-18 fluorodeoxyglucose positron emission tomography scanning: a preliminary report. Journal of clinical oncology. 2004;22:1949-56.
.204 Khosa F, Otero HJ, Prevedello LM, Rybicki FJ, Di Salvo DN. Imaging presentation of venous thrombosis in patients with cancer. AJR American journal of roentgenology. 2010;194:1099-108.
.205 Calcagno C, Cornily JC, Hyafil F, Rudd JH, Briley-Saebo KC, Mani V, et al. Detection of neovessels in atherosclerotic plaques of rabbits using dynamic contrast enhanced MRI and ^{18}F-FDG PET. Arteriosclerosis, thrombosis, and vascular biology. 2008;28:1311-7.
.206 Morales CH, Villegas MI, Villavicencio R, Gonzalez G, Perez LF, Pena AM, et al. Intra-abdominal infection in patients with abdominal trauma. Arch Surg. 2004;139:1278-85.
.207 Datz FL. Abdominal abscess detection: gallium, 111In-, and 99mTc-labeled leukocytes, and polyclonal and monoclonal antibodies. Seminars in nuclear medicine. 1996;26:51-64.
.208 Hooton TM, Stamm WE. Diagnosis and treatment of uncomplicated urinary tract infection. Infectious disease clinics of North America. 1997;11:551-81.

.209 Minoja G, Chiaranda M, Fachinetti A, Raso M, Dominioni L, Torre D, et al. The clinical use of 99m-Tc-labeled WBC scintigraphy in critically ill surgical and trauma patients with occult sepsis. Intensive care medicine. 1996;22:867-71.
.210 Yang MD, Jeng LB, Kao A, Lin CC, Lee CC. C-reactive protein and gallium scintigraphy in patients after abdominal surgery. Hepato-gastroenterology. 2003;50:354-6.
.211 Sailer J, Peloschek P, Schober E, Schima W, Reinisch W, Vogelsang H, et al. Diagnostic value of CT enteroclysis compared with conventional enteroclysis in patients with Crohn's disease. AJR American journal of roentgenology. 2005;185:1575-81.
.212 Mackalski BA, Bernstein CN. New diagnostic imaging tools for inflammatory bowel disease. Gut. 2006;55:733-41.
.213 Almer S, Granerus G, Strom M, Olaison G, Bonnet J ,Lemann M, et al. Leukocyte scintigraphy compared to intraoperative small bowel enteroscopy and laparotomy findings in Crohn's disease. Inflammatory bowel diseases. 2007;13(2):164-74. Epub 2007/01/09.
.214 Sciarretta G, Furno A, Mazzoni M, Basile C, Malaguti P. Technetium-99m hexamethyl propylene amine oxime granulocyte scintigraphy in Crohn's disease: diagnostic and clinical relevance. Gut. 1993;34:1364-9.
.215 Kresnik E, Mikosch P, Gallowitsch HJ, Heinisch M, Lind P. ^{18}F- fluorodeoxyglucose positron emission tomography in the diagnosis of inflammatory bowel disease. Clinical nuclear medicine. 2001;26:867.
.216 Kutsky P, Goodman FR. Calcium incorporation by smooth muscle subcellular fractions. The American journal of physiology. 1981;240:C248.
.217 Das CJ, Makharia G, Kumar R, Chawla M, Goswami P, Sharma R, et al. PET-CT enteroclysis: a new technique for evaluation of inflammatory diseases of the intestine. European journal of nuclear medicine and molecular imaging. 2007;34:2106-14.
.218 Zhuang H, Pourdehnad M, Lambright ES, Yamamoto AJ, Lanuti M, Li P, et al. Dual time point 18F-FDG PET imaging for differentiating malignant from inflammatory processes. Journal of nuclear medicine. 2001;42:1412-7.
.219 Gutman F, Alberini JL, Wartski M, Vilain D, Le Stanc E, Sarandi F, et al. Incidental colonic focal lesions detected by FDG PET/CT. AJR American journal of roentgenology. 2005;185:495-500.
.220 Kresnik E, Gallowitsch HJ, Mikosch P, Wurtz F, Alberer D, Hebenstreit A, et al. ^{18}F-FDG positron emission tomography in the early diagnosis of enterocolitis: preliminary results. European journal of nuclear medicine and molecular imaging. 2002;29:1389-92.
.221 Wittenberg J, Harisinghani MG, Jhaveri K, Varghese J, Mueller PR. Algorithmic approach to CT diagnosis of the abnormal bowel wall. Radiographics. 2002;22:1093-107.
.222 Lemberg DA, Issenman RM, Cawdron R, Green T, Mernagh J, Skehan SJ, et al. Positron emission tomography in the investigation of pediatric inflammatory bowel disease. Inflammatory bowel diseases. 2005;11:733-8.
.223 Loffler M, Weckesser M, Franzius C, Schober O, Zimmer KP. High diagnostic value of ^{18}F-FDG-PET in pediatric patients with chronic inflammatory bowel disease. Annals of the New York Academy of Sciences. 2006;1072:379-85.
.224 Neurath MF, Vehling D, Schunk K, Holtmann M, Brockmann H, Helisch A, et al. Noninvasive assessment of Crohn's disease activity: a comparison of ^{18}F-fluorodeoxyglucose positron emission tomography, hydromagnetic resonance imaging, and granulocyte

scintigraphy with labeled antibodies. The American journal of gastroenterology. 2002;97:1978-85.
.225 Towson JEC, Radiation protection and dosimetry in PET and PET/CT. In: Valk PE BD, Townsend DW, Maisey MN, editors. Positron emission tomography basic science and clinical practice. London: Springer; 2003. pp. 265–82.
.226 Spier BJ, Perlman SB, Jaskowiak CJ, Reichelderfer M. PET/CT in the evaluation of inflammatory bowel disease: studies in patients before and after treatment. Molecular imaging and biology 2010;12:85-8.
.227 Yoshida K, Toki F, Takeuchi T, Watanabe S, Shiratori K, Hayashi N. Chronic pancreatitis caused by an autoimmune abnormality. Proposal of the concept of autoimmune pancreatitis. Digestive diseases and sciences. 1995;40:1561-8.
.228 Kamisawa T, Okamoto A. Autoimmune pancreatitis: proposal of IgG4-related sclerosing disease. Journal of gastroenterology. 2006;41:613-25.
.229 Kamisawa T, Egawa N, Nakajima H, Tsuruta K, Okamoto A. Morphological changes after steroid therapy in autoimmune pancreatitis. Scandinavian journal of gastroenterology. 2004;39:1154-8.
.230 Deshpande V, Mino-Kenudson M, Brugge W, Lauwers GY. Autoimmune pancreatitis: more than just a pancreatic disease? A contemporary review of its pathology. Archives of pathology & laboratory medicine. 2005;129:1148-54.
.231 Nakamoto Y, Saga T, Ishimori T, Higashi T, Mamede M, Okazaki K, et al. FDG-PET of autoimmune-related pancreatitis: preliminary results. European journal of nuclear medicine. 2000;27:1835-8.
.232 Nakajo M, Jinnouchi S, Fukukura Y ,Tanabe H, Tateno R. The efficacy of whole-body FDG-PET or PET/CT for autoimmune pancreatitis and associated extrapancreatic autoimmune lesions. European journal of nuclear medicine and molecular imaging. 2007;34:2088-95.
.233 Kamisawa T, Takum K, Anjiki H, Egawa N, Kurata M, Honda G, et al. FDG-PET/CT findings of autoimmune pancreatitis. Hepato-gastroenterology. 2010;57:447-50.
.234 Okazaki K. Autoimmune pancreatitis: etiology, pathogenesis, clinical findings and treatment. The Japanese experience. JOP : Journal of the pancreas. 2005;6:89-96.
.235 Siemon JK, Siegfried GF, Waxman AD. The use of Ga-67 in pulmonary disorders. Seminars in nuclear medicine. 1978;3:235–49.
.236 Woolfenden JM, Carrasquillo JA, Larson SM, Simmons JT, Masur H, Smith PD, et al. Acquired immunodeficiency syndrome: Ga-67 citrate imaging. Radiology. 1987;162:383-7.
.237 Moinuddin M, Rockett J. Gallium scintigraphy in the detection of amiodarone lung toxicity. AJR American journal of roentgenology. 1986;147:607-9.
.238 Cook PS, Datz FL, Disbro MA, Alazraki NP, Taylor AT. Pulmonary uptake in indium-111 leukocyte imaging: clinical significance in patients with suspected occult infections. Radiology. 1984;150:557-61.
.239 Jones HA, Marino PS, Shakur BH, Morrell NW. In vivo assessment of lung inflammatory cell activity in patients with COPD and asthma. The European respiratory journal. 2003;21:567-73.
.240 Chen DL, Schuster DP. Positron emission tomography with [^{18}F]fluorodeoxyglucose to evaluate neutrophil kinetics during acute lung injury. American journal of physiology Lung cellular and molecular physiology. 2004;286:L834-40.

.241 Gremse DA. GERD in the pediatric patient: management considerations. MedGenMed : Medscape general medicine. 2004;6:13.
.242 Razak HR, Geso M ,Abdul Rahim N, Nordin AJ. Imaging characteristics of extrapulmonary tuberculosis lesions on dual time point imaging (DTPI) of FDG PET/CT. Journal of medical imaging and radiation oncology. 2011;55:556-62.
.243 Soussan M, Brillet PY, Mekinian A, Khafagy A, Nicolas P, Vessieres A, et al. Patterns of pulmonary tuberculosis on FDG-PET/CT. European journal of radiology. 2012;81:2872-6.
.244 Braun JJ, Kessler R, Constantinesco A, Imperiale A. 18F-FDG PET/CT in sarcoidosis management: review and report of 20 cases. European journal of nuclear medicine and molecular imaging. 2008;35:1537-43.
.245 Sobic-Saranovic D, Grozdic I, Videnovic-Ivanov J, Vucinic-Mihailovic V, Artiko V, Saranovic D, et al. The Utility of 18F-FDG PET/CT for Diagnosis and Adjustment of Therapy in Patients with Active Chronic Sarcoidosis. Journal of nuclear medicine. 2012;53:1543-9.
.246 Mostard RL, van Kuijk SM, Verschakelen JA, van Kroonenburgh MJ, Nelemans PJ, Wijnen PA, et al. A predictive tool for an effective use of 18[THIN SPACE]F-FDG PET in assessing activity of sarcoidosis. BMC pulmonary medicine. 2012;12:57.
.247 Alavi A, Gupta N ,Alberini JL, Hickeson M, Adam LE, Bhargava P, et al. Positron emission tomography imaging in nonmalignant thoracic disorders. Seminars in nuclear medicine. 2002;32:293-321.
.248 Mavi A, Basu S, Cermik TF, Urhan M, Bathaii M, Thiruvenkatasamy D, et al. Potential of dual time point FDG-PET imaging in differentiating malignant from benign pleural disease. Molecular imaging and biology. 2009;11:369-78.
.249 Umeda Y, Demura Y, Ishizaki T, Ameshima S, Miyamori I, Saito Y, et al. Dual-time-point ^{18}F-FDG PET imaging for diagnosis of disease type and disease activity in patients with idiopathic interstitial pneumonia. European journal of nuclear medicine and molecular imaging. 2009;36:1121-30.
.250 Nagai S, Kitaichi M, Itoh H, Nishimura K, Izumi T, Colby TV. Idiopathic nonspecific interstitial pneumonia/fibrosis: comparison with idiopathic pulmonary fibrosis and BOOP. The European respiratory journal. 1998;12:1010-9.
.251 Hamberg LM, Hunter GJ, Alpert NM, Choi NC, Babich JW, Fischman AJ. The dose uptake ratio as an index of glucose metabolism: useful parameter or oversimplification? Journal of nuclear medicine. 1994;35:1308-12.
.252 Hustinx R, Smith RJ, Benard F, Rosenthal DI, Machtay M, Farber LA, et al. Dual time point fluorine-18 fluorodeoxyglucose positron emission tomography: a potential method to differentiate malignancy from inflammation and normal tissue in the head and neck. European journal of nuclear medicine. 1999;26:1345-8.
.253 Kim IJ ,Lee JS, Kim SJ, Kim YK, Jeong YJ, Jun S, et al. Double-phase ^{18}F-FDG PET-CT for determination of pulmonary tuberculoma activity. European journal of nuclear medicine and molecular imaging. 2008;35:808-14.
.254 Schuster DP, Brody SL ,Zhou Z, Bernstein M, Arch R, Link D, et al. Regulation of lipopolysaccharide-induced increases in neutrophil glucose uptake. American journal of physiology Lung cellular and molecular physiology. 2007;292:845-51.
.255 Martin WG, Ristow KM, Habermann TM, Colgan JP, Witzig TE, Ansell SM. Bleomycin pulmonary toxicity has a negative impact on the outcome of patients with Hodgkin's lymphoma. Journal of clinical oncology. 2005;30 :20-7614

.256 Sleijfer S. Bleomycin-induced pneumonitis. Chest. 2001;120:617-24.
.257 von Rohr L, Klaeser B, Joerger M, Kluckert T, Cerny T, Gillessen S. Increased pulmonary FDG uptake in bleomycin-associated pneumonitis. Onkologie. 2007;30:320-3.
.258 Connerotte T, Lonneux M. Use of 2-[18F]fluoro-2-deoxy-D-glucose positron emission tomography in the early diagnosis of asymptomatic bleomycin-induced pneumonitis. Annals of hematology. 2008;87.5–943:
.259 Park IN, Ryu JS, Shim TS. Evaluation of therapeutic response of tuberculoma using F-18 FDG positron emission tomography. Clinical nuclear medicine. 2008;33:1-3.
.260 Chamilos G, Macapinlac HA, Kontoyiannis DP. The use of 18F-fluorodeoxyglucose positron emission tomography for the diagnosis and management of invasive mould infections. Medical mycology. 2008;46:23-9.
.261 Ozsahin H, von Planta M, Muller I, Steinert HC, Nadal D, Lauener R, et al. Successful treatment of invasive aspergillosis in chronic granulomatous disease by bone marrow transplantation, granulocyte colony-stimulating factor-mobilized granulocytes, and liposomal amphotericin-B. Blood. 1998;92:2719-24.
.262 Bleeker-Rovers CP, Warris A, Drenth JP, Corstens FH, Oyen WJ, Kullberg BJ. Diagnosis of Candida lung abscesses by 18F-fluorodeoxyglucose positron emission tomography. Clinical microbiology and infection. 2005;11:493-5.
.263 Win Z, Todd J, Al-Nahhas A. FDG-PET imaging in Pneumocystis carinii pneumonia. Clinical nuclear medicine. 2005;30:690-1.
.264 Little PJ, McPherson DR, Dewardener HE. The Appearance of the Intravenous Pyelogram during and after Acute Pyelonephritis. Lancet. 1965;1:1186-8.
.265 MacKenzie JR. A review of renal scarring in children. Nuclear medicine communications. 1996;17:176-90.
.266 Bykov S, Chervinsky L, Smolkin V, Halevi R, Garty I. Power Doppler sonography versus Tc-99m DMSA scintigraphy for diagnosing acute pyelonephritis in children :are these two methods comparable? .Clinical nuclear medicine. 2003;28:198-203.
.267 Traisman ES, Conway JJ, Traisman HS, Yogev R, Firlit C, Shkolnik A, et al. The localization of urinary tract infection with Tc-99mglucoheptonate scintigraphy. Pediatr Radiol 1986;16:403–6.
.268 Lin KY, Chiu NT, Chen MJ, Lai CH, Huang JJ, Wang YT, et al. Acute pyelonephritis and sequelae of renal scar in pediatric first febrile urinary tract infection. Pediatr Nephrol. 2003;18:362-5.
.269 Chiou YY, Wang ST, Tang MJ, Lee BF, Chiu NT. Renal fibrosis: prediction from acute pyelonephritis focus volume measured at 99mTc dimercaptosuccinic acid SPECT. Radiology. 2001;221:366-70.
.270 Wang YT, Chiu NT, Chen MJ, Huang JJ ,Chou HH, Chiou YY. Correlation of renal ultrasonographic findings with inflammatory volume from dimercaptosuccinic acid renal scans in children with acute pyelonephritis. The Journal of urology. 2005;173:190-4.
.271 Sakarya ME, Arslan H, Erkoc R, Bozkurt M, Atilla MK. The role of power Doppler ultrasonography in the diagnosis of acute pyelonephritis. British journal of urology. 1998;81:360-3.
.272 Majd M, Nussbaum Blask AR, Markle BM, Shalaby-Rana E ,Pohl HG, Park JS, et al. Acute pyelonephritis: comparison of diagnosis with 99mTc-DMSA, SPECT, spiral CT, MR imaging, and power Doppler US in an experimental pig model. Radiology. 2001;218:101-8.

.273 Torres VE, Harris PC. Autosomal dominant polycystic kidney disease: the last 3 years. Kidney international. 2009;76:149-68.
.274 Torres VE, Harris PC, Pirson Y. Autosomal dominant polycystic kidney disease. Lancet. 2007;369:1287-301.
.275 Sallee M, Rafat C, Zahar JR, Paulmier B, Grunfeld JP, Knebelmann B, et al. Cyst infections in patients with autosomal dominant polycystic kidney disease. Clinical journal of the American Society of Nephrology : CJASN. 2009;4:1183-9.
.276 Lahiri SA, Halff GA, Speeg KV, Esterl RM, Jr. ^{111}In-WBC scan localizes infected hepatic cysts and confirms their complete resection in adult polycystic kidney disease. Clinical nuclear medicine. 1998;23:33-4.
.277 Palestro CJ, Love C, Bhargava KK. Labeled leukocyte imaging: current status and future directions. Q J Nucl Med Mol Imaging. 2009;53:105-23.
.278 Jimenez-Bonilla JF, Quirce R, Calabia ER, Banzo I, Martinez-Rodriguez I, Carril JM. Hepatorenal polycystic disease and fever: diagnostic contribution of gallium citrate Ga 67 scan and fluorine F 18 FDG-PET/CT. European urology. 2011;59:297-9.
.279 Piccoli G, Arena V, Consiglio V. Positron emission tomography in the diagnostic pathway for intracystic infection in adpkd and “cystic” kidneys. a case series. BMC Nephrology. 2011:12:48.
.280 Lyra M, Voliotopoulos V, Vlachos L, Limouris G. Practical dosimetric consideration and imaging evaluation in infection scintigraphy. edit. Limouris G.S. Bender,H.F. Voliotopoulos V. Mediterra, Athens. 1998: 105-109.
.281 Gemmel F, Dumarey N, Welling M. Future diagnostic agents. Seminars in nuclear medicine. 2009;39:11-26.
.282 Gemmel F, Dumarey N, Palestro CJ. Radionuclide imaging of spinal infections. European journal of nuclear medicine and molecular imaging. 2006;33:1226-37.

دور المَسح الذرِّى المقطعى بواسطة الانبعاث البُوزيتروني المُدمَج بالأشَعة المَقطعية في الألتهابات والعدوى الميكروبية

مقالة

توطئة للحصول على درجة الماجستير في الطب النووي والنظائر المشعة

مقدمة من

الطبيبة: شيماء أحمد عبد المنعم الرصد

تحت إشراف

الأستاذة الدكتورة/ شاهندة سالم صبري

أستاذ الطب النووي
كلية الطب- جامعة القاهرة

الأستاذ الدكتور/ صالح عبده محمد جودة

أستاذ النظائر المشعة - طب نووي
كلية الطب- جامعة القاهرة

الدكتورة/ محاسن أمين أبو جبل

مدرس الطب النووي
كلية الطب-جامعة القاهرة

كلية الطب
جامعة القاهرة
٢٠١٢